NON-LINEAR EXCITATIONS

IN

MODULATED CRYSTALS

J.J.M. SLOT

1987

NON-LINEAR EXCITATIONS IN MODULATED CRYSTALS

PROEFSCHRIFT

TER VERKRIJGING VAN DE GRAAD VAN
DOCTOR IN DE WISKUNDE EN NATUURWETENSCHAPPEN
AAN DE KATHOLIEKE UNIVERSITEIT TE NIJMEGEN,
OP GEZAG VAN DE RECTOR MAGNIFICUS
PROF.DR. B M.F. VAN IERSEL
VOLGENS BESLUIT VAN HET COLLEGE VAN DECANEN
IN HET OPENBAAR TE VERDEDIGEN OP
VRIJDAG 18 DECEMBER 1987
DES NAMIDDAGS TE 1.30 UUR PRECIES

DOOR

JOHAN JOSEPHUS MACHIEL SLOT

GEBOREN TE TERNEUZEN

DRUK INTERNATIONALE PUBLICITEITS DIENSTEN (IPD)
TERNEUZEN 1987

Promotor:

PROF.DR. A.G.M. JANNER

Co-referenten:

DR. Th.W.J.M. JANSSEN

DR. H.J.F. KNOPS

NON-LINEAR EXCITATIONS IN MODULATED CRYSTALS

NON-LINEAR EXCITATIONS IN MODULATED CRYSTALS

PROEFSCHRIFT

TER VERKRIJGING VAN DE GRAAD VAN
DOCTOR IN DE WISKUNDE EN NATUURWETENSCHAPPEN
AAN DE KATHOLIEKE UNIVERSITEIT TE NIJMEGEN
OP GEZAG VAN DE RECTOR MAGNIFICUS
PROF DR B M F VAN IERSEL
VOLGENS BESLUIT VAN HET COLLEGE VAN DECANEN
IN HET OPENBAAR TE VERDEDIGEN OP
VRIJDAG 18 DECEMBER 1987
DES NAMIDDAGS TE 1 30 UUR PRECIES

DOOR

JOHAN JOSEPHUS MACHIEL SLOT

GEBOREN TE TERNEUZEN

DRUK INTERNATIONALE PUBLICITEITS DIENSTEN (IPD)
TERNEUZEN 1987

Promotor

PROF.DR. A.G.M. JANNER

Co-referenten

DR. Th.W.J.M. JANSSEN

DR. H.J.F. KNOPS

ter nagedachtenis van mijn vader
voor mijn moeder
voor Corine

Graag wil ik eenieder bedanken, die op enigerlei wijze een bijdrage geleverd heeft aan de totstandkoming van dit proefschrift.

In het bijzonder wil ik Maria Straatman bedanken voor de enorme inzet die zij getoond heeft bij het scheppen van het uiteindelijke manuscript met behulp van de tekstverwerker*) Zonder haar grote kennis op dit gebied en zonder haar grote bereidheid om 's avonds en 's nachts te werken, vaak ook in de weekeinden, zou het proefschrift nooit geworden zijn, wat het nu is, zeker niet binnen de gestelde termijn

Verder wil ik ook mijn ouders bedanken voor het in mij gestelde vertrouwen en voor hun altijd aanwezige steun gedurende de jaren. Het is jammer dat mijn vader de laatste periode niet heeft mogen meemaken.

Als laatste wil ik Corine bedanken voor het grote geduld dat zij heeft willen opbrengen tijdens mijn vaak geprikkelde buien in de laatste fase van de totstandkoming van het proefschrift maar ook voor de plezierige tijd die ik met haar tot op heden heb mogen beleven.

*) Voor de grafische uitvoering van dit proefschrift werd gebruik gemaakt van het tekstverwerkingsprogramma "troff", werkend onder het bedrijfssysteem UNIX.

Models are, for the most part, caricatures of reality, but if they are good, then, like good caricatures, they portray, though perhaps in a distorted manner, some of the features of the real world The main role of models is not so much to explain and to predict - though ultimately these are the main functions of science - as to polarise thinking and to pose sharp questions. Above all, they are fun to invent and to play with, and they have a peculiar life of their own. The "survival of the fittest" applies to models even more than it does to living creatures. They should not, however, be allowed to multiply indiscriminantly without real necessity or real purpose.

M. Kac, "Some Mathematical Models in Science"
Science, vol. 166, p. 699 (November 1969)

CONTENTS

CHAPTER 1

INTRODUCTION

The main subject of this thesis concerns statics and dynamics of domain walls in modulated crystals. Domains walls or phase boundaries are also found in many other condensed matter systems such as ferromagnets [1] where they are known as Bloch walls, ferroelectrics [2], fluid mixtures [3] etc. and it is by now well established that they are to be looked upon as large local variations of the (thermodynamic) ground state order-parameter of the system. Therefore it is clear that a state of the system with domain walls cannot be reached in any finite order of perturbation theory starting from the ground state. So in order to describe domain walls and their properties one needs a non-linear theory in which the non-linearities are taken properly into account. In a general sense one can view a domain wall as a static excitation (excited state) of the system.

In a modulated crystal the equilibrium positions of the atoms or molecules are shifted (displaced) with respect to points of a structure having three-dimensional space group symmetry, the displacement being periodic. Therefore the three-dimensional lattice translational symmetry is lost or at least reduced as in the case of a superstructure. Actually there are two main classes of modulated crystals observed in nature, crystals with a displacive modulation and crystals with an occupational modulation. In this thesis only the former class is considered. So the word modulated here will always refer to displacively modulated. If the wave vector of the periodic deformation has one irrational component with respect to the reciprocal basis of the underlying lattice one has an incommensurate crystal. However, when all components are rational one has a commensurate crystal (superstructure). Incommensurate crystals is the collective name for a large and still growing group of solid state systems which, broadly speaking, can be characterised by having a definite long range order but no three-dimensional space group symmetry. In [4] one can find a recent list of compounds which belong to the group of incommensurate crystals. A superstructure still has a three dimensional space group symmetry, but it has a unit-cell which is a multiple (possibly large) of the original unit-cell. The lost (reduced) translational symmetry of a modulated crystal can be restored by a mathematical construction which is known by the name "superspace embedding". This construction, which is due to de Wolff [5] and Janner and Janssen [6], boils

down to embedding the modulated crystal into a higher dimensional space in such a way that the embedded crystal again has a space group symmetry albeit a higher (>3) dimensional one The original modulated crystal can be recovered as a three-dimensional intersection of this embedded super-crystal" This "superspace' approach has been very successfully applied to the crystallography of modulated structures For instance it is possible to explain systematic extinctions in X-ray diffraction patterns on the basis of these higher dimensional space groups [7] However applications of this superspace' idea to the physics of modulated crystals such as the existence of domain walls and their behaviour has up to now run into non-trivial conceptual problems Therefore this superspace approach is not used here

In nearly all crystals which show an incommensurate (IC) phase, one observes that the latter is just one of the many thermodynamical phases in which the crystal can exist For instance in K_2SeO_4 [8] which represents a generic case of a modulated crystal one observes three phases depending on temperature First of all there is a so-called high temperature phase where the system exhibits a three-dimensional space group symmetry with a transition at a temperature T_i to an intermediate modulated incommensurate phase and a low-temperature superstructure phase below T_c In approaching T_i from above one of the lattice modes with wave vector $\mathbf{q}$ becomes soft i e its frequency $\omega(\mathbf{q}\ 1)$ decreases and eventually vanishes at T_i Just below T_i non-linear (anharmonic) forces stabilise this lattice instability resulting in a modulated phase with a wave vector which is initially given by the wave vector $\mathbf{q}$ of the soft mode Further down below T_i the wave vector generally varies with respect to the average structure parameters, as a function of temperature The region just below T_i is called the sinusoidal region, because there the displacement pattern is very accurately described by a single sine-function This incommensurate (unlocked) phase ends at a lower temperature T_c At this temperature the system undergoes a second phase transition, which is known as the lock in transition Below T_c one still has a modulated phase, but with a wave vector which is locked (fixed) to a commensurate value in other words below T_c one has a superstructure of the original high-temperature phase In the incommensurate phase just above T_c, one has the so-called discommensuration - or soliton regime [9] In this part of the incommensurate phase the modulation function is non sinusoidal, i e contains contributions from the higher harmonics of the modulation wave vector The crystal in this regime consists of nearly commensurate domains separated by domain walls The structure within such a domain is nearly that of the locked phase below T_c Due to these domain walls the overall modulation periodicity is still incommensurate This is the reason why these domain walls are also called discommensurations The name soliton is of course due to the fact that domain walls are

described, as was mentioned before as localised solutions of certain non-linear equations They are, however not always solitons in the true sense of the word [10] In the beginning of this regime one has small domains with relatively broad domain walls The strong mutual interaction of the domain walls then forces them to be equidistant Such a structure is known as a discommensuration (or soliton) lattice In approaching T_c the size of the domains grows Now because their mutual interaction decreases with distance the walls will no longer be bound together This results in domains of all kinds of sizes This situation is analogous to the situation just above the paramagnetic to ferromagnetic phase transition in ferromagnets There one has magnetised domains (Weiss domains) of all kinds of sizes, but with a zero total magnetisation At T_c there will be one large superstructure One can also formulate this by saying that the average spacing between the domain walls is a critical quantity, i e diverges at the phase transition It is therefore clear that in order to understand the kinetics of the lock-in transition, i e the way the commensurate low-temperature phase is formed in space and time [11], one needs to understand the statics, i e the structure, and the dynamics of these domain walls in modulated systems

Up to now nothing is mentioned about the origin of the incommensurate phase, i e the mechanisms which lead to an instability of the high-temperature phase In this thesis actually two mechanisms play a central role The first mechanism which is considered is the well-known Peierls instability [12] in quasi-one-dimensional coupled electron-phonon systems such as polyacetylene [13] In this mechanism the lattice mode with wave vector $2k_F$ becomes unstable because this leads to the opening of a gap at the Fermi level which is located at the points $\pm k_F$ in the first Brillouin zone This opening of a gap at the Fermi level implies that the occupied electronic levels are lowered in energy On the other hand the appearance of a periodic lattice deformation with wave vector $2k_F$ in the system costs elastic energy Now Peierls showed that the decrease in electronic band energy outweights the increase in elastic energy So it is always energetically favourable to create a periodic lattice deformation with wave vector $2k_F$ and because this k_F can be located anywhere in the zone one can have an incommensurate modulated phase The original argument of Peierls was a zero temperature argument Now in a finite temperature mean field version of this argument, the instability occurs at a temperature T_p which is known as the Peierls temperature This temperature which is of course the equivalent of the earlier mentioned T_c is predominantly determined by a very important parameter in these quasi-one-dimensional coupled electron-phonon systems namely the electron-phonon coupling constant λ or α as it is called in the third chapter The Peierls temperature T_p depends on λ in the following way

$$T_p \quad \exp(-\frac{1}{\lambda}) \qquad (1.1)$$

This means that for small λ one has a negligible T_p. This formed the reason to calculate λ for the well-known incommensurate metallic compound $Hg_{3-\delta}AsF_6$ [14] together with M. Weger form the Hebrew University in Jerusalem and M.H. Boon from Nijmegen. In this compound the conduction is along linear chains of Hg atoms which makes it a quasi one dimensional conductor. A long-standing problem concerning this material was the fact that no Peierls transition was ever observed. The claim was that it has something to do with the intra-chain electron phonon coupling constant λ which has to be very small. This problem forms the subject of the second chapter.

A generic model for many quasi one dimensional coupled electron phonon systems of the so-called charge transfer type is given by the well-known Su-Schrieffer-Heeger (SSH) model which was put forward to explain many phenomena in trans polyacetylene $(CH)_x$ [15]. Trans polyacetylene is a quasi-one dimensional organic conductor which has many interesting optical, electrical and magnetic properties at low temperatures [13]. All these properties are connected with the fact that below some temperature the system forms a two-fold superstructure for a half filled band ($k_F = \frac{\pi}{2a}$). This means that there are two degenerate ground states and thus that one can have domain walls between these ground state phases. The analytical form of these domain walls was found in a continuum version of the original SSH model which is known as the Takayama-Lin-Liu-Maki [TLM] model [16]. Also the soliton lattice was found in this model [17]. In the third chapter of this thesis the original SSH model is extended by including a strong coupling between the one dimensional chains. This leads to quite a different ground state for the half-filled band case and also to quite different domain walls in the system.

The mechanism of the IC phase formation in insulators such as the earlier mentioned K_2SeO_4 is different. In the last two chapters a model is investigated where the instability is caused by a phenomenon known as frustration. Frustration is the competition between two or more conflicting influences, for instance like two forces which favour different length scales. The model which is considered is known by the name Discrete Frustrated ϕ^4 (DIFFF) model or also the Janssen-Tjon model [18,19]. It consists of a one-dimensional chain of classical particles with harmonic interactions up to next nearest neighbours and an anharmonic fourth order on-site potential. In this model domain walls play a two fold role. First of all they lead to the stabilisation of the incommensurate phase just above the lock in transition. That is to say a system consisting of nearly commensurate domains separated by domain walls has a lower free energy than the

corresponding commensurate system. Secondly, domain walls appear in this model as static excitations of the commensurate low-temperature phase. Infinitesimally above the lock-in transition the average spacing between domain walls is very large. Therefore, in this situation one has nearly free domain walls, i.e the interaction between the walls is negligibly small. This forms the subject of chapter 4, where the dynamics (including the statics) of single domain walls or kinks is studied. Higher up in the discommensuration regime, one has a soliton - or discommensuration lattice, whose statics and dynamics is the subject of chapter 5.

References

[1] U. Enz, Phys. Acta **37** (1964) 245

[2] Y. Ishibashi, J. Phys. Soc. Jpn **54** (1985) 2017.

[3] B. Widom in: "Statistical Mechanics and Statistical Methods in Theory and Application", ed U. Landman, Plenum, New York (1977).

[4] A.U. Sheleg and V.V. Zaretskii in: "Incommensurate Phases in Dielectrics", part two: Materials, ed R. Blinc and A.P. Levanyuk in the series "Modern Problems in Condensed Matter Sciences", North-Holland, Amsterdam (1986).

[5] P.M de Wolff, Acta Cryst. A **30** (1974) 777.

[6] A Janner and T. Janssen, Phys. Rev. B **15** (1977) 643.

[7] A Yamamoto, Acta Cryst. B **38** (1982) 1451.

[8] J.D. Axe, M. Iizumi and G. Shirane, Phys. Rev. B **22** (1980) 3408.

[9] K.K. Fung, S. Mckernan, J.W. Steeds and J.A Wilson, J. Phys. C **14** (1981) 5417.

[10] A.R. Bishop, J.A. Krumhansl and S.E. Trullinger, Physica **1D** (1980) 1.

[11] K. Kawasaki and S. Yamanaka, Phys. Rev. B **34** (1986) 7986.

[12] R.E. Peierls: Quantum theory of solids, Clarendon Press, Oxford (1955).

[13] See for instance: J.R. Schrieffer in: "Highlights of Condensed-Matter Theory", proceedings of the international school of physics, "Enrico Fermi", course 89, ed. F. Basani, F. Fumi and M.P. Tosi, North-Holland, Amsterdam (1985).

[14] J.J.M. Buiting, thesis, Catholic University of Nijmegen (1985) and references therein.

[15] W.P. Su, J.R. Schrieffer and A.J. Heeger, Phys. Rev. B **22** (1980) 2099.

[16] H Takayama, Y R Lin-Liu and K Maki, Phys Rev B **21** (1980) 2388
[17] B Horovitz, Phys Rev Lett **46** (1981) 742
[18] T Janssen and J A Tjon, Phys Rev B **24** (1981) 2245
[19] T Janssen in "Incommensurate Phases in Dielectrics", part one Fundamentals, ed R Blinc and A P Levanyuk in the series "Modern Problems in Condensed Matter Sciences", North-Holland, Amsterdam (1986)

CHAPTER 2†

CALCULATION OF THE ELECTRON-PHONON COUPLING CONSTANT λ FOR THE INCOMMENSURATE METAL $Hg_{3-\delta}AsF_6$

J J M Slot and M H Boon

Institute for Theoretical Physics, Faculty of Science, Toernooiveld, Nijmegen, 6525 ED, The Netherlands

and

M Weger

Racah Institute of Physics, Hebrew University, Jerusalem, Israel

Abstract

We carry out an ab-initio calculation of the electron-phonon coupling constant λ for the incommensurate linear chain metal $Hg_{3-\delta}AsF_6$. We find that the intra-chain coupling $\lambda_{//}$ is very weak, less than 0.1, while the inter-chain coupling $\lambda_{\perp}$ is very strong, close to 1. This value of λ accounts for the resistivity in the normal state, for the absence of a Peierls transition, and also for bulk superconductivity with a transition temperature of several degrees.

---

† Solid State Communications, vol. 56, No. 8, pp. 645-649, 1985, Pergamon Press Ltd.

2.1 Introduction

Over the last few years there has been a growing interest in the intergrowth material $Hg_{3-\delta}AsF_6$ because of its peculiar lattice and electronic properties [1,2,3,4,5]. This material consists of mercury chains in the a and b directions. The Hg-Hg distance d = 2.67Å is incommensurate with the period of the AsF_6-lattice of a = b = 7.45Å (a = (3−δ)d, δ≈ 0.21). Above 130 K, the mercury chains form a one-dimensional liquid with no long range order [6]. Below 120 K, the chains interlock and long-range order is established [7]. The electrical conductivity is very anisotropic and mainly in the a-b plane [2]. In spite of the incommensurability, sharp dHvA oscillations are observed [3] indicating plane sheets of the Fermi surface. The temperature-dependent resistivity is large, indicating strong electron-phonon coupling [8], while the residual resistivity is small in spite of the large concentration of AsF_6-vacancies. The material remains metallic down to the lowest observed temperatures with no Peierls transition, in spite of the strong electron-phonon coupling. The material displays a rather mysterious superconductivity ; the Philadelphia group claims [9] it is an anisotropic bulk superconductivity, while Datars et al. claim [10] that the superconductivity is due to extruded mercury. The electronic bandstructure indicates strong inter-chain coupling [11] and novel selection-rules that strongly suppress the effect of the incommensurability on the electronic states [12].

Because of these numerous unusual properties, we carry out here a conventional calculation of McMillan's electron-phonon coupling constant λ, which plays a key role in many of these phenomena. We calculate both the intra-chain coupling $\lambda_{//}$ and the inter-chain coupling $\lambda_{\perp}$. We find that $\lambda_{//}$ is exceedingly small, while $\lambda_{\perp}$ is unexpectedly large. On the basis of these features, we account for some of the unusual properties of this material

2.2 The intra-chain electron-phonon coupling constant $\lambda_{//}$

The intra-chain electron-phonon coupling constant $\lambda_{//}$ is due to the coupling of an electron near the Fermi level with the longitudinal acoustic deformation of the mercury chain. $\lambda_{//}$ is given by the McMillan expression [13,14,15]:

$$\lambda_{//} = \frac{\alpha_{//}^2 \, N(E_F)}{2M\omega_{2k_F}^2} \qquad (1)$$

The mercury-mercury distance within a chain is small (2 67 Å) compared to the mercury mercury distance in elemental mercury ($\approx$ 3 Å) therefore the LA phonons along the chain have a very high Debye temperature Θ_{1D} ($\hbar\omega_{1D}=k_B\Theta_{1D}$) For ω_q we use the expression

$$\omega_q = \omega_{1D} \sin(qd/2) \tag{2}$$

Various values of Θ_{1D} are quoted in the literature Wei et al [21] quote Θ_{1D}=596 K Moses et al [21] quote Θ_{1D}=540 K These values are based on the continuum model, for which ω=vq For the Born Von Karman model for which ω is given by (2), we have to reduce the value of ω_{1D} by a factor of $2/\pi$ Hastings et al [6] quote a value of v=4 4×10^5 cm/sec which for a continuum model yields ω_{1D}=387 K, and for the Born Von Karman model ω_{1D}=243 K All these values are very high the value of ω_{1D} [2] being one to two orders higher than in elemental mercury where ω_D=80 K This hardening may be due in part to the closer distance between Hg nearest neighbours being 2 67 Å (instead of 3 Å), for a 6-12 Lennard Jones potential this increases the force constant by a factor of 5 Also since there are only 2 nearest neighbours (rather than 6, as in elemental Hg) the bonds may be stronger leading to additional hardening In the following table we present values of λ for both the highest (600 K) and lowest (243 K) values quoted in the literature $N(F_F)$ is the density of states at the Fermi level, calculated in [11] (about 0 2 states/eV per mercury atom for both spin directions), α is the value of the derivative of the electronic gap Δ_{k_F} with respect to the amplitude u of the longitudinal acoustic deformation of the chain at u=0 M is the atomic mass of mercury (3 33×10^{-25} kg)

In order to calculate λ we did a bandstructure calculation for an infinite mercury chain with a displacive cosine modulation $x_n = nd + u_n$ where $u_n = u\cos(qnd)$ For the modulation wave-vector q we took $8\pi/5d$ which is the value of $2k_F$ given in [12] This gives us a five-fold superstructure with four gaps in addition to the gap at the band edge The potential we use for the bandstructure calculation is a Gaussian fitted to a Heine Abarenkov [16] pseudopotential for mercury (Fig 1) Gaussian (a) has the same depth as the Heine-Abarenkov pseudopotential (c) at q=0 while the width is so chosen as to give the best least square fit The other Gaussian (b) is so chosen as to coincide with the pseudopotential over a wide q-range The Gaussian potential (a) gives a value for the mercury 6s 6p gap of about 90 mRy This value is in good agreement with a 3D pseudopotential calculation done by Butting et al [11]

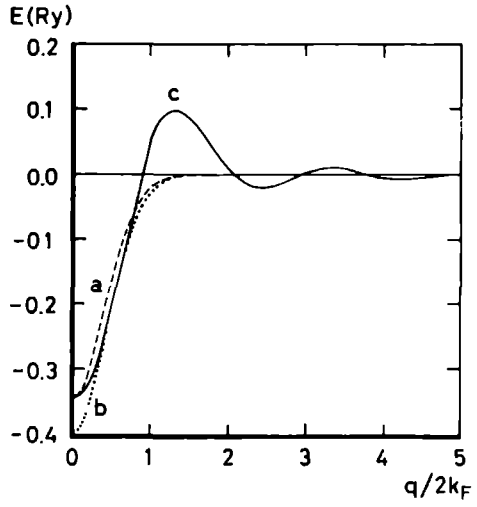

Figure 1. The potentials employed in this work (a) Gaussian fitted to the Hg-pseudopotential in second moment (least square fit) and depth at q = 0 (b) Gaussian fitted to the Hg-pseudopotential over a wide q range (c) The Heine-Abarenkov pseudopotential for Hg

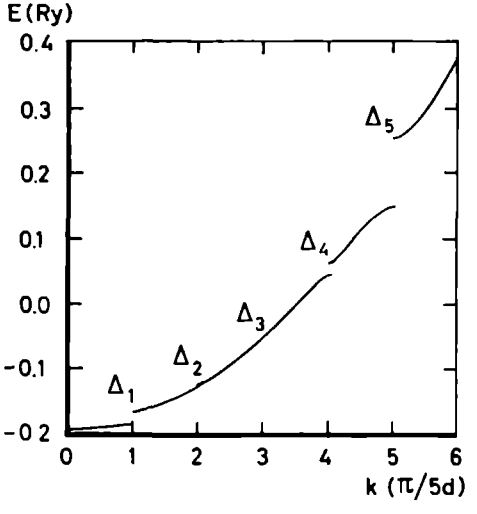

Figure 2. The bandstructure arising from a 5% lattice distortion (frozen $2k_F$ phonon) Δ_1 and Δ_4 are first order gaps, Δ_2 and Δ_3 are second-order gaps, and Δ_5 is the gap between the 6s and 6p bands

When we use the Heine-Abarenkov pseudopotential directly rather than this Gaussian fit, we obtain a 6s-6p gap of about 340 mRy which is inconsistent with the 3D pseudopotential calculation [11] This is because the pseudopotential in r-space is close to a δ-function spherical shell of radius d/2, which for the present structure is somewhat unrealistic As a basis set we take wavefunctions which are plane waves along the direction of the chain and Gaussians perpendicular to the chain

$$<\mathbf{r}|k,n> = C \exp\{i(k - n\frac{2\pi}{5d})x\} \exp\{-\beta(y^2+z^2)\}$$

$$-\frac{\pi}{5d} < k \leq \frac{\pi}{5d} \qquad (3)$$

where n is an integer and C is a normalisation constant In the real crystal the y and z directions are inequivalent, but we treat both directions on a equal footing, following Buiting et al [17] The Gaussian potentials give a very rapid convergence By taking a basis set containing 11 states (n = -5 5) we get a convergence to better than 1 mRy The gaps are illustrated in Fig 2 for the case of Gaussian (b) with a modulation amplitude of 5% of the Hg-Hg distance (2 67 Å) and a perpendicular fall-off parameter β= 0 35Å^{-2} For this structure one observes in addition to the band-gap (Δ_5, about 105 mRy) the appearance of four more gaps due to the modulation Their values are given in the last column of the table This table gives the results of some of the calculations For the perpendicular fall-off parameter β we take the values 0 35 Å^{-2} and 0 55 Å^{-2} The value 0 35 Å^{-2} followed from the logarithmic derivative $t_{\perp}^{-1}\frac{\partial t_{\perp}}{\partial \epsilon}$ for two mercury atoms 3 1 Å apart [18] while the other value 0 55 Å^{-2} was given in [17]

The band-gap (Δ_5, between the Hg 6s and 6p bands) is almost independent of the modulation Gaps Δ_1 and Δ_4 have a non zero derivative as function of the modulation amplitude at zero amplitude, while the second-order gaps Δ_2 and Δ_3 have a zero first order derivative at the origin Gap Δ_4 is the gap at the Fermi level Gap Δ_1 gives us the values of α and λ for forward scattering This value of λ is important for the so-called 'g-ology" diagrams [19] The values of $\alpha_{//}$ and $\lambda_{//}$ for forward scattering are larger than the corresponding values for backward scattering, as can be seen in the table

	pseudo - potential (c)		gaussian (a)		gaussian (b)	
$\beta(Å^{-2})$	0 55	0 35	0 55	0 35	0 55	0 35
Δ_1(mRy)	33	25	21	17	25	20
Δ_2(mRy)	7	3	2	1	3	2
Δ_3(mRy)	3	1	0	0	0	0
Δ_4(mRy)	23	19	18	16	21	19
Δ_5(mRy)	337	183	92	76	130	105
α_1(eV/Å)	3 40	2 56	2 13	1 78	2 49	2 08
α_4(eV/Å)	2 39	1 93	1 83	1 61	2 17	1 96
$\lambda_{//1}$ Θ_{1D}=600K	0 026	0 015	0 011	0 007	0 015	0 011
$\lambda_{//4}$ Θ_{1D}=600K	0 011	0 007	0 007	0 007	0 011	0 007
$\lambda_{//1}$ Θ_{1D}=234K	0 16	0 09	0 07	0 04	0 09	0 07
$\lambda_{//4}$ Θ_{1D}=243K	0 07	0 04	0 04	0 04	0 07	0 04

2.3 The inter-chain electron-phonon coupling constant $\lambda_\perp$

The inter-chain electronic matrix element is given by a McMillan-like expression

$$\alpha_\perp = 2 \frac{\partial t_\perp}{\partial c} \tag{4}$$

where $t_\perp$ is the inter-chain transfer integral, and we use a modified tight-binding approximation [20] because of the large separation of the Hg atoms along the c-direction (3 1 Å)

The value of $t_\perp$ for two isolated Hg atoms 3 06 Å apart is 1 2 eV, and its derivative is $\partial t_\perp/\partial c$ = 2 eV/Å This value of $\alpha_\perp$, together with a phonon frequency of Θ_{3D} = 70 K [21], yields a value of $\lambda_\perp$ = 0 8

The band calculations - the self-consistent ASW calculation [11] as well as the pseudopotential calculation for the 3D structure [11] - yielded similar values of $t_\perp$ The Wannier-function fit to the ASW calculation [17] yields a parameter E_{15} = 1 3 eV which is essentially our $t_\perp$ Some small corrections to this value

arise from several causes

i) There is one bond in the c-direction for every $(3-\delta)/2 = 1\ 4$ Hg atoms only This reduces $<\alpha_\perp^2>$ and $\lambda_\perp$ by $1/1\ 4 \approx 0\ 7$

ii) The next-nearest neighbor inter chain integrals contribute to $<\alpha_\perp^2>$ as well The value of these integrals is approximately 20-25% of the nearest-neighbor inter-chain integrals Since there are 4 of them (for each n n integral), their contribution increases $<\alpha_\perp^2>$ by about 20 25%

Effects (i) and (ii) together reduce $<\alpha_\perp^2>$ and $\lambda_\perp$ by about 10%

The largest uncertainty in $\lambda_\perp$ comes from the uncertainty of the phonon frequency The Debye temperature determined from the specific heat, $\Theta_{3D} = 70$ K is an *average* over all modes , while we consider here the modulation of the inter-chain distance only The phonon spectrum of this material is extremely anisotropic ~500 K for LA phonons along the chain, a 3D Debye temperature of 70 K, and a phason mode at 1 5 K [22] Therefore the value of $<1/\omega^2>$ entering the expression for the resistivity can be quite different from the value determined by the specific heat We estimate an uncertainty of about a factor two in the value of $<1/\omega^2>$

2.4 Discussion

2.4.1 Resistivity

The value of $\lambda_\perp \approx 0\ 8$ is consistent with the measured resistivity in the region 30-300 K ϱ/T is approximately flat above 70 K, and falls below this temperature [23], which is consistent with a Debye temperature of 70 K Around 300 K, ϱ/T rises with T This rise can be accounted for by

i) A temperature dependence of Θ_{3D} (like $T^{-1\,4}$, approximately) [24]

ii) A contribution from high frequency phonons, like the LA branch , according to the present calculation of $\lambda_\perp$ this is possible for $\Theta_{1D} \approx 300$ K

iii) Deviations from the first Born approximation [23]

iv) A T^2 term due to the soft transverse phonons [25], or the damped diffusive motion along the chain direction

At low temperatures, the resistivity follows approximately a T^2 law This can be due to relaxation by multiple transitions, as in the classical Bloch theory A theory along these lines has been proposed by Kaveh and Ehrenfreund [24] Relaxation near the corners of the Fermi surface is fast because the phonons can have a small value of q and thus of ω Diffusion to the corners is also caused by low q phonons Some support for this is provided by anisotropy of the Dingle temperature, which is higher near the corners [26] Datars et al [27] postulate that the coupling constant C (related essentially to McMillan's α) is the same for the inter-chain and intra-chain processes As for the phonons they take $q = 2k_F$ in the first Brillouin zone of the 3D lattice, i e instead of $q = 8\pi/5d$ they take $q = 8\pi/5d - 4\pi/a$ which yields a phonon frequency considerably lower than ours, and thus a value of $\lambda_{//}$ one to two orders larger than ours, and also enhanced relaxation at low temperatures However, for such an umklapp process C is lower by an order-of-magnitude, since the electronic wavefunction is nearly free-electron like along the chain

Also, a few soft modes can possibly account for the enhanced relaxation at low temperatures (over the Bloch-Gruneisen curve), as for example the phason modes [22]

2.4.2 Absence of a Peierls transition

A long-standing mystery regarding this compound is the absence of a Peierls transition The resistivity indicates that $\lambda \approx 1$, and thus [21] $T_P \approx E_F \exp(-(1 + \lambda)/\lambda)$ should be around 1000 K For T_P to be lower than 2-3 K (where superconductivity sets in), λ must be smaller than 0 1 Also, inter-chain coupling can suppress the Peierls transition only if $\lambda_{//}$ is that small [28] The present calculation shows that indeed $\lambda_{//} < 0$ 1 The inter-chain electron-phonon coupling $\lambda_\perp$ does *not* produce a Peierls transition, since the inter-chain wavevectors are not nested

2.4.3 Superconductivity

The values of λ and $\Theta_{3D} \approx 70$ K are very similar to those of elemental mercury Therefore T_c could be close to that of elemental mercury ($T_c = 4$ 1 K). The Philadelphia group [9] indeed claims that this is the case Datars et al [10] claim that superconductivity is due to extruded mercury Schirber et al [29] showed that the *onset* of superconductivity under pressure is the same as for elemental mercury However, Moses et al [30] showed that the superconductivity

that occurs at T_c of elemental mercury under pressure gives rise to only a very small Meissner effect ($\approx$ 1%), while a big Meissner effect ($\approx$ 20%) occurs at lower temperatures - about 3 K at low pressures falling below 1 K above 10 kbar This strong pressure dependence does *not* follow elemental mercury However, it can here be accounted for by a stronger pressure dependence of the phonon frequency than in elemental mercury A stronger pressure dependence is indeed expected here, since the inter-chain Hg-Hg distance is larger than in elemental mercury

2.4.4 Mass enhancement

Another dilemma in this material concerns the absence of mass enhancement The dHvA data indicate [31] that the effective mass is essentially the band mass [11] The resistivity indicates that λ is large ($\lambda \approx 1$) which should cause a large mass enhancement - $m^* = m_{band}(1 + \lambda)$ The present work shows that because of the anisotropy of λ, only the transverse mass m_c^* is enhanced The mass measured in the dHvA experiment is the effective mass in the a-b plane, which is not enhanced, since λ is small

2.5 Conclusion

We have carried out an ab initio calculation of McMillan s λ for $Hg_{3-\delta}AsF_6$ We have found that λ is extremely anisotropic , in the a-b plane, λ is essentially zero, while in the c-direction $\lambda_\perp$ is of order unity This large value of $\lambda_\perp$ accounts for the large resistivity observed in the normal state The (practical) vanishing of $\lambda_{//}$ accounts for the absence of a Peierls transition in this linear chain system The value of λ calculated here is consistent with the strange superconductivity found in this material

Acknowledgements - The calculation of $t_\perp$ and its derivative was carried out by R A de Groot We benefitted from discussions with him and with J J M Butting and M Methfessel

2.6 References

[1] I O Brown, B D Cutforth, C G Davies, R J Gillespie, P R Freland and J E Verkis, Can J Chem **52**, 791 (1974)

[2] D P Chakraborty, R Spal, C K Chiang, A Denenstein, A J Heeger and A G MacDiarmid, Solid State Commun **27**, 849 (1978)

[3] F S Razavi, W R Datars, D Chartier and R J Gillespie, Phys Rev Lett **42**, 1181 (1979)

[4] A Janner and T Janssen, Acta Cryst A **36**, 399 (1980)

[5] J J M Buiting, thesis Catholic University of Nijmegen (1985)

[6] J M Hastings, J P Pouget, G Shirane, A J Heeger, N D Miro and A G MacDiarmid, Phys Rev Lett **39**, 1484 (1977)

[7] J P Pouget, G Shirane, J M Hastings, A J Heeger, N D Miro and A G MacDiarmid, Phys Rev B **18**, 3645 (1978)

[8] C K Chiang, R Spal, A Denenstein, A J Heeger, N D Miro and A G MacDiarmid, Solid State Commun **22**, 293 (1977)

[9] R Spal, C K Chiang, A Denenstein, A J Heeger, N D Miro and A G MacDiarmid, Phys Rev Lett **39**, 650 (1977)

[10] W R Datars, A van Schyndel, J S Lass, D Chartier and R J Gillespie, Phys Rev Lett **40**, 1184 (1978)

[11] J J M Buiting, M Weger and F M Mueller, Solid State Commun **46**, 857 (1983) R A de Groot, J J M Buiting, M Weger and F M Mueller, Phys Rev B **31**, 2881 (1985)

[12] J J M Buiting, M Weger and F M Mueller, J Phys F, **14**, 2343 (1984)

[13] W L McMillan, Phys Rev **167**, 331 (1968)

[14] G A Toombs, Physics Reports C **40**, 181 (1978)

[15] M J Rice and S Strassler, Lecture Notes in Physics **34**, Springer Verlag, Berlin (1974)

[16] V Heine and I V Abarenkov, Phil Mag **9**, 451 (1964) I V Abarenkov and V Heine, Phil Mag **12**, 529 (1965)

[17] J J M Buiting, M Weger and F M Mueller, J Phys F **15**, 1293 (1985)

[18] R A de Groot, private communication

[19] H Gutfreund, Physica **109**, 1866 (1982)

[20] A Birnboim and H Gutfreund, Phys Rev B **12**, 2682 (1975)

[21] D Moses, A Denenstein, A J Heeger, P J Nigrey and A G MacDiarmid, Phys Rev Lett **43**, 369 (1979) T Wei, A F Garito, C K Chiang and N D Miro Phys Rev B **16**, 3373 (1977)

[22] J D Axe and P Bak, Phys Rev B **26**, 4963 (1982) W Finger and T M Rice, Phys Rev B **28** 340 (1983)

[23] S Marianer, V Zevin, M Weger and D Moses, J Phys C, **15**, 3877 (1982)

[24] M Kaveh and E Ehrenfreund, Solid State Commun **31**, 709 (1979)
[25] O Entin-Wohlman, M Kaveh, H Gutfreund, M Weger and N F Mott, Phil Mag B **50**, 251 (1984)
[26] A P J van Deursen, J J M Buiting, M Weger and D Moses, J Phys F, **14**, L101 (1984)
[27] E Batalla and W R Datars, Can J Phys , **60**, 1348 (1982)
[28] B Horovitz, H Gutfreund and M Weger, Phys Rev B **12**, 3174 (1975)
[29] J E Schirber, A J Heeger and P J Nigrev, Phys Rev B **26**, 6291 (1982)
[30] D Moses, A Denenstein, M Weger, Phys Rev B **28**, 6325 (1983)
[31] E Batalla, F S Razavi and W R Datars, Phys Rev B **25**, 2109 (1982)

CHAPTER 3†

GROUND STATE AND NON-LINEAR EXCITATIONS OF TWO STRONGLY COUPLED SU-SCHRIEFFER-HEEGER CHAINS

J J M Slot and H J F Knops

Institute for Theoretical Physics University of Nijmegen, Toernooiveld, 6525 ED Nijmegen, The Netherlands

Abstract

A two-chain version of the original Su-Schrieffer-Heeger model with a strong inter-chain coupling is analysed for the case of a half filled band using a self-consistent iteration procedure and a continuum description in conjunction with bosonisation techniques The problem of the stability of the iteration procedure is addressed and it is shown that the iteration converges to the (local) minima of the total ground state energy The ground state of the present model is a trimerisation but also other homogeneous (metastable) phases are possible The solitons in the model are of phason, amplitudon and intermediary type, but other more complicated solitons are also observed

---

† Zeitschrift fur Physik B Condensed Matter 66 107 123 1987 Springer Verlag

3.1 Introduction

Since Su, Schrieffer and Heeger [1] introduced their soliton model to interpret various kinds of optical, electrical and magnetic phenomena in trans-polyacetylene $(CH)_x$ with a half-filled π band, a lot of interest has arisen in this relatively simple but rich model. Within the model that neglects any form of coupling between the $(CH)_x$-chains, the half-filled π band leads, via a Peierls instability [2], to a dimerised ground state. The low-lying excitations consist of charged ($\pm e$) and neutral solitons, with spin 0 and spin ½ respectively [3]. The same model but now with an one-third-filled band, exhibits a trimerised ground state and fractionally charged ($\pm\frac{1}{3}e, \pm\frac{2}{3}e$) solitons [4]. Because of the latter , many studies [5-8] were devoted to this case. Another direction into which the original SSH model can be extended is to include a coupling between chains. Baeriswyl and Maki [9] studied the effect of a weak inter-chain coupling in a two-chain version of the original SSH model. They assume that both chains are dimerised and show that due to the inter-chain coupling an out-of-phase ordering of the dimerisations on both chains is favoured. Furthermore they find a confinement of solitons due to the inter-chain coupling.

The object of this paper is to study the opposite limit of two strongly coupled chains where the inter-chain overlap equals the intra-chain overlap which, as we will see later, leads to a Peierls instability that induces (amongst others) a trimerisation for a half-filled band. The present model encompasses two novel features: 1) The fact that the trimerisation occurs for a half-filled band changes the boundary conditions used to create a soliton (like addition of an extra site or electron) in an essential way. 2) In addition to the trimerisation also other modes can and sometimes will interfere in the construction of solitons. We study the model numerically on finite chains using a method which iteratively solves the self-consistent equations, which determine the lattice configuration. This method has been extensively used in the single-chain case [6-8,10-13]. We show that the stable fixed points of the non-linear iteration correspond to the (local) minima of the total ground state energy and vice versa. A fact which is often taken for granted, but which is non-trivial seen in the light of some recent insights in the field of non-linear dynamics [14-16]. We further use a continuum description combined with bosonisation techniques which provides a qualitative understanding of some of the solitons observed in the numerical analysis of the model. In section 3.2 we analyse the ground state and other homogeneous phases of the system. We show that the ground state is a trimerised

homogeneous phase Section 3 3A is devoted to the analysis of the stability properties of the iteration procedure and in section 3 3B the numerical results are presented for the ground state and the other (metastable) homogeneous phases of the system The continuum description and the subsequent bosonisation is treated in section 3 4A, while the numerical results for the soliton excitations are given in section 3 4B

3.2 Ground state and other homogeneous phases of the model

Consider a system consisting of two chains of atoms (also called sites), with one valence orbital per atom and a nearly half-filled band In the model we include the coupling of the (valence) electrons to the longitudinal lattice modes of each chain These modes $\{u_n^{(j)}\}$, where $u_n^{(j)}$ is the displacement of the nth site along the direction of chain j (j=1,2), are the only lattice degrees of freedom in this model The chains are coupled though a non zero overlap between orbitals centered around equivalent sites on both chains and through an elastic energy term The Hamiltonian that describes this situation is a direct generalisation of the Su Schrieffer-Heeger (SSH) Hamiltonian [1] for a single chain

$$
\begin{aligned}
H = & - \sum_{ns} \sum_{j=1}^{2} \{[t_0 - \alpha(u_{n+1}^{(j)} - u_n^{(j)})](C_{n+1,s}^{(j)} C_{ns}^{(j)} + h.c.) \\
& - \mu\, C_{ns}^{(j)}\, C_{ns}^{(j)}\} - \eta \sum_{ns} (C_{ns}^{(1)}\, C_{ns}^{(2)} + h.c.) \qquad (1) \\
& + \frac{1}{2} K_1 \sum_{n} \sum_{j=1}^{2} (u_{n+1}^{(j)} - u_n^{(j)})^2 + \frac{1}{2} K_2 \sum_{n} (u_n^{(2)} - u_n^{(1)})^2 \\
& \qquad\qquad\qquad\qquad\qquad\qquad t_0, \alpha, \eta, K_1, K_2 > 0
\end{aligned}
$$

where $C_{ns}^{(j)}$ ($C_{ns}^{(j)}$) creates (annihilates) an electron with spin s on site n of chain j, μ is the chemical potential, $4t_0$ is the bandwidth and K_1, K_2 are bare lattice force constants We have left out the lattice kinetic energy (the $M \to \infty$ limit), because we only consider classical static deformations of the chains Finally we do not take into account any form of direct electron-electron interaction In this section we will restrict ourselves to an exactly half filled band

If there is no inter-chain coupling ($\eta = K_2 = 0$), the Hamiltonian (1) reduces to a sum of two independent Hamiltonians, each describing a chain with a half-filled band As was shown by Su, Schrieffer and Heeger [1] the ground state of each chain is then a dimerised homogeneous phase with a gap in the electronic spectrum at the Fermi energy which separates a filled valence band from an

empty conduction band. This is of course the well-known Peierls instability of one-dimensional metals [2]. If there is an inter-chain overlap ($\eta \neq 0$) the ground state of the system will be quite different, and may become incommensurate. As we mentioned in the introduction there are several interesting reasons to study the case of $\eta = t_0$, so let us start analysing the homogeneous phases allowed by (1) for this choice of η. We separate (1) into three parts

$$H = H_0 + H_1 + H_2$$

where

$$H_0 \equiv -t_0 \sum_{nj\sigma} (C^{(j)\dagger}_{n+1,\sigma} C^{(j)}_{n\sigma} + \text{h.c.}) - t_0 \sum_{n\sigma} (C^{(1)\dagger}_{n\sigma} C^{(2)}_{n\sigma} + \text{h.c.}) \qquad (2)$$

$$+ \mu \sum_{nj\sigma} C^{(j)\dagger}_{n\sigma} C^{(j)}_{n\sigma}$$

and

$$H_1 \equiv \alpha \sum_{nj\sigma} (u^{(j)}_{n+1} - u^{(j)}_n)(C^{(j)\dagger}_{n+1,\sigma} C^{(j)}_{n\sigma} + \text{h.c.}) \qquad (3)$$

and

$$H_2 \equiv \frac{1}{2} K_1 \sum_{nj} (u^{(j)}_{n+1} - u^{(j)}_n)^2 + \frac{1}{2} K_2 \sum_n (u^{(2)}_n - u^{(1)}_n)^2. \qquad (4)$$

We assume periodic boundary conditions with period N along both chains, i.e.

$$\begin{cases} u^{(j)}_{N+1} = u^{(j)}_1 \\ \\ C^{(j)}_{N+1} = C^{(j)}_1 \end{cases} \qquad (j=1,2).$$

The following transformation will diagonalise (2)

$$C^{(j)}_{n\sigma} = \frac{1}{\sqrt{2N}} \sum_k \exp[ikna] \{C^{(1)}_{k\sigma} + (-1)^{j+1} C^{(2)}_{k\sigma}\} \qquad (5)$$

where the sum runs over the discrete k-values consistent with the periodic boundary conditions within the first Brillouin zone $(-\pi/a, \pi/a]$. (Notice that the upper indices of the operators that create or annihilate a Fourier mode refer to a band number and no longer to a chain number). This results in

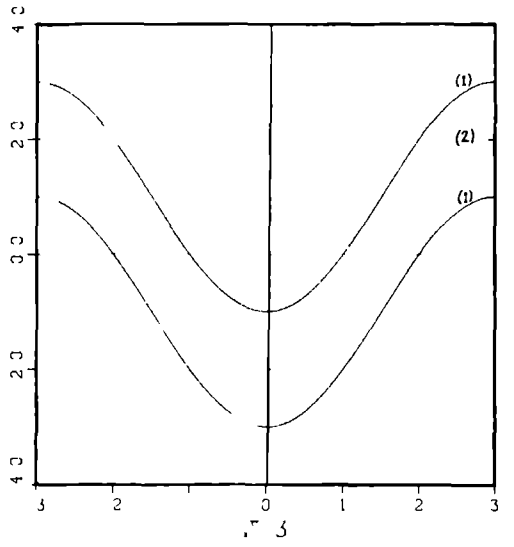

Figure 1 Bandstructure in the absence of an electron phonon coupling (α=0) (1) for two coupled chains (2) for a single chain

$$H_0 = \sum_{kjs} \varepsilon_k^{(j)} C_{ks}^{(j)\dagger} C_{ks}^{(j)} \tag{6}$$

where

$$\varepsilon_k^{(j)} - \mu = -t_0(2\cos ka + (-1)^{j+1}) \tag{7}$$

To simplify our notation we will shift our zero of energy to the Fermi energy μ, so that $\varepsilon_k^{(j)} - \mu \rightarrow \varepsilon_k^{(j)}$ As follows immediately from Fig 1(1) the 'Fermi surface" consists (in the absence of an electron-phonon coupling) of the following four points

$$k = \pm k_F^{(1)} = \pm \frac{2\pi}{3a} \quad , \quad k = \pm k_F^{(2)} = \pm \frac{\pi}{3a} \tag{8}$$

In order to deal with the electron phonon coupling it is convenient to switch to new chain variables Although there are 2N displacements $u_n^{(j)}$, only 2N-1 of them are independent as is clear from the Hamiltonian (1) Therefore, we choose $u_1^{(1)}=0$ Instead of taking the remaining u's as independent variables, we will use

$$\Delta_n^{(j)} \equiv u_{n+1}^{(j)} - u_n^{(j)} \qquad (n=1,\ldots,N;\ j=1,2)$$

and

$$\Omega \equiv u_1^{(2)} \tag{9}$$

These are not all independent, but because of the periodic boundary conditions we have $\sum_n \Delta_n^{(j)}=0$ (j=1,2). The u's are given in these variables by

$$\begin{cases} u_n^{(1)} = \sum_{m=1}^{n-1} \Delta_m^{(1)} \\ \\ u_n^{(2)} = \Omega + \sum_{m-1}^{n-1} \Delta_m^{(2)} \end{cases} \qquad (n=1,\ldots,N)\ . \tag{10}$$

The variable Ω describes the relative orientation of the second chain with respect to the first chain. The "electron-phonon" part H_1 (3) and the "phonon" part H_2 (4) now become

$$H_1 = \alpha \sum_{njs} \Delta_n^{(j)} (C_{n+1,s}^{(j)\dagger} C_{ns}^{(j)} + \text{h.c.}) \tag{11}$$

and

$$H_2 = \frac{1}{2} K_1 \sum_{nj} \{\Delta_n^{(j)}\}^2 + \frac{1}{2} K_2 \sum_n (\Omega + \sum_{m-1}^{n-1} [\Delta_m^{(2)} - \Delta_m^{(1)}])^2 . \tag{12}$$

This rigid shift Ω is a trivial degree of freedom and can easily be eliminated as it does not couple to the electronic degrees of freedom. Passing to Fourier-transformed variables

$$\Delta_n^{(j)} = \frac{1}{\sqrt{2N}} \sum_{q \neq 0} \exp[iqna] \{\Delta_q^{(1)} + (-1)^{j+1} \Delta_q^{(2)}\} \tag{13}$$

we get

$$H_2 = \frac{1}{2} \sum_{q \neq 0} \{K_1 \Delta_q^{(1)} \Delta^{(1)}_{\bar{q}} + [K_1 + \frac{K_2}{1-\cos qa}] \Delta_q^{(2)} \Delta^{(2)}_{\bar{q}}\} \tag{14}$$

and

$$H_1 = \alpha \sqrt{\frac{2}{N}} \sum_{ks} \sum_{q \neq 0} \exp[-\tfrac{1}{2} iqa] \cos[(k - \tfrac{1}{2}q)a] \{\Delta_q^{(1)} (C_{ks}^{(1)\dagger} C^{(1)}_{k-q,s} + C_{ks}^{(2)\dagger} C^{(2)}_{k-q,s})$$

$$+ \Delta_q^{(2)}(C_{k\sigma}^{(1)} C_{k-q\sigma}^{(2)} + C_{k\sigma}^{(2)} C_{k-q\sigma}^{(1)})\} \tag{15}$$

This latter part of the Hamiltonian will change the bandstructure as given by Fig 1(1)

If α is 'small' compared to the bandwidth only states in the immediate neighbourhood of the Fermi energy will be modified This is the so-called "weak coupling limit' It is in this limit that we will analyse our model In this limit only phonon modes which couple electron states close to the Fermi level have to be taken into account From Fig 1(1) it is clear that there are three relevant phonon modes One mode, which we will describe by an amplitude Δ_3 and a phase θ_3, is an in-phase trimerisation of both chains and leads to scattering of states belonging to the same band ($C^{(1)}$ $C^{(1)}$ and $C^{(2)}$ $C^{(2)}$) The other two modes, which we will describe by $\{\Delta_6,\theta_6\}$ and $\{\Delta_2,\theta_2\}$, lead to scattering of states between the two bands ($C^{(1)}$ $C^{(2)}$ and $C^{(2)}$ $C^{(1)}$) The mode $\{\Delta_6,\theta_6\}$ is an out-of phase hexamerisation of the chains, while $\{\Delta_2\ \theta_2\}$ is an out-of-phase dimerisation of the chains As the phase of a dimerisation mode can be absorbed into the sign of its amplitude, we shall choose $\theta_2=0$ The wave numbers of these three modes are

$$Q_3 = 2k_F^{(2)} = \frac{2\pi}{3a} = \quad 2k_F^{(1)}+G \tag{16a}$$

$$Q_6 = k_F^{(1)}-k_F^{(2)} = \frac{\pi}{3a} \tag{16b}$$

$$Q_2 = k_F^{(1)}+k_F^{(2)} = \frac{\pi}{a} \tag{16c}$$

From (15) it is clear that a direct scattering from $k_F^{(2)}$ to $k_F^{(1)}$ or from $-k_F^{(1)}$ to $-k_F^{(2)}$ or vice versa via the mode Δ_6 is not possible, simply because the "matrix elements" for these transitions are all zero Therefore, we will neglect this mode for the moment in our present analysis Apart from the relevant electron states near the Fermi level we must also take into account some states which are far away from the Fermi level These are the states that act as intermediary states in multiple scattering processes which connect the relevant states near the Fermi level In this case only states in the neighbourhood of $k=0$ of the first band and $k=\pi/a$ of the second band occur in this way So the electron states which enter into the description in the weak coupling limit are

$$\begin{cases} C^{(1)}_{ks\,1} \equiv C^{(1)}_{k+k_F^{(1)}\,s} \quad , \quad \tilde{C}^{(1)}_{ks\,2} \equiv C^{(1)}_{k-k_F^{(1)}\,s} \\ \tilde{C}^{(2)}_{ks\,1} \equiv C^{(2)}_{k+k_F^{(2)}\,s} \quad , \quad \tilde{C}^{(2)}_{ks\,2} \equiv C^{(2)}_{k-k_F^{(2)}\,s} \end{cases} \tag{17a}$$

and

$$\begin{cases} C^{(1)}_{ks\,3} = C^{(1)}_{ks} \\ C^{(2)}_{ks\,3} \equiv C^{(2)}_{k+\frac{\pi}{a}\,s} \end{cases} \tag{17b}$$

where $|k| \simeq 0$ In the weak coupling limit the dominant periodicities of the ground state and the low-lying excited states are determined by the Fermi points (8) The dispersion around these points, as in (17a), leads to slowly varying deviations of these dominant periodicities if we also would take into account dispersion around the phonon wave numbers (16a-c) These phenomena including solitons are in a natural way described by a continuum model, which we will discuss in section 3 4 In this section, however, we are concerned with the ground state and possible other homogeneous phases of the system In our description of the system we will take a linearised energy dispersion with a cut-off k_c around the Fermi points

$$\varepsilon^{(j)}_{k\pm k_F^{(j)}} \simeq \pm v_F k, \quad |k| \leq k_c \qquad (j=1,2) \tag{18}$$

where the Fermi velocity v_F is given by $\sqrt{3}t_0 a$ for both bands The intermediary states (17b) are far away from the Fermi level, therefore, we will neglect their dispersion in energy Because in our description we only have the phonon modes Δ_2 and Δ_3, the effective Hamiltonian in the Hilbert space of the electron states (17a-b) consists of a direct sum of 6×6 hermitean matrices labelled by k

The rows and columns of this matrix are labelled in the following way $(^1_1)\leftrightarrow1$, $(^2_1)\leftrightarrow2$, $(^2_2)\leftrightarrow3$, $(^1_2)\leftrightarrow4$, $(^1_3)\leftrightarrow5$ and $(^2_3)\leftrightarrow6$ (see (17a-b)) Its matrix elements can directly be obtained from (15) and are conveniently expressed in terms of the complex phonon amplitudes

$$v \equiv \alpha\sqrt{\frac{2}{N}}\Delta_3 \exp[i(\theta_3 - \frac{\pi}{3})] \tag{19a}$$

$$w \equiv -\frac{1}{2}i\alpha\sqrt{\frac{6}{N}}\Delta_2 \tag{19b}$$

In the matrix we will neglect all k-dependence except the linear k-dependence of the first four diagonal elements, because this k-dependence removes the

degeneracy at the Fermi level. So the matrix becomes

$$\begin{pmatrix} v_F k & 0 & w & -\bar{v} & \tfrac{1}{2}v & 0 \\ 0 & v_F k & v & w & 0 & -\tfrac{1}{2}\bar{v} \\ \bar{w} & \bar{v} & -v_F k & 0 & 0 & -\tfrac{1}{2}v \\ -v & \bar{w} & 0 & -v_F k & \tfrac{1}{2}\bar{v} & 0 \\ \tfrac{1}{2}\bar{v} & 0 & 0 & \tfrac{1}{2}v & -E & 0 \\ 0 & -\tfrac{1}{2}v & -\tfrac{1}{2}v & 0 & 0 & E \end{pmatrix} \equiv H_k \tag{20}$$

where $E=3t_0$. We will now use the fact that the intermediary states 5 and 6 are far away from the Fermi level, i.e. that E is large. States near the Fermi level have a very long life-time [17]. On such a time-scale the time-derivative of an intermediary state wave function averages to zero. This means that the Heisenberg equations of motion for the intermediary state operators become

$$[H_k, \tilde{C}^{(1)}_{ks,3}]_- = 0 \tag{21a}$$

and

$$[H_k, \tilde{C}^{(2)}_{ks,3}]_- = 0. \tag{21b}$$

Our effective Hamiltonian H_k (20) can be written as

$$H_k = -E(\tilde{C}^{(1)\dagger}_{ks,3} C^{(1)}_{ks,3} - \tilde{C}^{(2)\dagger}_{ks,3} \tilde{C}^{(2)}_{ks,3}) + \sum_{i,j=1}^{2} \sum_{m,n=1}^{2} A_{ij,mn} \tilde{C}^{(i)\dagger}_{ks,j} \tilde{C}^{(m)}_{ks,n}$$

$$+ \sum_{i,j=1}^{2} \sum_{m-1}^{2} \{B_{ij,m3} \tilde{C}^{(i)\dagger}_{ks,j} \tilde{C}^{(m)}_{ks,3} + \bar{B}_{ij,m3} \tilde{C}^{(m)\dagger}_{ks,3} \tilde{C}^{(i)}_{ks,j}\} \tag{22}$$

where the explicit form of A and B is clear from (20). The Heisenberg equations of motion (21a-b) now become

$$-E\, \tilde{C}^{(1)}_{ks,3} + \sum_{i,j=1}^{2} \bar{B}_{ij\,13}\, \tilde{C}^{(i)}_{ks,j} = 0 \tag{23a}$$

and

$$E\, \tilde{C}^{(2)}_{ks,3} + \sum_{i,j=1}^{2} \bar{B}_{ij,23}\, \tilde{C}^{(i)}_{ks,j} = 0. \tag{23b}$$

By eliminating the intermediary states, using (23a-b), in (22) we get

$$H_k = \sum_{i\,n=1}^{2}\sum_{m\,n=1}^{2}\{A_{ij\,mn} + \frac{1}{E}[B_{ij\,13}\bar{B}_{mn\,13} - B_{ij\,23}\bar{B}_{mn\,23}]\}\bar{C}^{(i)}_{ks\,j}C^{(m)}_{ks\,n}$$

$$\equiv \sum_{i\,n=1}^{2}\sum_{m\,n=1}^{2}\tilde{H}_{ij\,mn}\bar{C}^{(i)}_{ks\,j}\bar{C}^{(m)}_{ks\,n} \tag{24}$$

where

$$\tilde{H} = \begin{bmatrix} v_F k + \frac{|v|^2}{4E} & 0 & w & -\bar{v}+\frac{v^2}{4E} \\ 0 & v_F k - \frac{|v|^2}{4E} & v - \frac{v^2}{4E} & w \\ -w & \bar{v} - \frac{v^2}{4E} & -v_F k & \frac{|v|^2}{4E} \\ -v + \frac{\bar{v}^2}{4E} & -w & 0 & -v_F k + \frac{|v|^2}{4E} \end{bmatrix} \tag{25}$$

Let us first take $E=\infty$, when $\tilde{H}$ can easily be diagonalised The eigenvalues in the original variables (see (19)) are given by

$$\lambda_{1\,4}(k) = \mp\sqrt{v_F^2k^2+\frac{2\alpha^2}{N}(\Delta_1+\frac{1}{2}\sqrt{3}\Delta_2)^2} \tag{26a}$$

$$\lambda_{2\,3}(k) = \mp\sqrt{v_F^2k^2+\frac{2\alpha^2}{N}(\Delta_1-\frac{1}{2}\sqrt{3}\Delta_2)^2} \tag{26b}$$

By using (14) and (26) the ground state energy of the system becomes

$$\varepsilon = 2\sum_{k\,\leq k_c}\{\lambda_1(k)+\lambda_2(k)\} + \frac{1}{2}K_1\Delta_1^2 + \frac{1}{2}[K_1+\frac{1}{2}K_2]\Delta_2^2 \tag{27}$$

Passing from the sum to an integral and scaling Δ_2 and Δ_1 by $\alpha\sqrt{2/N}$ we end up with the following expression for the ground state energy per site

$$\frac{\varepsilon}{2N} = -\frac{1}{\pi v_F}\int_0^{v_F k_c}\left\{\sqrt{x^2+(\tilde{\Delta}_1+\frac{1}{2}\sqrt{3}\tilde{\Delta}_2)^2} + \sqrt{x^2+(\tilde{\Delta}_1-\frac{1}{2}\sqrt{3}\tilde{\Delta}_2)^2}\right\}dx$$

$$+\frac{K_1}{8\alpha^2}\tilde{\Delta}_1^2 + \frac{1}{8\alpha^2}[K_1+\frac{1}{2}K_2]\Delta_2^2 \tag{28}$$

The integral can easily be evaluated, leading to

$$\frac{1}{2\pi v_F}\{U^2\ell n|U|+V^2\ell n\ V_\perp\}+D_0+\frac{1}{2}D_1\{U^2+V^2\}+O(U^4,V^4) \qquad (29)$$

where we define

$$U=\tilde{\Delta}_1+\frac{i}{2}\sqrt{3}\tilde{\Delta}_2 \qquad (30a)$$

$$V=\tilde{\Delta}_1-\frac{1}{2}\sqrt{3}\tilde{\Delta}_2 \qquad (30b)$$

The cut-off dependent constant D_0 merely shifts our zero of energy and can therefore be neglected D_1 is also cut-off dependent but his term can be absorbed into the elastic contribution by a redefinition of the force constants Therefore the equations which determine the minima are of following form

$$U\ \ell n|U|+\beta U-\gamma U=0 \qquad (31a)$$

$$V\ \ell n|V|+\beta V-\gamma V=0 \qquad (31b)$$

where $\beta=\frac{\pi v_F}{48\alpha^2}(7K_1+2K_2)+\pi v_F D_1+\frac{1}{2}$ and $\gamma=\frac{\pi v_F}{48\alpha^2}(K_1+2K_2)$ Now γ is large (weak coupling limit), therefore the only solutions of (31a-b) are

$$1)\qquad -U=V=\pm V_0=\pm\exp[-(\beta+\gamma)] \qquad (32a)$$

$$2)\qquad U=V=\pm U_0=\pm\exp[-(\beta-\gamma)] \qquad (32b)$$

Using (30a-b) we see that the solutions of 1) correspond to dimerisations and those of 2) to trimerisations Because the phase of a dimerisation can be absorbed into the sign of its amplitude, the dimerisations form a degenerate pair The phase of the trimerisations is at this level not yet determined, this will be fixed in higher order Both trimerisations have the same energy, but the symmetry operation that shifts the phase by $\pm 2\pi/3$ does not connect them Their degeneracy is accidental If we calculate the lowest order corrections for finite E, using ordinary perturbation theory, to the eigenvalues (26a-b) at k=0, we get

$$\lambda_{1,4}(0)=\mp[\tilde{\Delta}_1+\frac{1}{2}\sqrt{3}\tilde{\Delta}_2+\frac{1}{4E}\tilde{\Delta}_1^2\cos(3\theta_1)]+O(\frac{1}{E^2}) \qquad (33a)$$

$$\lambda_{2,3}(0)=\mp[\tilde{\Delta}_1-\frac{1}{2}\sqrt{3}\tilde{\Delta}_2+\frac{1}{4E}\tilde{\Delta}_1^2\cos(3\theta_1)]+O(\frac{1}{E^2}) \qquad (33b)$$

Now if $\tilde{\Delta}_1=U_0$ and $\tilde{\Delta}_2=0$ then the sum of the lowest two eigenvalues at k=0 is $\lambda_1(0)+\lambda_2(0)=-2U_0-1/2E\ U_0^2\cos(3\theta_1)+O(1/E^2)$ On the other hand when $\tilde{\Delta}_1=-U_0$ and $\tilde{\Delta}_2=0$ the same sum equals $\lambda_3(0)+\lambda_4(0)-$

$-2U_0+1/2E\ U_0^2\cos(3\theta_1)+O(1/E^2)$ Because the eigenvalues depend continuously on k, the trimerisation with amplitude U_0 will have a lower energy then the trimerisation with amplitude $-U_0$ By using some simple algebra it is not hard to see that the dimerisation has a higher energy than the trimerisations, which means that the trimerisation with the positive amplitude is the ground state of the model

3.3 Numerical analysis for finite chains

This section is mainly devoted to a discussion of a method for performing an, in principle, exact calculation of the lattice ground state of a finite system described by the Hamiltonian (1) At the end of this section some results will be presented for the ground state and other (metastable) homogeneous phases of the system, which corroborate the analytical results of the previous section

A. Self-consistent method and stability analysis

Since Su, Schrieffer and Heeger introduced their discrete model to describe poly-acetylene [1], i e the one-chain version of (1) much work has been devoted to performing calculations on finite chains especially to determine the lattice ground state, the low-lying excitations and the phonon modes around these configurations [3,4,6-8,10-13] Su and Schrieffer [3 4] use an equation of motion method while others [6 8,10-13] use the self-consistent method The results of both approaches are in agreement with one another Although many groups use the self-consistent method the stability of this method has been taken for granted However, in general it is certainly not always the case that the fixed points which are attractive for an iterative solution of self-consistent equations correspond to (local) minima of the energy [14 16] For this reason we find it worthwhile to settle this point in the present case We will now describe this method for the two-chain model

First we bring the Hamiltonian (1) in a more convenient form by applying the following scale transformations,

$$u_n^{(j)} \rightarrow \frac{t_0}{\alpha}\, u_n^{(j)} \tag{34a}$$

$$K_j \rightarrow \frac{\alpha^2}{t_0}\, K_j \tag{34b}$$

$$H \rightarrow t_0 H \tag{34c}$$

to (1) with $\eta = t_0$ and $\mu = 0$ This results in

$$H = -\sum_{njs}[1-(u_{n+1}^{(j)}-u_n^{(j)})](C_{n+1,s}^{(j)}C_{ns}^{(j)}+h\,c\,) - \sum_{ns}(C_{ns}^{(1)}\,C_{ns}^{(2)}+h\,c\,)$$

$$+\frac{1}{2}K_1\sum_{nj}(u_{n+1}^{(j)}-u_n^{(j)})^2 + \frac{1}{2}K_2\sum_{n}(u_n^{(2)}-u_n^{(1)})^2 \equiv H_e+\varepsilon_{el\,is} \tag{35}$$

We will always take periodic boundary conditions over the length N of the chains For a given lattice configuration $\{u_1^{(1)}=0,u_2^{(1)},\ \ u_N^{(1)},u_1^{(2)},\ \ ,u_N^{(2)}\}$, the $2N\times 2N$ matrix H_e can be diagonalised numerically Let S_{nj}^{mj} be the orthogonal matrix whose columns are the eigenvectors of H_e When there are N_e^+ electrons present in the system with spin-up, the electronic ground state $|\Phi_+>$ for the up-spin electrons is formed by the set $mj'\epsilon M(+)$ of the N_e^+ lowest eigenvectors Similarly we define $M(-)$ as the set of the lowest eigenvectors corresponding to N_e^- down-spin electrons The total ground state energy for a given set $\{u_n^{(j)}\}$ then becomes

$$\varepsilon = <\Phi_+|H_e(+)|\Phi_+> + <\Phi\ |H_e(-)|\Phi_->$$

$$+\frac{1}{2}K_1\sum_{nj}(u_{n+1}^{(j)}-u_n^{(j)})^2 + \frac{1}{2}K_2\sum_{n}(u_n^{(2)}-u_n^{(1)})^2 \tag{36}$$

To find the lattice ground state we have to minimise ε with respect to the $2N-1$ lattice degrees of freedom $\{u_2^{(1)},\ \ ,u_N^{(1)},u_1^{(2)},\ \ ,u_N^{(2)}\}$ It is clear that the electronic ground state $|\Phi>\equiv|\Phi_+>\otimes|\Phi\ >$ depends implicitly on these lattice degrees of freedom However, the Hellmann-Feynman theorem [18,19] states that

$$\frac{\partial}{\partial u_n^{(j)}}<\Phi|H_e|\Phi> - <\Phi|\frac{\partial H_e}{\partial u_n^{(j)}}|\Phi> \tag{37}$$

The remaining terms $<\frac{\partial\Phi}{\partial u_n^{(j)}}|H_e|\Phi> + <\Phi|H_e|\frac{\partial\Phi}{\partial u_n^{(j)}}>$ are equal to $\varepsilon_e\frac{\partial}{\partial u_n^{(j)}}<\Phi|\Phi>$, which is zero by normalisation The self-consistent method is an iterative method to solve the following set of equations

$$\frac{\partial\epsilon}{\partial u_n^{(j)}} = 0 \qquad \text{and} \qquad \begin{matrix} n=2\ \ ,N \quad \text{for} \quad j=1 \\ n=1,\ \ ,N \quad \text{for} \quad j=2 \end{matrix} \tag{38}$$

By using (35-37) this set of equations becomes

$$K_1(2u_n^{(1)}-u_{n-1}^{(1)}-u_{n+1}^{(1)}) + K_2(u_n^{(1)}-u_n^{(2)}) = 2\sum_s \sum_{(mj)\in M(s)} S_{nj}^{mj}(S_{n+1\,1}^{mj}-S_{n-1\,1}^{mj})$$

$$n=2, \quad ,N$$

and

$$K_1(2u_n^{(2)}-u_{n-1}^{(2)}-u_{n+1}^{(2)}) + K_2(u_n^{(2)}-u_n^{(1)}) = 2\sum_s \sum_{(mj)\in M(s)} S_{nj}^{mj}(S_{n+1\,2}^{mj}-S_{n-1\,2}^{mj})$$

$$n=1, \quad ,N \qquad (39)$$

which can formally be written as $\mathbf{L}\,\mathbf{u} = \mathbf{w}(\mathbf{u})$ where $\mathbf{u}=(u_2^{(1)}, \quad ,u_N^{(1)},u_1^{(2)}, \quad ,u_{N-1}^{(2)})^T$ The $(2N-1)\times(2N-1)$-matrix $\mathbf{L}$ can be inverted, at least numerically, to give $\mathbf{L}^{-1}$ We can therefore write (39) as

$$\mathbf{u} = \mathbf{L}^{-1}\,\mathbf{w}(\mathbf{u}) \qquad (40)$$

This last equation leads in a natural way to the following transformation

$$\mathbf{u}' = \mathbf{L}^{-1}\,\mathbf{w}(\mathbf{u}) \qquad (41)$$

which defines the iteration So the procedure we have to follow is start with some configuration $\mathbf{u}$, diagonalise H_e (35), calculate $\mathbf{w}$ (39) using the eigenvectors obtained in the diagonalisation, and determine via (41) the new configuration $\mathbf{u}'$ We then repeat this procedure until convergence is reached After each loop we compare the new configuration $\mathbf{u}'$ with the old one $\mathbf{u}$ by calculating

$$\gamma = \frac{\sum_n (u_n-u_n)^2}{\sum_n (u_n)^2} \qquad (42)$$

The convergence criterion we use is that this parameter γ must be equal or less than some prescribed number In the actual calculations this number is 10^{-12} The matrix $\mathbf{L}$ only has to be inverted once, because it only depends on K_1 and K_2 and does not change during the iteration process

We now want to address the stability of the non-linear transformation (41) We want to show that whenever the iteration process converges to some fixed point, that this fixed point corresponds to a (local) minimum of the total ground state energy and vice versa To see this let us expand the total ground state energy ε (36) around such a fixed point $\mathbf{u}$ Locally the electronic ground state energy will look like

$$\varepsilon_e = \varepsilon_e^{(0)} + \sum_{nj}{}' A_{nj}\delta_n^{(j)} + \frac{1}{2}\sum_{njn'j'} B_{nj\,n'j'}\delta_n^{(j)}\delta_{n'}^{(j')} + O(3) \tag{43}$$

where $\delta_n^{(j)} \equiv u_n^{(j)} - u_n^{(j)}$ and the prime means that we have to omit $n=j=1$ in the summations The total ground state energy ε (36) now becomes

$$\varepsilon = \varepsilon_e^{(0)} + \varepsilon_{elas}^{(0)} + \frac{1}{2}\boldsymbol{\delta}\,(\mathbf{L}+\mathbf{B})\,\boldsymbol{\delta} + O(3) \tag{44}$$

where terms linear in $\boldsymbol{\delta}$ drop out because $\mathbf{u}$ is a fixed point The "self consistent" equations (38) now lead to

$$\boldsymbol{\delta}' = -(\mathbf{L}^{-1}\,\mathbf{B})\,\boldsymbol{\delta} \qquad \text{(compare with (41))} \tag{45}$$

Suppose now that $\tilde{\mathbf{u}}$ is a (local) minimum of the total ground state energy ε, or stated differently that $\mathbf{L}+\mathbf{B}$ is a positive definite matrix (i e is symmetric and possesses positive eigenvalues)

$$\mathbf{L}+\mathbf{B} > 0 \tag{46}$$

Now $\mathbf{L}$ is also positive definite, but because $\mathbf{B}$ in general does not commute with $\mathbf{L}$, one can only conclude that the matrix

$$\mathbf{L}^{-1}\,(\mathbf{L}+\mathbf{B}) = 1+\mathbf{L}^{-1}\,\mathbf{B} \tag{47}$$

has positive eigenvalues [20] This matrix is not positive definite in general because it is not symmetric in general Thus the eigenvalues of $-\mathbf{L}^{-1}\,\mathbf{B}$ are smaller than 1 In order for $\tilde{\mathbf{u}}$ to be a stable fixed point of (41), we not only need (in view of (45)) the eigenvalues of $-\mathbf{L}^{-1}\,\mathbf{B}$ to be bounded above by 1 but also to be bounded below by -1 This last inequality is guaranteed by the fact that $\mathbf{B}$ is a negative definite matrix, a result which follows from the convexity of the electronic ground state energy This we will now show The electronic part of the Hamiltonian H_e (35) can formally be written as

$$H_e(\mathbf{u}) = H_e^{(0)} + \mathbf{u}\,\mathbf{H}_e^{(1)} \tag{48}$$

As before let us expand around the (local) minimum of the total ground state energy $\mathbf{u}$, but now using a scale factor λ which varies between 0 and 1

$$\mathbf{u} = \tilde{\mathbf{u}} + \lambda\boldsymbol{\delta} \tag{49}$$

So we fix $\boldsymbol{\delta}$ and vary λ (48) now becomes

$$H_e(\lambda) \equiv H_e(\bar{u}+\lambda\delta) = H_e(\bar{u})+\lambda\delta.H_e^{(1)} \equiv H_e(0)+\lambda \frac{dH_e}{d\lambda}(0). \tag{50}$$

Let us denote the normalised ground state of (50) by $|\Phi(\lambda)>$. Using the variational principle of quantum mechanics we get

$$\varepsilon_e(\lambda) \equiv <\Phi(\lambda)|H_e(\lambda)|\Phi(\lambda)> \leq <\Phi(0)|H_e(\lambda)|\Phi(0)>$$

or

$$\varepsilon_e(\lambda) \leq <\Phi(0)|H_e(0)+\lambda \frac{dH_e}{d\lambda}(0)|\Phi(0)>. \tag{51}$$

Thus using the Hellmann-Feynman theorem (see (37)) this leads to

$$\varepsilon_e(\lambda) \leq \varepsilon_e(0)+\lambda \frac{d\varepsilon_e}{d\lambda}(0). \tag{52}$$

Upon expanding $\varepsilon_e(\lambda)$ around $\lambda=0$ we have

$$\varepsilon_e(\lambda) = \varepsilon_e(0)+\lambda \frac{d\varepsilon_e}{d\lambda}(0)+\frac{1}{2}\lambda^2 \frac{d^2\varepsilon_e}{d\lambda^2}(0) + O(\lambda^3). \tag{53}$$

By combining (52) and (53) we get the following result

$$\frac{d^2\varepsilon_e}{d\lambda^2}(0) \leq 0 \tag{54}$$

which expresses the convexity of the electronic ground state energy, a very general property. In the case of (49), ε_e (43) becomes

$$\varepsilon_e(\lambda) = \varepsilon_e^{(0)}+\lambda\mathbf{A}.\boldsymbol{\delta} + \frac{1}{2}\lambda^2\boldsymbol{\delta}.\mathbf{B}.\boldsymbol{\delta} + O(\lambda^3). \tag{55}$$

Thus (54) implies, using (55)

$$\boldsymbol{\delta}.\mathbf{B}.\boldsymbol{\delta} \leq 0 \qquad \text{for an arbitrary } \boldsymbol{\delta}. \tag{56}$$

Because $\mathbf{B}$ can be chosen to be symmetric, we have that $\mathbf{B}$ is a negative definite matrix. From this fact we can deduce using a similar reasoning as before that the eigenvalues of $-\mathbf{L}^{-1}.\mathbf{B}$ are all greater than zero. So we are led to the conclusion that the (local) minima of the total ground state energy ε (36) are also the stable fixed points of the non-linear transformation (41). Conversely one can argue in a similar way that the stable fixed points of the iteration procedure correspond to (local) minima of the total ground state energy.

We end this part with the following observation There is some freedom in defining a transformation with the above mentioned properties in order to solve

$$\mathbf{L}\,\mathbf{u} = \mathbf{w}(\mathbf{u}) \tag{39}$$

That is to say our choice $\mathbf{u}' = \mathbf{L}^{-1}\,\mathbf{w}(\mathbf{u})$ (41) is not the only possibility For instance Ono, Ohfuti and Terai [7] and Ohfuti and Ono [8] use a different transformation in the one-chain case They use the fact that $\mathbf{L}$ has a constant diagonal part K so that (39) can be written as

$$\mathrm{K}\mathbf{u} = \mathbf{w}(\mathbf{u}) - \mathbf{L}^{\mathrm{nd}}\,\mathbf{u} \tag{39a}$$

where $\mathbf{L}^{\mathrm{nd}}$ is the remaining non-diagonal part of $\mathbf{L}$ Their transformation is then given by

$$\mathbf{u}' = \frac{1}{\mathrm{K}}[\mathbf{w}(\mathbf{u}) \quad \mathbf{L}^{\mathrm{nd}}\,\mathbf{u}] \tag{41a}$$

It is easy to prove, using similar arguments as in the case of (41), that this transformation has the desired stability properties The linearised transformations corresponding to (41) and (41a) around some fixed point $\hat{\mathbf{u}}$ are given by

$$\boldsymbol{\delta}' = -(\mathbf{L}^{-1}\,\mathbf{B})\,\boldsymbol{\delta} \tag{45}$$

and

$$\boldsymbol{\delta}' = \frac{1}{\mathrm{K}}\,(\mathbf{B}-\mathbf{L}^{\mathrm{nd}})\,\boldsymbol{\delta} \tag{45a}$$

Although it is hard to prove, because in general $\mathbf{L}$ and $\mathbf{B}$ do not commute, it is intuitively clear that in the weak coupling limit where $\mathbf{L}$ is large compared to $\mathbf{B}$, the majority of eigenvalues of (45) will be close to zero, while for (45a) this majority will be close to one So one would expect a better convergence in using (41) instead of (41a) Ono, Ohfuti and Terai [7] notice that in choosing as a convergence criterion $\gamma \leq 10^{-6}$ the convergence becomes very slow In our calculations we observed a very fast convergence up to $\gamma - 10^{-12}$ So although our transformation is not the only possible one it appears to be superior from the point of view of convergence

B. Results for the ground state and other (metastable) homogeneous phases

In the previous section we found that in the weak coupling limit the ground state of the system is an in-phase trimerisation of both chains, a triply degenerate homogeneous phase We further found two other homogeneous phases One of them is also an in-phase trimerisation The other one in an out-of-phase dimerisation of both chains a doubly degenerate homogeneous phase In doing calculations on finite versions of the two-chain model the chain length plays an important role In order to find the homogeneous phases of the system we have to avoid topologically constraining the system via the periodic boundary conditions, to exhibit a kink Since we expect to find either a trimerised or a dimerised phase it is necessary to choose the chain length a multiple of six In the next section we will modify this length in order to observe domain walls The chain length we take is 66 This means that in the half-filled band case, which is the one we have here, the system contains 132 electrons The bare lattice force constants we take are $K_1=1,75$ and $K_2=2$ With these values we are still in the weak coupling regime The chain length is large enough to display the domain walls (solitons), i e the width of a typical soliton is considerably smaller than the chain length (see the next section) The specific choice of all these parameters is, however, arbitrary In order to find each of the homogeneous phases and their degenerate partners we have to take different initial configurations for the self-consistent iteration procedure The number of iterations needed to obtain convergence varies between 5 and 250 The results for the homogeneous phases can be summarised as follows There are two phases corresponding to a trimerisation One is given in terms of the difference variables $\Delta_n^{(j)}\equiv u_{n+1}^{(j)}-u_n^{(j)}$ by $\Delta_n^{(1)}=\Delta_n^{(2)}=\Delta\cos(2\pi n/3+\theta)$ with $\Delta\sim 0\,2750$ and $\theta=0,2\pi/3,4\pi/3$ for the three degenerate phases Its energy (relative to $\varepsilon(\Delta=0)$) equals $\varepsilon\sim\ 0\,976131$ The other trimerised phase has an amplitude with a negative sign $\Delta\simeq-0\,2510$ and a larger energy $\varepsilon\simeq-0\,840571$ in accordance with our findings in the previous section Furthermore we observed a dimerised phase with $\Delta_n^{(1)}=-\Delta_n^{(2)}=\Delta\cos(\pi n+\theta)$ with $\Delta\simeq 0\,1459$ and $\theta=0,\pi$ The energy of this phase is $\varepsilon\simeq-0\,867397$ For the ground state the energy per unit cell (2×3 sites) is given by $\varepsilon=-0\,976131/22=-0\,044370$ In appendix A the exact trimerised ground state energy per unit cell is calculated for the infinite system The result is $-0\,039614$, which is somewhat higher The amplitude is 0 2750, which is also the value we found for the finite system By using Poisson summation one can deduce that the leading finite-size corrections to the ground state energy per unit cell will go as $1/N^2$ for large N, which is also what we find in our calculations as is clearly shown in Fig 2

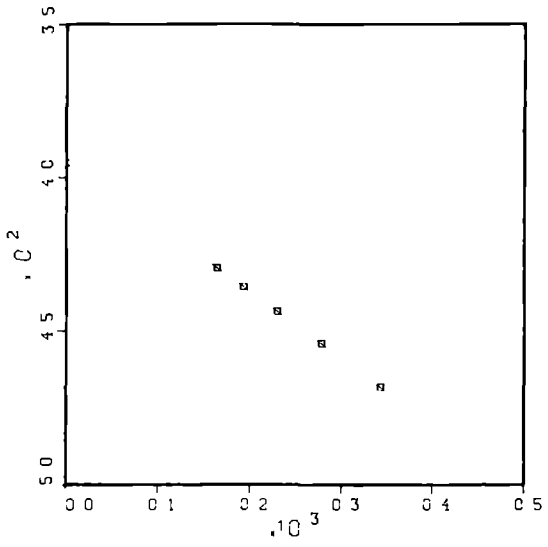

Figure 2 Ground state energy per unit cell versus 1/N. The squares correspond to systems with chain length N = 54, 60, 66, 72 and 78. The dashed line gives the energy for N→∞.

3.4 Soliton excitations

In section 3.3 we introduced the weak coupling limit and argued that in this limit only electron states near the Fermi level determine "the physics" of the system and only those phonon modes which couple these relevant electron states have to be taken into account. Furthermore we mentioned that the slowly varying deviations of the dominant periodicities present in the system are due to dispersion of the electron states (17a) around the Fermi points (8), which are coupled through phonon modes dispersed around the dominant wave numbers Q_1, Q_2 and Q_3 (16a-c). Slowly varying meaning here varying slowly on the scale of the intra-chain lattice constant a. These slowly varying deviations correspond to the low-lying excitations of the system and are in a natural way described by a continuum model. In the case of trans-polyacetylene with a half filled band, these low-lying excitations are charged ($\pm e$) and neutral kinks with spin 0 and spin ½ respectively. These solitons were found in a numerical analysis by Su and Schrieffer [3]. Takayama, Lin-Liu and Maki were the first to analyse the SSH model in the continuum limit [21]. They found that the neutral kink,

proposed by Su and Schrieffer [3], is an exact solution of the equations which determine the displacement pattern in their continuum model Somewhat later Horovitz [22] established a similar result for the charged kinks within this continuum model Since then on a great number of articles appeared (and still appears) in the literature on such a continuum approach to various (quasi-) one-dimensional systems with soliton excitations Of direct interest to our case is the work by Tinka Gammel and Krumhansl [23] and Horovitz and Krumhansl [24], which both study continuum models for a one-dimensional system with an arbitrary rational band filling

The way to analyse numerically the nature of the possible low-lying excitations of the model is to change the chain length and/or the number of electrons in the system and observe what kind of self-consistent lattice configuration is generated Although many properties of the system can be studied on the basis of a continuum model description, we will use such a description here solely to get a qualitative insight in what may be expected to happen if one changes the length of the chains and/or the number of electrons in the system For this purpose it is convenient to bosonise the continuum Hamiltonian A technique which was introduced for the one-chain SSH model by Hara and Fukuyama [25] and which is based on the bosonisation method devised by Tomonaga [26] and by Luther et al [27,28] for the one-dimensional interacting electron gas In part A of this section we will first derive a continuum version of the discrete Hamiltonian (35) and then bosonise the resulting continuum Hamiltonian In part B we will analyse the effects of the above mentioned changes on the system and compare this with numerical results

A. Continuum model description and bosonisation

Because the ground state of the system consists of an in-phase trimerisation of both chains, one expects that the low-lying excitations will consist of domain walls (kinks) between degenerate ground state phases As we saw in section 3 2 the system also exhibits other (metastable) homogeneous phases, such as an out-of-phase dimerisation It is therefore conceivable that other, more complicated, low-lying excitations are possible in the system For instance excitations which involve degenerate phases of both the in-phase trimerisation and the out-of-phase dimerisation Because the theoretical analysis of such excitations is far from trivial, we will postpone this to a subsequent article However, in part B of this section we will show some numerical examples of such complex non-linear excitations So here we only take into account slowly varying deviations of the in-phase trimerised ground state As we will see later this already leads to an understanding of some of the kinks that we find numerically

In the continuum limit we only take into account the electron states (17a b) as argued in section 3 2 It is customary to write the Hamiltonian in terms of the real space operators corresponding to the annihilation operators of (17a b) as

$$\psi_{\ell s}^{(j)}(x) \equiv \frac{1}{\sqrt{Na}} \sum_{k<k_c} e^{ikx} \tilde{C}_{ks\ell}^{(j)} \qquad \text{where } x=na \tag{57}$$

In terms of these fields the electronic part of the Hamiltonian H_0 becomes in the continuum limit

$$H_0 = \sum_s \int dx\{-iv_F \sum_{j=1}^{2} [\psi_{1s}^{\{j\}}(x)\frac{d}{dx}\psi_{1s}^{\{j\}}(x) - \psi_{2s}^{\{j\}}(x)\frac{d}{dx}\psi_{2s}^{\{j\}}(x)]$$

$$3[\psi_{4s}^{\{1\}}(x)\psi_{4s}^{\{1\}}(x) - \psi_{3s}^{\{2\}}(x)\psi_{3s}^{\{2\}}(x)]\} \tag{58}$$

The appearance of a derivative in this expression is a result of the linearisation of $\varepsilon_k^{(j)}$ around the Fermi points (see (18)) The intermediary fields $\psi_{3s}^{\{1\}}(x)$ and $\psi_{3s}^{\{2\}}(x)$ belong to states far away from the Fermi level for which the dispersion in energy can be neglected In the continuum limit we further write

$$\Delta_n^{(1)} = \Delta_n^{(2)} \equiv \Delta_n = \Delta(x)\cos(2k_F^{\{2\}}na+\theta(x)) \tag{59}$$

where $\Delta(x)$ and $\theta(x)$ are slowly varying fields, just as the $\psi_{\ell s}^{(j)}(x)$ in (57) So at this point we restrict the analysis, as explained above, to excitations brought about by the interaction with the trimerised mode only The elastic energy then becomes

$$H_{ph} = \frac{1}{2}K_1 \int dx\ \Delta^2(x) \qquad \text{with } K_1 = \frac{K_1}{2a} \tag{60}$$

Finally, the electron-phonon part of the Hamiltonian (35) becomes after some algebra in the continuum limit

$$H_{e-ph} = \sum_s \int dx\ \Delta(x)\{\exp[i(\theta(x)-\frac{\pi}{3})]\ [2(\psi_{1s}^{\{2\}}(x)\psi_{2s}^{\{2\}}(x)-\psi_{2s}^{\{1\}}(x)\psi_{1s}^{\{1\}}(x))$$

$$+ \psi_{1s}^{\{1\}}(x)\psi_{3s}^{\{1\}}(x)+\psi_{3s}^{\{1\}}(x)\psi_{2s}^{\{1\}}(x)-\psi_{2s}^{\{2\}*}(x)\psi_{4s}^{\{2\}}(x)$$

$$- \psi_{4s}^{\{2\}}(x)\psi_{1s}^{\{2\}}(x)] + h.c.\} \tag{61}$$

Just as we did in section 3 2, we eliminate the intermediary fields $\psi_{3s}^{\{1\}}(x)$ and

$\psi^{(2)}_{3s}(x)$ in (58) and (61) by using the Heisenberg equations of motion for these fields

$$-3\psi^{(1)}_{3s}(x) = -[\exp[i(\theta(x)-\frac{\pi}{3})]\ \Delta(x)\psi^{(1)}_{2s}(x)+\exp[-i(\theta(x)-\frac{\pi}{3})]\ \Delta(x)\psi^{(1)}_{1s}(x)]$$

$$-3\psi^{(2)}_{3s}(x) = \exp[i(\theta(x)-\frac{\pi}{3})]\ \Delta(x)\psi^{(2)}_{1s}(x)+\exp[-i(\theta(x)-\frac{\pi}{3})]\ \Delta(x)\psi^{(2)}_{2s}(x) \tag{62a-b}$$

Now by substituting (62a-b) in (58) and (61) and neglecting terms which renormalise the chemical potential, we finally arrive at

$$H_0+H_{e-ph} = \sum_s \int dx\{-iv_F \sum_j [\psi^{(j)*}_{1s}(x)\frac{d}{dx}\psi^{(j)}_{1s}(x)-\psi^{(j)}_{2s}(x)\frac{d}{dx}\psi^{(j)}_{2s}(x)\}]$$

$$+ 2\Delta(x)\exp[i(\theta(x)-\frac{\pi}{3})](\psi^{(2)}_{1s}(x)\psi^{(2)}_{2s}(x)-\psi^{(1)}_{2s}(x)\psi^{(1)}_{1s}(x))$$

$$+ \frac{1}{3}\Delta^2(x)\exp[i(2\theta(x)+\frac{\pi}{3})](\psi^{(2)}_{2s}(x)\psi^{(2)}_{1s}(x)-\psi^{(1)*}_{1s}(x)\psi^{(1)}_{2s}(x))+h.c.\} \tag{63}$$

The continuum Hamiltonian is the sum of (60) and (63)

We are now going to bosonise the fermion fields $\psi^{(j)}_{\ell s}(x)$ in this Hamiltonian All the necessary information concerning this technique is given in appendix B The way to bosonise these fermion fields is to write them in the following form

$$\psi^{(j)}_{\ell s}(x) = \frac{1}{\sqrt{2\pi\eta}}\exp\{i(-1)^{\ell}\phi^{(j)}_{\ell s}(x)\} \tag{B 1}$$

where the explicit form of $\phi^{(j)}_{\ell s}(x)$ and the meaning of η are given in appendix B In H_0+H_{e-ph} (63) four different bilinear products of fermion fields appear, namely $\psi^{(1)*}_{1s}(x)\psi^{(1)}_{2s}(x)$, $\psi^{(2)*}_{1s}(x)\psi^{(2)}_{2s}(x)$ and their hermitean conjugates By using (B 4), (B 5a-b), (B 9a-b) and the fact that the $\phi^{(j)}_{\ell s}(x)$ mutually commute, these products can be written as

$$\begin{cases} \psi^{(j)*}_{1s}(x)\psi^{(j)}_{2s}(x) = \frac{1}{2\pi\eta}\exp\{i(-1)^{j+1}[\phi^{(j)}(x)+s\sigma^{(j)}(x)]\} \\ \qquad\qquad\qquad\qquad\qquad\qquad\qquad\qquad (j=1\ 2) \\ \psi^{(j)}_{2s}(x)\psi^{(j)}_{1s}(x) = \frac{1}{2\pi\eta}\exp\{-i(-1)^{j+1}[\phi^{(j)}(x)+s\sigma^{(j)}(x)]\} \end{cases} \tag{64}$$

This result together with the results of appendix B for the "kinetic energy" of the fermion fields leads directly to the boson representation of (63). Here we only need this representation to reach a qualitative understanding of the type of solitons to be expected. As shown by Hara and Fukuyama [25] for the one-chain case it then suffices to consider a static limit where (canonically conjugated) momentum fields are neglected. The Hamiltonian is then expressed in terms of classical phase fields, after shifting $\phi^{(j)}(x) \rightarrow \phi^{(j)}(x) - \pi/3$, as

$$H = \int dx \{ \mu \sum_j [(\frac{d\phi^{(j)}(x)}{dx})^2 + (\frac{d\sigma^{(j)}(x)}{dx})^2] + \frac{1}{2} K_1 \Delta^2(x)$$

$$+ \nu\Delta(x)[\cos(\theta(x) - \phi^{(2)}(x))\cos(\sigma^{(2)}(x)) - \cos(\theta(x) \quad \phi^{(1)}(x))\cos(\sigma^{(1)}(x))]$$

$$+ \frac{1}{3}\nu\Delta^2(x)[\cos(2\theta(x) + \phi^{(2)}(x))\cos(\sigma^{(2)}(x)) - \cos(2\theta(x) + \phi^{(1)}(x))\cos(\sigma^{(1)}(x))]\} \tag{65}$$

with $u = v_F/4\pi$ and $v = 4/\pi\eta$. Passing to the following lattice fields

$$\Delta_1(x) = \Delta(x)\cos(\theta(x)) \tag{66a}$$

$$\Delta_2(x) = \Delta(x)\sin(\theta(x)) \tag{66b}$$

the $\Delta - \theta$ dependent part of (65) becomes

$$\int dx \{ \frac{1}{2} K_1 (\Delta_1^2(x) + \Delta_2^2(x)) + \nu P(x)(\Delta_1(x) + \frac{1}{3}[\Delta_1^2(x) - \Delta_2^2(x)])$$

$$+ \nu Q(x)(\Delta_2(x) - \frac{2}{3}\Delta_1(x)\Delta_2(x))\} \tag{67}$$

with

$$P(x) \equiv \cos(\phi^{(2)}(x))\cos(\sigma^{(2)}(x)) - \cos(\phi^{(1)}(x))\cos(\sigma^{(1)}(x)) \tag{68a}$$

and

$$Q(x) \equiv \sin(\phi^{(2)}(x))\cos(\sigma^{(2)}(x)) - \sin(\phi^{(1)}(x))\cos(\sigma^{(1)}(x)) \tag{68b}$$

Minimising with respect to $\Delta_1(x)$ and $\Delta_2(x)$ yields the equations

$$\begin{bmatrix} 1 + \frac{2}{3}\xi P(x) & -\frac{2}{3}\xi Q(x) \\ -\frac{2}{3}\xi Q(x) & 1 - \frac{2}{3}\xi P(x) \end{bmatrix} \begin{bmatrix} \Delta_1(x) \\ \Delta_2(x) \end{bmatrix} = \xi \begin{bmatrix} P(x) \\ Q(x) \end{bmatrix} \tag{69}$$

with $\xi = v/K_1$, which is small quantity in the weak coupling limit We therefore get up to second order in ξ

$$\begin{pmatrix}\Delta_1(x)\\ \Delta_2(x)\end{pmatrix} = -\xi \begin{pmatrix}P(x)\\ Q(x)\end{pmatrix} + \frac{2}{3}\xi^2 \begin{pmatrix}P^2(x)-Q^2(x)\\ -2P(x)Q(x)\end{pmatrix} + O(\xi^3) \tag{70}$$

By substituting this into the integrand of (67) we get an "effective potential" $U(\phi^{(1)},\phi^{(2)},\sigma^{(1)},\sigma^{(2)})$, which is up to order ξ^2 given by

$$\begin{aligned} U(\phi^{(1)},\phi^{(2)},\sigma^{(1)},\sigma^{(2)}) &= -\frac{1}{2}v\xi[\cos^2(\sigma^{(1)})+\cos^2(\sigma^{(2)}) \\ &- 2\cos(\phi^{(1)}-\phi^{(2)})\cos(\sigma^{(1)})\cos(\sigma^{(2)})] \\ &- v\xi^2[\cos(3\phi^{(1)})\cos^3(\sigma^{(1)})+3\cos(\phi^{(1)}+2\phi^{(2)})\cos(\sigma^{(1)})\cos^2(\sigma^{(2)}) \\ &- \cos(3\phi^{(2)})\cos^3(\sigma^{(2)})-3\cos(2\phi^{(1)}+\phi^{(2)})\cos^2(\sigma^{(1)})\cos(\sigma^{(2)})]+O(\xi^3) \end{aligned} \tag{71}$$

So the effective Hamiltonian for the electronic phase fields reads

$$H = \int dx\{\mu \sum_j [(\frac{d\phi^{(j)}}{dx})^2 + (\frac{d\sigma^{(j)}}{dx})^2] + U(\phi^{(1)}\,\phi^{(2)}\,\sigma^{(1)},\sigma^{(2)})\} \tag{72}$$

For the ground state these phase fields have to be constant, their values follow from minimising U From (71) it is clear that this yields the following four classes of solutions

1) $\{\sigma^{(1)},\sigma^{(2)}\}=\{0,0\}$ together with $\{\phi^{(1)},\phi^{(2)}\}=\{0,-\pi\},\{\frac{2\pi}{3},-\frac{\pi}{3}\}$ or $\{\frac{4\pi}{3},\frac{\pi}{3}\}$

2) $\{\sigma^{(1)},\sigma^{(2)}\}=\{\pi,\pi\}$ together with $\{\phi^{(1)},\phi^{(2)}\}=\{\pi,0\},\{-\frac{\pi}{3},-\frac{4\pi}{3}\}$ or $\{\frac{\pi}{3},-\frac{2\pi}{3}\}$

3) $\{\sigma^{(1)},\sigma^{(2)}\}=\{\pi,0\}$ together with $\{\phi^{(1)},\phi^{(2)}\}=\{\pi,\pi\},\{-\frac{\pi}{3},-\frac{\pi}{3}\}$ or $\{\frac{\pi}{3},\frac{\pi}{3}\}$

4) $\{\sigma^{(1)},\sigma^{(2)}\}=\{0,\pi\}$ together with $\{\phi^{(1)},\phi^{(2)}\}=\{0,0\},\{\frac{2\pi}{3},\frac{2\pi}{3}\}$ or $\{\frac{4\pi}{3},\frac{4\pi}{3}\}$

(73)

Of course in each class we have the freedom to add an arbitrary multiple of 2π to each of the phase field values Each of these classes corresponds to the three degenerate ground states Solitons are excitations for which the phases vary as a function of x between two values corresponding to different ground states The soliton is localised because $U(\phi^{(1)},\phi^{(2)},\sigma^{(1)},\sigma^{(2)})$ favours the ground state values.

the actual width is a result of a competition between this effect and the gradient terms which favour a widely spread excitation The total phase shift is directly connected to the constraints laid upon the system such as excess charge q and excess spin m Indeed upon using (B 11) and (B 12) one has

$$-\frac{1}{\pi}\Delta\phi \equiv -\frac{1}{\pi}[\phi^{(1)}(x)-\phi^{(2)}(x)]\Big|_{-\infty}^{\infty} = \int_{-\infty}^{\infty} dx\varrho(x) = q \tag{74a}$$

and

$$-\frac{1}{2\pi}\Delta\sigma \equiv -\frac{1}{2\pi}[\sigma^{(1)}(x)-\sigma^{(2)}(x)]\Big|_{-\infty}^{\infty} = \int_{-\infty}^{\infty} dx\mu(x) = m \tag{74b}$$

The type of lattice deformation to be expected for a soliton with a given trajectory in the four-dimensional phase space spanned by $\phi^{(1)}$, $\phi^{(2)}$, $\sigma^{(1)}$ and $\sigma^{(2)}$ can be seen from (70) which may be written, using the definitions of P(x) and Q(x) (68a-b), as

$$\Delta(x)\begin{bmatrix}\cos(\theta(x))\\ \sin(\theta(x))\end{bmatrix} \equiv \begin{bmatrix}\Delta_1(x)\\ \Delta_2(x)\end{bmatrix} = \xi\cos(\sigma^{(1)}(x))\begin{bmatrix}\cos(\phi^{(1)}(x))\\ \sin(\phi^{(1)}(x))\end{bmatrix}$$

$$-\xi\cos(\sigma^{(2)}(x))\begin{bmatrix}\cos(\phi^{(2)}(x))\\ \sin(\phi^{(2)}(x))\end{bmatrix} + O(\xi^2) \tag{75}$$

From this equation one sees that the lattice deformation is the sum of two vectors with amplitudes $\xi\cos(\sigma^{(1)}(x))$ and $-\xi\cos(\sigma^{(2)}(x))$ and phases $\phi^{(1)}(x)$ and $\phi^{(2)}(x)$ Accordingly we expect to find three different types of solitons

1) A soliton of the "phason" type (i e $|\Delta(x)|$=constant) This occurs when the spin phases $\sigma^{(j)}(x)$ remain constant (i e no excess spin according to (74b)) and the vectors move in phase $\Delta\phi^{(1)}=\Delta\phi^{(2)}$ (i e no excess charge according to (74a))

2) A soliton of the "amplitudon" type (i e $\Delta(x)$ passes (almost) through zero) This happens for example when the two vectors move in opposite phase, e g $\Delta\phi^{(1)}=2\pi/3$ and $\Delta\phi^{(2)}=-4\pi/3$, while the spin phases $\sigma^{(j)}(x)$ remain constant This corresponds in view of (74a-b) to the case $q=-2$ and $m=0$

3) A soliton of an intermediate type where $\Delta(x)$ decreases to about half its original value One expects to find this case, which does not occur for the single chain, when only one of the two vectors mentioned above passes through zero This happens when a single spin phase, e g $\sigma^{(1)}(x)$, goes from π to 0 This phase shift must be accompanied with a phase shift $\Delta\phi^{(1)}=5\pi/3$ in order that the kink connects two ground states (see (73)) If now the phase shift $\Delta\phi^{(2)}$ of the other vector equals $2\pi/3$ we see from (74a-b) that this then corresponds to the case $q=-1$ and $m=+\frac{1}{2}$

The next subsection where our numerical results for the soliton excitations are presented all cases will indeed be met

B. Numerical results for the soliton excitations

As we already mentioned at the beginning of this section, the way to analyse numerically the nature of the possible soliton excitations in the system is to change the chain length and/or the number of electrons present in the system and to observe what kind of self-consistent solution is generated The reference system in all our calculations is the one we took in our calculations of the homogeneous phases in the previous section, i e the system with chain length $N^{(0)}=66$, number of electrons $N_e^{(0)}=132$ (half-filled band) and force constants $K_1=1\ 75$, $K_2=2$ Because we are interested in small deviations from the ground state we will restrict the analysis to systems with $N=N^{(0)}+\Delta N$, $\Delta N=0,1$ and with $|q|\leq 2$, where the excess charge or kink charge q is defined by

$$q = N_e - 2N \tag{76}$$

According to (74a) this quantity is equal to $-\Delta\phi/\pi$ The excess spin is $m=\pm\frac{1}{2}$ when $q=\mp 1$ In the other cases ($q=0,\pm 2$) when the total number of electrons is even, the excess spin is taken zero Its value is connected to the total spin phase shift by $m=-\Delta\sigma/2\pi$ (74b) The excitation energy $\Delta\varepsilon_{sol}$ of a soliton is estimated using

$$\Delta\varepsilon_{sol} = \varepsilon(N) - \frac{N}{N^{(0)}}\varepsilon(N^{(0)}) \tag{77}$$

where $\varepsilon(N)$ is the total ground state energy of a system with length N The lattice deformations that are obtained in the various cases are collected in Figs 3-7 It turns out that there is a fundamental distinction between the cases $\Delta N=1$ and $\Delta N=0$ Let us first discuss the case $\Delta N=1$ The kink must now connect two different homogeneous phases in view of the periodic boundary conditions We

find that the basic assumption made in the theoretical analysis of the previous subsection namely that the kink can be described as a modulation of the in-phase trimerisation only, is valid This is evident from Figs 3a) 4a) and 5a) The qualitative predictions that follow from the bosonisation analysis are indeed correct the soliton with kink charge $q=0$ is a phason, the soliton with $q=-2$ is an amplitudon and the soliton with $q=-1$ is an excitation of the intermediate type This is made more clear in Figs 3b) 4b) and 5b) where the amplitude of the lattice deformation is plotted and in Figs 3c), 4c) and 5c) where the phase of the lattice deformation is plotted The excitation energies of these solitons are $\Delta\varepsilon_{sol}=0\ 112497$, $0\ 365205$ and $0\ 284106$ for $q=0$, -2 and 1 respectively

When $\Delta N=0$ a soliton is an object that harbours again the excess charge (and spin) but now it is a kink within the *same* homogeneous phase The bosonisation analysis of this kink in the case of single chain shows that it will decay into a soliton-antisoliton pair [25] This cannot happen for the double chain with kink charge $q=-1,-2$ (and $\Delta N=0$) where the lattice deformation is a sum of two vectors (see (75)) Consider, to illustrate this, the case $q=-2$ The total phase shift $\Delta\phi=\Delta\phi^{(1)}-\Delta\phi^{(2)}$, according to (74a), then equals 2π Furthermore the condition $\Delta N=0$ implies that both vectors should reach a final orientation which is equal to the original orientation Hence only one of the two vectors rotates over 2π Along this path no other homogeneous phases are found (see (73)) so that the kink cannot decay Although this type of kink in principle can and perhaps also will exist, it turns out that the system chooses in practice more readily a different solution This solution exhibits a kink within the same homogeneous trimerised phase but involves also a modulation of the out-of-phase dimerisation It shows that our theoretical analysis does not exhaust all the possible types of solitons that can be created In Figs 6) and 7) the numerical results for the cases $q=-1$, respectively $q=-2$ ($\Delta N=0$) are given Figs 6a) and 7a) give the lattice deformation for the sum mode showing a kink within the trimerised phase In Figs 6b) and 7b) the difference of the lattice deformations of the two chains are shown From these Figs it is clear that the kink is accompanied by a modulation of the out-of-phase dimerised mode The excitation energies are $\Delta\varepsilon_{sol}=0\ 248108$ and $0\ 362251$ for $q=-1$ and $q=-2$ respectively A theoretical analysis of this type of soliton along the lines of section 3 4 A is underway

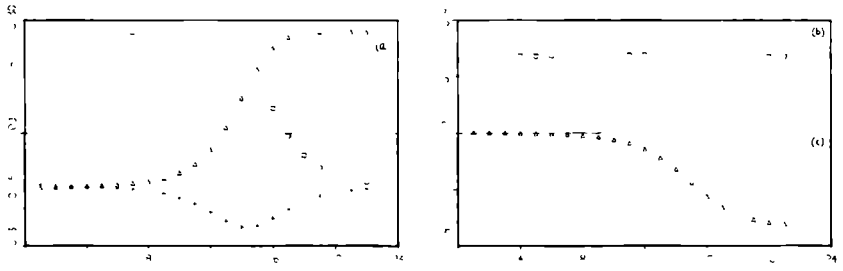

Figure 3. Soliton of the phason type with charge q=0 (a) Displacement pattern $\Delta^{(1)}_{n\ 2}=\Delta^{(2)}_{n-2}$(□), $\Delta^{(1)}_{n\ 1}-\Delta^{(2)}_{n\ 1}$(Δ) and $\Delta^{(1)}_{n}=\Delta^{(2)}_{n}$(+), (b) Amplitude Δ(n), (c) Phase θ(n), defined by $\Delta^{(1)}_{n-p}=\Delta^{(2)}_{n-p}=\Delta(n)\cos(\theta(n)+\frac{2\pi}{3}(p-2))+C_n$, p=0,1,2

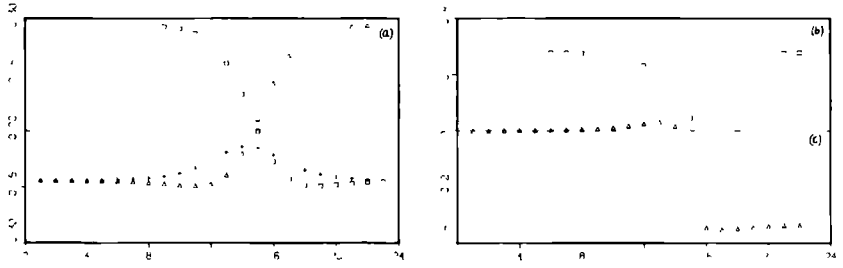

Figure 4. Soliton of amplitudon type with q=−2 (a) Displacement pattern $\Delta^{(1)}_{n-2}=\Delta^{(2)}_{n}$(□), $\Delta^{(1)}_{n\ 1}=\Delta^{(2)}_{n\ 1}$(Δ) and $\Delta^{(1)}_{n}=\Delta^{(2)}_{n}$(+), (b) Amplitude Δ(n), (c) Phase θ(n), defined by $\Delta^{(1)}_{n\ p}=\Delta^{(2)}_{n-p}=\Delta(n)\cos(\theta(n)+\frac{2\pi}{3}(p-2))+C_n$, p=0,1,2

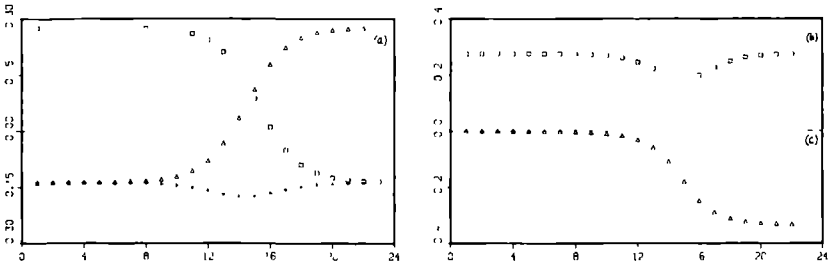

Figure 5. Soliton of intermediate type with $q=-1$. (a) Displacement pattern $\Delta^{\{1\}}_{n-2}=\Delta^{\{2\}}_{n-2}(\sqcup)$, $\Delta^{\{1\}}_{n-1}=\Delta^{\{2\}}_{n-1}(\Delta)$ and $\Delta^{\{1\}}_{n}=\Delta^{\{2\}}_{n}(+)$, (b) Amplitude $\Delta(n)$, (c) Phase $\theta(n)$, defined by $\Delta^{\{1\}}_{n-p}=\Delta^{\{2\}}_{n-p}=\Delta(n)\cos(\theta(n)+\frac{2\pi}{3}(p-2))+C_n$, $p=0,1,2$

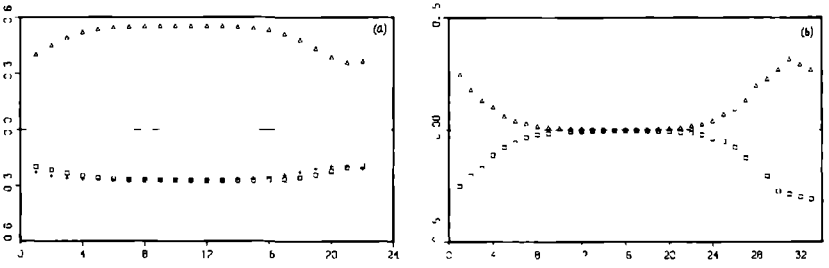

Figure 6. Excitation for $\Delta N=0$ with $q=-1$ (a) Displacement pattern of the sum mode $\Delta^{\{1\}}_{n-2}+\Delta^{\{2\}}_{n-2}(\sqcup)$, $\Delta^{\{1\}}_{n-1}+\Delta^{\{2\}}_{3n-1}(\Delta)$ and $\Delta^{\{1\}}_{n}+\Delta^{\{2\}}_{n}(+)$ $(n=1,\ldots,22)$, (b) Displacement pattern of the difference mode $\Delta^{\{1\}}_{2n-1}-\Delta^{\{2\}}_{2n-1}(\square)$ and $\Delta^{\{1\}}_{2n}-\Delta^{\{2\}}_{2n}(\Delta)$ $(n=1,\ldots,33)$

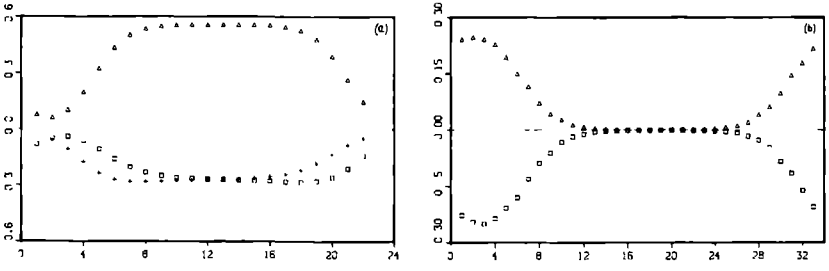

Figure 7. Excitation for $\Delta N=0$ with $q=-2$ (a) Displacement pattern of the sum mode $\Delta^{\{1\}}_{n-2}+\Delta^{\{2\}}_{3n-2}(\sqcap)$, $\Delta^{\{1\}}_{3n-1}+\Delta^{\{2\}}_{n-1}(\Delta)$ and $\Delta^{\{1\}}_{n}+\Delta^{\{2\}}_{n}(+)$ $(n=1,\ldots,22)$, (b) Displacement pattern of the difference mode $\Delta^{\{1\}}_{2n-1}-\Delta^{\{2\}}_{2n-1}(\sqcap)$ and $\Delta^{\{1\}}_{2n}-\Delta^{\{2\}}_{2n}(\Delta)$ $(n=1,\ldots,33)$.

3.5 Appendix A

In this appendix we will give an exact treatment of an in-phase trimerisation for the infinite system The Hamiltonian for this case is give by

$$H = -\sum_{njs}[1-\Delta_n](C^{(j)\dagger}_{n+1\,s}C^{(j)}_{ns}+h\,c\,) - \sum_{ns}(C^{(1)\dagger}_{ns}C^{(2)}_{ns}+h\,c\,)$$

$$+ K_1\sum_n \Delta_n^2 \qquad (A\ 1)$$

where $\Delta_n=\Delta\cos(2\pi/3\ n+\theta)$ Δ and θ will be determined by minimising the total ground state energy of the system We will assume periodic boundary conditions over the chain length N, which we take accordingly a multiple of three, say 3N′ and let eventually N′ go to infinity The elastic energy becomes

$$K_1\sum_{n=1}^{3N}\Delta_n^2 = K_1\Delta^2\sum_{n=1}^{3N}\cos^2(\frac{2\pi}{3}n+\theta) = \frac{3}{2}N'K_1\Delta^2 \qquad (A\ 3)$$

The intra-chain part of the Hamiltonian (A 1) corresponding to chain j is rewritten in terms of Fourier-transformed operators $C^{(j)}_{ks\,\mu}$, where k runs over the discrete k-values consistent with the periodic boundary conditions within the new Brillouin zone $(-\pi/3a,\pi/3a]$ and $\mu=1,2,3$ is a band label, as

$$\sum_{ks}\sum_{\mu\nu}M_{\mu\nu}\,C^{(j)\dagger}_{ks\,\mu}C^{(j)}_{ks\,\nu} \qquad (j=1,2) \qquad (A\ 4)$$

with M the following 3×3 matrix

$$M = \begin{Bmatrix} -2\cos ka & \tfrac{1}{2}\Delta\{e^{i(ka-\theta+\frac{2\pi}{3})}+e^{i(ka+\theta)}\} & \tfrac{1}{2}\Delta\{e^{i(ka+\theta-\frac{2\pi}{3})}+e^{i(ka-\theta)}\} \\ \tfrac{1}{2}\Delta\{e^{-i(ka-\theta+\frac{2\pi}{3})}+e^{i(ka-\theta)}\} & 2\cos(ka+\frac{2\pi}{3}) & \tfrac{1}{2}\Delta\{e^{i(ka-\theta-\frac{2\pi}{3})}+e^{i(ka+\theta-\frac{2\pi}{3})}\} \\ \tfrac{1}{2}\Delta\{e^{-(ka+\theta-\frac{2\pi}{3})}+e^{i(ka-\theta)}\} & \tfrac{1}{2}\Delta\{e^{i(ka+\theta-\frac{2\pi}{3})}+e^{(ka+\theta+\frac{2\pi}{3})}\} & -2\cos(ka-\frac{2\pi}{3}) \end{Bmatrix} \qquad (A\ 5)$$

The secular equation associated with M is given by

$$\varepsilon^3 - 3(1+\frac{1}{2}\Delta^2)\varepsilon+2(1-\frac{3}{4}\Delta^2-\frac{1}{4}\Delta^3\cos3\theta)\cos3k = 0 \qquad (A\ 6)$$

The three solutions of this equation correspond to three electronic bands ε_{kv} $(v=1,2,3)$ Thus (A 4) can be written as

$$\sum_{kss} \varepsilon_{ks} a^{(j)}_{ks\nu} a^{(j)}_{ks\nu} \qquad (j=1\ 2) \tag{A 7}$$

where the $a^{(j)}_{ks\nu}$ are related to the $C^{(j)}_{ks\mu}$ by a unitary transformation In terms of these new operators the inter-chain part in (A 1) is trivially given by

$$-\sum_{kss} (a^{(1)}_{ks\nu} a^{(2)}_{ks\nu} + h\ c\ ) \tag{A 8}$$

So the total electronic part of the Hamiltonian (A 1) now becomes

$$\sum_{kss} \sum_{j} \varepsilon_{ks} a^{(j)}_{ks\nu} a^{(j)}_{ks\nu} - \sum_{kss} (a^{(1)}_{ks\nu} a^{(2)}_{ks\nu} + h\ c\ ) \tag{A 9}$$

which is easily diagonalised by

$$a^{(j)}_{ks\nu} = \frac{1}{\sqrt{2}} \{\tilde{a}^{(1)}_{ks\nu} + (-1)^{j+1} a^{(2)}_{ks\nu}\} \tag{A 10}$$

giving

$$\sum_{kss} \{[\varepsilon_{ks}-1] a^{(1)}_{ks\nu} a^{(1)}_{ks\nu} + [\varepsilon_{ks}+1] \tilde{a}^{(2)}_{ks\nu} a^{(2)}_{ks\nu}\}$$

$$= \sum_{kvjs} \varepsilon^{(j)}_{kv} \tilde{a}^{(j)}_{ks\nu} a^{(j)}_{ks\nu} \tag{A 11}$$

Now let ε_{k1} denote the lowest and ε_{k3} the highest of the three electronic bands and let ε_{k2} denote the band in between It is now easy to see that in the half-filled band case the electronic ground state in obtained by filling all the levels of the bands $\varepsilon^{(1)}_{k1}$, $\varepsilon^{(1)}_{k2}$ and $\varepsilon^{(2)}_{k1}$ So the electronic ground state energy ε_e is given by

$$\varepsilon_e = 2 \sum_{k < \frac{\tau}{3a}} \{2\varepsilon_{k1} + \varepsilon_{k2} - 1\} \tag{A 12}$$

The electronic ground state energy per cell becomes in the limit of N′ going to infinity

$$\tilde{\varepsilon}_e = \frac{\varepsilon_e}{N'} = \frac{3}{\pi} a \int_{-\frac{\tau}{3a}}^{\frac{\tau}{3a}} dk \{2\varepsilon_{k1} + \varepsilon_{k2} - 1\} \tag{A 13}$$

So the total ground state energy per cell for the infinite system is

$$\varepsilon = \varepsilon_e + \frac{3}{2} K_1 \Delta^2 \qquad \text{(A 14)}$$

The phase θ is determined by $\partial\varepsilon_e/\partial\theta=0$ Now θ is found to be given by $\cos 3\theta=1$ i e $\theta=0$ $2\pi/3$ and $4\pi/3$ The amplitude Δ is determined by numerically solving $\partial\varepsilon/\partial\Delta=0$ Or using (A 14) by solving

$$\Delta = \frac{a}{\pi K_1} \int_{-\frac{\pi}{3a}}^{\frac{\pi}{3a}} dk \{2 \frac{\partial \varepsilon_{k1}}{\partial \Delta} + \frac{\partial \varepsilon_{k2}}{\partial \Delta}\} \qquad \text{(A 15)}$$

For $K_1=1$ 75 this yields $\Delta=0$ 2750 and -0 039614 for the total ground state energy per cell

3.6 Appendix B

In this appendix we will derive the formulae and give the definitions necessary for the bosonisation of the fermion fields in the continuum Hamiltonian For further details one is referred to the original articles e g Luther and Peschel [27], Luther and Emery [28] and an excellent review article by Emery [29] The bosonisation technique is based on the fact that in (1+1)-dimensions there is an equivalence between fermion field theories and boson field theories, i e in (1+1)-dimensions a fermion field can be represented by a boson field Luther and Peschel [27] introduced such a representation for the well-known Luttinger model [30] Luther [31] later showed that such a representation can also be constructed for some (3+1) dimensional models One starts with the following representation for the fermion field $\psi_{\xi}^{(j)}(x)$ (see e g [27])

$$\psi_{\xi}^{(j)}(x) = \frac{1}{\sqrt{2\pi\eta}} \exp\{i(-1)^j \phi_{\xi}^{(j)}(x)\} \qquad \text{(B 1)}$$

where the boson field $\phi_{\xi}^{(j)}(x)$ is defined by

$$\phi_{\xi}^{(j)}(x) \equiv \frac{2\pi i}{L} \sum_{q\neq 0} \frac{\exp[-iqx - \frac{1}{2}\eta|q|]}{q} \varrho_{\xi}^{(j)}(q) \qquad \text{(B 2)}$$

$L=Na$ is the length of the chains, η is a short distance cut off parameter which is inversely proportional to k_c and $\varrho_{\xi}^{(j)}(q)$ is a Fourier coefficient of the density $\varrho_{\xi}^{(j)}(x) \equiv \psi_{\xi}^{(j)\dagger}(x)\psi_{\xi}^{(j)}(x)$ defined through

$$\varrho_{\ell\varsigma}^{(j)}(q) = \int dx\, e^{iqx}\varrho_{\ell\varsigma}^{(j)}(x) \tag{B.3a}$$

$$\varrho_{\ell\varsigma}^{(j)}(x) = \frac{1}{L}\sum_{q\neq 0} e^{-iqx}\varrho_{\ell\varsigma}^{(j)}(q). \tag{B.3b}$$

Because there is no $q=0$ contribution in (B.3b), $\varrho_{\ell\varsigma}^{(j)}(x)$ is related to the excess charge density as we will see later. By using $\varrho_{\ell\varsigma}^{(j)^{-}}(q)=\varrho_{\ell\varsigma}^{(j)}(-q)$ it is easily seen that $\phi_{\ell\varsigma}^{(j)}(x)$ is hermitean

$$\phi_{\ell\varsigma}^{(j)^{+}}(x) = \phi_{\ell\varsigma}^{(j)}(x). \tag{B.4}$$

We now define new operators representing the charge and spin collective coordinates by summing over the spin variable $s=\pm 1$

$$\phi_{\ell}^{(j)}(x) \equiv \frac{1}{\sqrt{2}}\sum_{s}\phi_{\ell s}^{(j)}(x) \tag{B.5a}$$

$$\sigma_{\ell}^{(j)}(x) \equiv \frac{1}{\sqrt{2}}\sum_{s} s\phi_{\ell s}^{(j)}(x). \tag{B.5b}$$

Similarly we define

$$\varrho_{\ell}^{(j)}(x) \equiv \frac{1}{\sqrt{2}}\sum_{s}\varrho_{\ell s}^{(j)}(x) \tag{B.6a}$$

$$\mu_{\ell}^{(j)}(x) \equiv \frac{1}{\sqrt{2}}\sum_{s} s\varrho_{\ell s}^{(j)}(x). \tag{B.6b}$$

From the definition of $\phi_{\ell s}^{(j)}(x)$ (B.2), one derives easily the following identity

$$\frac{d}{dx}\,\phi_{\ell s}^{(j)}(x)\,|_{\eta\downarrow 0} = 2\pi\varrho_{\ell s}^{(j)}(x). \tag{B.7}$$

The limit $\eta\downarrow 0$ is actually the continuum limit, because

$$\eta \sim k_c^{-1} \sim \text{intra-chain distance } a$$

which goes to zero in the continuum limit. Combining (B.5a-b), (B.6a-b) and (B.7a-b) we get

$$\frac{1}{2\pi}\,\frac{d}{dx}\,\phi_{\ell}^{(j)}(x)\,|_{\eta\downarrow 0} = \varrho_{\ell}^{(j)}(x) \tag{B.8a}$$

$$\frac{1}{2\pi}\,\frac{d}{dx}\,\sigma_{\ell}^{(j)}(x)\,|_{\eta\downarrow 0} = \mu_{\ell}^{(j)}(x). \tag{B.8b}$$

It is now useful to define the following operators

$$\phi^{(j)}(x) = \frac{(-1)^{j+1}}{\sqrt{2}} \{\phi_1^{(j)}(x)+\phi_2^{(j)}(x)\} \tag{B 9a}$$

$$\sigma^{(j)}(x) = \frac{(-1)^{j+1}}{\sqrt{2}} \{\sigma_1^{(j)}(x)+\sigma_2^{(j)}(x)\} \tag{B 9b}$$

and

$$\Pi_\phi^{(j)}(x) = \frac{(-1)^{j+1}}{\sqrt{2}} \{\varrho_1^{(j)}(x)-\varrho_2^{(j)}(x)\} \tag{B 10a}$$

$$\Pi_\sigma^{(j)}(x) = \frac{(-1)^{j+1}}{\sqrt{2}} \{\mu_1^{(j)}(x)-\mu_2^{(j)}(x)\} \tag{B 10b}$$

It is easy to see, using (B 6a), (B 8a) and (B 9a) that the total excess charge density $\varrho(x)$ in the system is given by

$$\varrho(x) = \sqrt{2}\sum_{\ell j} \varrho_\ell^{(j)}(x) = -\frac{1}{\pi}\frac{d}{dx}\{\phi^{(1)}(x)-\phi^{(2)}(x)\}\,|_{\eta\to 0} \tag{B 11}$$

Similarly the total excess spin density $\mu(x)$ in the system is given by

$$\mu(x) = \frac{1}{\sqrt{2}}\sum_{\ell j} \mu_\ell^{(j)}(x) = -\frac{1}{2\pi}\frac{d}{dx}\{\sigma^{(1)}(x)-\sigma^{(2)}(x)\}\,|_{\eta\downarrow 0} \tag{B 12}$$

One of the results of the bosonisation method, which we will not derive here, is that $(\phi^{(j)},\Pi_\phi^{(j)})$ and $(\sigma^{(j)},\Pi_\sigma^{(j)})$ are pairs of canonically conjugated operators, i e

$$[\phi^{(j)}(x),\Pi_\phi^{(j')}(x')]_- = [\sigma^{(j)}(x)\,\Pi_\sigma^{(j')}(x')]_- = -i\delta_{jj'}\,\delta(x-x') \tag{B 13}$$

Because $\varrho(x)$ and $\mu(x)$, defined through (B 11) and (B 12), are the important physical quantities in the theory, it is clear that $\phi^{(j)}(x)$ and $\sigma^{(j)}(x)$ are the relevant fields $\Pi_\phi^{(j)}(x)$ and $\Pi_\sigma^{(j)}(x)$ are the canonical momenta corresponding to these fields In the so-called 'static limit', in which we analyse the bosonised Hamiltonian, we neglect these 'momenta"

Finally we will indicate how 'the kinetic energy" of the fermion fields $\psi_{\ell\xi}^{(j)}(x)$

$$H_0 = -iv_F\sum_{j\xi}\int dx\{\psi_{1\xi}^{(j)}(x)\frac{d}{dx}\psi_{1\xi}^{(j)}(x)-\psi_{2\xi}^{(j)}(x)\frac{d}{dx}\psi_{2\xi}^{(j)}(x)\} \tag{B 14}$$

can be expressed into the boson fields $\phi^{(j)}(x)$ and $\sigma^{(j)}(x)$ in the "static limit For this we need a result which was introduced by Mattis and Lieb [32] in their

study of the Luttinger model They showed that (B 14) can be represented in terms of density operators by

$$H_0 = \frac{2\pi v_F}{L} \sum_j \sum_{q>0} \{\varrho_+^{(j)}(q)\varrho_+^{(j)}(-q)+\varrho_-^{(j)}(-q)\varrho_-^{(j)}(q)$$

$$+ \mu_+^{(j)}(q)\mu_+^{(j)}(-q)+\mu_-^{(j)}(-q)\mu_-^{(j)}(q)\} \qquad \text{(B 15)}$$

which in real space becomes

$$H_0 = \pi v_F \sum_{j\ell} \int dx\{[\varrho_\ell^{(j)}(x)]^2+[\mu_\ell^{(j)}(x)]^2\} \qquad \text{(B 16)}$$

If we now substitute (B 8a-b), (B 9a-b) and (B 10a-b) in (B 16) and take the "static limit" we finally get

$$H_0 = \frac{v_t}{4\tau} \sum_j \int dx\{[\frac{d\phi^{(j)}(x)}{dx}]^2 + [\frac{d\sigma^{(j)}(x)}{dx}]^2\} \qquad \text{(B 17)}$$

which is used in order to arrive at (65)

Acknowledgements

The authors wish to thank Professor A G M Janner and Dr Th W J M Janssen for useful discussions

3.7 References

[1] Su, W P , Schrieffer J R , Heeger A J Phys Rev Lett **42**, 1698 (1979) and Phys Rev B **22**, 2099 (1980)

[2] Peierls, R E Quantum Theory of Solids, Clarendon Press, Oxford (1955)

[3] Su, W P , Schrieffer, J R Proc Natl Acad Sci U S A **77**, 5626 (1980)

[4] Su, W P , Schrieffer, J R Phys Rev Lett **46**, 738 (1981)

[5] Su, W P Phys Rev B **27**, 370 (1983)

[6] Stafstrom, S Phys Rev B **31**, 6058 (1985)

[7] Ono Y , Ohfuti, Y Terai, A J Phys Soc Japan **54**, 2641 (1985)

[8] Ohfuti Y , Ono, Y J Phys Soc Japan **54**, 4680 (1985)
[9] Baeriswyl, D Maki, K Phys Rev B **28** 2068 (1983)
[10] Stafstrom, S , Chao, K A Phys Rev B **29**, 2255 (1984)
[11] Stafstrom, S , Chao, K A Phys Rev B **30**, 2098 (1984)
[12] Chao, K A , Wang, Y J Phys C Solid State Phys **18**, L1127-L1132 (1985)
[13] Terai, A , Ono, Y J Phys Soc Japan **55**, 213 (1986)
[14] Janssen, T , Tjon, J A J Phys A General Physics **16**, 673 (1983)
[15] Allroth, E , Muller-Krumbhaar, H Phys Rev A **27**, 1575 (1983)
[16] Aubry, S , Le Daeron, P Y Physica D **8**, 381 (1983)
[17] Landau L D Sov Phys JETP **3**, 920 (1957), **5**, 101 (1957), and **8**, 70 (1959)
[18] Hellmann, H Einfuhrung in die Quantenchemie, Deuticke, Leipzig (1937)
[19] Feynman, R P Phys Rev **56**, 340 (1939) and undergraduate thesis MIT (1939) (unpublished)
[20] e g Hohn, F E Elementary Matrix Algebra, first edition, MacMillan, New York, (1958), p 270
[21] Takayama, H , Lin-Liu, Y R , Maki, K Phys Rev B **21**, 2388 (1980)
[22] Horovitz, B Phys Rev B **22**, 1101 (1980)
[23] Tinka Gammel, J , Krumhansl, J A Phys Rev B **27**, 7659 (1983)
[24] Horovitz, B , Krumhansl, J A Phys Rev B **29**, 2109 (1984)
[25] Hara, J , Fukuyama, H J Phys Soc Japan **52**, 2128 (1983)
[26] Tomonaga, S Prog Theor Phys **5**, 544 (1950)
[27] Luther, A , Peschel, I Phys Rev B **9**, 2911 (1974)
[28] Luther, A , Emery, V Phys Rev Lett **33**, 589 (1974)
[29] Emery, V Theory of the one-dimensional electron gas, in Higly Conducting One-Dimensional Solids, Devreese, J T , Evrard, R P, van Doren, V E (eds) Plenum Press, New York (1979)
[30] Luttinger, J M J Math Phys **4**, 1154 (1963)
[31] Luther, A Phys Rev B **9**, 320 (1979)
[32] Mattis, D C , Lieb, E H J Math Phys **6**, 304 (1965)

CHAPTER 4†

DYNAMICS OF KINKS IN MODULATED CRYSTALS

J J M Slot and T Janssen

Institute for Theoretical Physics, University of Nijmegen, Toernooiveld, 6525 ED Nijmegen, The Netherlands

Abstract

The dynamics of kinks (domain walls) in a linear chain system with frustration, in which incommensurate phases occur, is studied

In this both numerical and analytical techniques are used The kinks, which can be interpreted as discommensurations in incommensurate phases, are found to be unstable, in a continuum approximation, but their life-time may be long near the lock-in transition due to pinning effects

---

† Submitted for publication to Physica D, Nonlinear Phenomena, North-Holland

4.1 Introduction

Discrete non-linear systems bearing solitary waves have been studied in detail, especially the Frenkel Kontorova model and the discrete ϕ^4 model, a chain of particles residing in double well potentials and interacting via harmonic nearest-neighbour interactions [1 11 and references therein]

Linear chains with non-linear forces between the particles have also been proposed as model for crystals with a quasiperiodic distortion incommensurate displacively modulated crystal structures Essential in these models (ANNNI and frustrated discrete ϕ^4 model) is the competition between first and second neighbour interaction

The ground state of these models is, depending on the parameters, the undistorted chain, a periodically modulated or an incommensurately modulated chain The IC phase is intermediate between the undistorted and the periodic structure Near the phase boundary commensurate - incommensurate (the so-called lock-in) the structure may be described as a periodic structure in which domain walls occur Variation of the parameters then influences the domain wall (discommensuration) structure

Therefore, kink-like excitations are important in the statics and kinetics of IC phases This is the reason to study the influence of frustrating interactions on the possibility of having solitary waves

The procedure is, as in the case of the original ϕ^4 chain, based on an analytical treatment of a continuum approximation to the model, and on numerical integration for the discrete system When the displacement at site n is x_n one may take as model Hamiltonian

$$\mathcal{H} = \sum_n \{\frac{p_n^2}{2m} + \frac{A}{2}x_n^2 + \frac{1}{4}x_n^4 + Bx_nx_{n-1} + Dx_nx_{n-2}\} \qquad (1\ 1)$$

This is one version of a system that possibly shows IC phases Another version is a linear chain with non-linear first neighbour and harmonic second and third neighbour interactions If the potential energy for displacements u_n is

$$V = \sum_n \{\frac{\alpha}{2}(u_n-u_{n-1})^2 + \frac{1}{4}(u_n-u_{n-1})^4 + \frac{\beta}{2}(u_n-u_{n-2})^2 + \frac{\delta}{2}(u_n-u_{n-3})^2\} \quad (1\ 2)$$

it is of the same form as in (1 1) with the change of variables $x_n = u_n-u_{n-1}$ and of parameters

$$A = \alpha+2\beta+3\delta \quad B = \beta+2\delta, \quad D = \delta \tag{1 3}$$

These relations are given to make the comparison possible with phase diagrams given earlier

The ground state of (1 1) may be the undistorted chain ($x_n = 0$), an N-period distorted chain ($x_{n+N} = x_n$) or an incommensurate chain Only in certain regions of the parameter space the solutions are different from the 3 simple structures

$$\begin{aligned} &\text{a) } N = 1, \quad x_n = 0 \\ &\text{b) } N = 1, \quad x_n = \pm \sqrt{-(A+2B+2D)} \\ &\text{c) } N = 2, \quad x_n = \pm(-1)^n \sqrt{-(A-2B+2D)} \end{aligned} \tag{1 4}$$

These ground states may form the basis for non-linear excitations in the form of kinks, as found for D = 0 For example, in the case of (1 4c) one may approximate (1 1) by a continuum expression Putting

$$x_n = (-1)^n Q_n \tag{1 5}$$

and assuming that Q_n depends only slowly on n, one may write the equations of motion as

$$-mQ + 2(B-2D)Q = (A-2B+2D)Q + Q^3 \tag{1 6}$$

This equation has as solitary wave solution

$$Q(\xi,t) = \sqrt{-(A-2B+2D)} \tanh\left((\xi-\xi_0-vt)\sqrt{\frac{-A+2B-2D}{4B-8D-mv^2}}\right) \tag{1 7}$$

The properties of these solutions are the same as those for the ordinary ϕ^4 chain, which corresponds to D = 0

For other structures kink solutions may also be found For the general case a continuum approximation is discussed in section 4 2 The equations of motion are identical to those of a particle in a 2-dimensional potential and an external magnetic field H One may distinguish two qualitatively different cases H = 0 and H ≠ 0, which are treated in sections 4 3 and 4 4 In the chosen approximation the kinks are not pinned Pinning mechanisms are discussed in section 4 5 A special case is a structure near a period 4 solution This is the subject of section 4 6 Finally discrete systems are discussed in section 4 7

4.2 Continuum model

The model which we consider consists of a one-dimensional chain of classical particles Each particle has one degree of freedom denoted by x_n, and is harmonically coupled to its nearest and next-nearest neighbours Furthermore, each particle moves in an anharmonic site potential The potential energy of the chain is

$$V = \sum_n \{\tfrac{1}{2}Ax_n^2 + \tfrac{1}{4}x_n^4 + Bx_nx_{n-1} + Dx_nx_{n-2}\} \qquad (2\ 1)$$

A possible interpretation of x_n is that of a molecular torsion angle as in biphenyl [12] The ground state of the system (2 1) has been studied in detail as function of the parameters α, β and δ [13] (see (1 3) for the relations between α, β, δ and A, B, D) Fig 1 shows the stable configurations with the lowest energy as function of A/D and B/D The hatched regions correspond to incommensurate phases These IC phases only occur for $D \neq 0$ If $|B/D| < 4$ the ground state may be incommensurate There is a simple argument from which one can conclude that the parameters of the model are effectively dependent on temperature An increase in A corresponds to an increase in temperature This agrees with the results of a mean-field approximation [14]

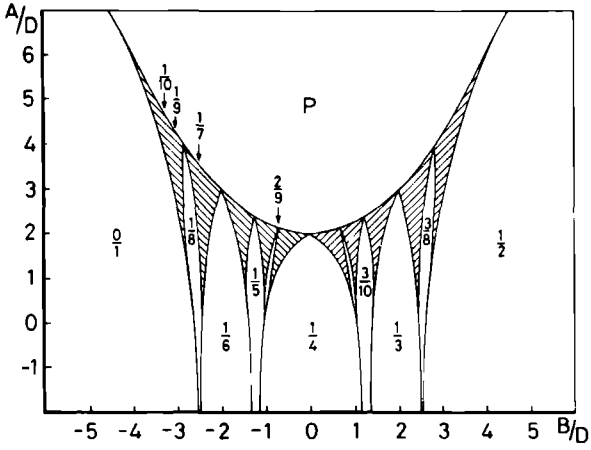

Figure 1. Phase diagram of the discrete frustrated ϕ^4 model Each point in this diagram corresponds to a ground state of the model Indicated are the small period commensurate phases by their wave vector The hatched regions correspond to incommensurate phases and to long period commensurate phases

The Hamiltonian of the chain is given by eq (1 1) Because the potential energy (2 1) is not translationally invariant, there will be no acoustic mode present in the dynamics determined by (1 1) The equations of motion associated with (1 1) are (m = 1)

$$\ddot{x}_n = - Ax_n - x_n^3 - B(x_{n-1}+x_{n+1}) - D(x_{n-2}+x_{n+2}) \qquad (2\ 2)$$

One cannot solve this set of coupled non-linear equations analytically The appropriate way to analyse them is to integrate these equations numerically for a finite system This will be the subject of section 4 7

Now the interesting non-linear excitations consist of localised deviations from the ground state, with finite energies relative to the infinite energy of the ground state, traveling through the system without changing their shape If these deviations vary slowly on the scale of the lattice-constant a which we will take equal to one from now on, an approximate analytical treatment of the equations of motion (2 2) is possible In that case we can study the model in a suitably defined continuum limit, which leads in a natural way to a classical field theory in 1+1 dimensions In this limit the original infinite set of coupled non-linear ordinary differential equations (2 2) will be replaced by a finite set of coupled non-linear partial differential equations, for which exact solutions can be looked for We start by defining this limit and derive the form of the resulting continuum Hamiltonian and of the equations of motion

For given parameters A, B and D the ground state is periodic or incommensurate We approximate the latter also with a commensurate modulation vector

$$q = 2\pi \frac{L}{N} \qquad (2\ 3)$$

where L an N are relative prime and possibly very large In the analysis we have to distinguish four different cases depending on the value of N N = 1,2,4 and the rest We will not treat the cases N = 1 and N = 2 because in these cases the continuum model for D ≠ 0 is qualitatively the same as the continuum model for D = 0, which was studied in depth by several authors [2,4,7 8] The other two cases do not arise when D = 0 One can easily show that when D = 0, one can only have a phase transition at the center (N = 1) or at the boundary (N = 2) of the Brillouin zone A non-zero value of D is needed to have a phase transition at a general point of the Brillouin zone The case N = 4 is somewhat special and that is why we will treat it separately in section 4 6 In the rest of this section we will treat the remaining case N ≠ 1, 2 or 4

Because a phase transition in this model is of the soft-mode type, the region in the phase diagram just below the transition point is characterised by the fact that the ground state is 'sinusoidally modulated with the q-vector of the soft-mode The higher harmonics are also present but they have a very small amplitude The ground state configuration in that region is approximately described by

$$x_n^{(0)} = \Delta \sin(qn+\phi) \tag{2 4}$$

For a N-fold superstructure (2 3) the ground state will be M-fold degenerate, where M = N if N is even and M = 2N if N is odd The phase-angle ϕ can take on M values

$$\phi = \phi^{(j)} \equiv \frac{2\pi}{M} j + \text{constant} \qquad (j = 0, \ldots, M-1) \tag{2 5}$$

while the amplitude Δ for each of these degenerate phases will be the same

The low lying excitations in the system consist of domain walls or kinks between different degenerate ground state phases Such a domain wall is characterised by a so-called topological charge (or winding number η), defined by

$$\eta \equiv \frac{\Delta\phi}{2\pi} \tag{2 6}$$

where $\Delta\phi$ is the phase difference between degenerate ground states which the wall separates The lowest excitation is a single kink with $\eta = \pm 1/N$ when N is even and $\eta = \pm 1/2N$ when N is odd Because both the phase and the amplitude are coupled degrees of freedom, both will vary while going through the kink This leads us to the following Ansatz for the derivation of the continuum Hamiltonian in the "sinusoidal" region

$$x_n(t) = e^{iqn}Q(n,t) + e^{-iqn}Q^*(n,t) \tag{2 7}$$

with $Q(\xi,t)$ a slowly varying function of ξ By slowly varying we mean that if

$$Q = O(1) \text{ then } Q \equiv \frac{\partial Q}{\partial \xi} = O(\varepsilon) \text{ and } Q\,,\, Q = O(\varepsilon^2) \text{ etc} \tag{2 8}$$

where $\varepsilon \ll 1$ If we now substitute our Ansatz (2 7) in the Hamiltonian (2 3), sum out all fast varying terms (i e terms which have as a factor some power of exp(iqn)), replace the sum by an integral and eliminate all appearing "surface" terms, we end up with the following continuum Hamiltonian which is correct to $O(\varepsilon^2)$

$$\mathcal{H} = \int_{-\infty}^{\infty} d\xi \{ |P|^2 + a|Q|^2 + \frac{3}{2}|Q|^4 + ib(Q'Q^* - QQ^{*'}) + c^2|Q'|^2 \} \qquad (2.9)$$

with P the canonical momentum conjugate to Q^*

$$P = \dot{Q} \qquad (2.10)$$

and

$$a \equiv A + 2B\cos(q) + 2D\cos(2q) \qquad (2.11)$$
$$b \equiv B\sin(q) + 2D\sin(2q) \qquad (2.12)$$
$$c^2 \equiv -[B\cos(q) + 4D\cos(2q)]. \qquad (2.13)$$

The details of this derivation are given in appendix A. The term with the coefficient b is well-known from Landau's phenomenological theory of phase transitions by the name of Lifshitz-term [15].

The ground state is given by Q = constant for a certain mode with wave vector q, for which b vanishes. Above the phase transition Q = 0. For decreasing value of A, with B and D fixed, the first mode that becomes unstable satisfies (if $|B/4D| < 1$)

$$\cos(q) = -\frac{B}{4D}. \qquad (2.14)$$

Below the transition non-linear terms stabilize the system. It is easy to see that for this q-vector a (2.11) will have a minimum, which is negative below the transition point, b (2.12) will vanish and c^2 will be positive.

The equations of motion are given by Hamilton's equations

$$\dot{P} = -\frac{\delta\mathcal{H}}{\delta Q^*} + \left(\frac{\delta\mathcal{H}}{\delta Q^{*'}}\right)' \qquad (2.15)$$

$$\dot{Q} = \frac{\delta\mathcal{H}}{\delta P^*} + \text{their complex conjugates.} \qquad (2.16)$$

These equations of motion are

$$\begin{aligned} \ddot{Q} - c^2Q'' + 2ib\,Q' &= -aQ - 3|Q|^2Q \\ \ddot{Q}^* - c^2Q^{*''} - 2ib\,Q^{*'} &= -aQ^* - 3|Q|^2Q^*. \end{aligned} \qquad (2.17)$$

Instead of working with the complex field Q it is more convenient to work with the following pair of real fields u and v

$$u \equiv Q+Q^* \tag{2 18}$$
$$v \equiv i(Q-Q^*) \tag{2 19}$$

The equations of motion (2 17) become in terms of these fields

$$\begin{aligned} u - \frac{1}{c^2}u - Hv &= ru + su(u^2+v^2) \\ v - \frac{1}{c^2}v + Hu &= rv + sv(u^2+v^2) \end{aligned} \tag{2 20}$$

with

$$r \equiv \frac{a}{c^2}<0, \quad H \equiv \frac{2b}{c^2} \quad \text{and} \quad s \equiv \frac{3}{4c^2}>0 \tag{2 21}$$

Solitary waves are solutions of (2 20) which depend on ξ and t in the combination $\xi - vt$ Every solution of this type can be obtained from a solution in the rest frame ($v = 0$) by applying the following boost

$$\begin{aligned} &\xi \to \chi \equiv \gamma(\xi - vt) \\ &H \to \gamma H \quad \text{with} \quad \gamma \equiv \frac{1}{\sqrt{1 - v^2/c^2}} \end{aligned} \tag{2 22}$$

It is easy to check that the role of "the speed of light" c is played here by the phason velocity This is the slope of the dispersion curve for q at the stability limit, i e of $\omega = \sqrt{A+2B\cos(q+k)+2D\cos 2(q+k)}$ for q (2 15) and k small (cf 2 14) The problem in the rest frame is

$$\begin{aligned} u &= ru + Hv + su(u^2 + v^2) \\ v &= rv - Hu + sv(u^2 + v^2) \end{aligned} \tag{2 23}$$

A well-known way to look at such a stationary problem is to make an analogy with a problem in classical mechanics By interpreting ξ as a "time" variable we can view (2 23) as the equation-of-motion of a classical particle with a unit mass and a unit charge moving in a plane (coordinates u and v) perpendicular to a homogeneous magnetic field (strength H) in a non-linear central potential

$$U(\varrho) = -\frac{1}{2}r\varrho^2 - \frac{1}{4}s\varrho^4 - \frac{r^2}{4s} \tag{2 24}$$

where $\varrho^2 \equiv u^2+v^2$ Because r is negative and s is positive this potential is also known by the name "inverted Mexican hat' This mechanical system is conservative, i e its energy ϵ given by

$$\varepsilon = \frac{1}{2}(u'^2+v'^2)+U(\varrho) \tag{2 25}$$

is a constant of the motion The perpendicular "magnetic field" of course does not contribute to ε Also the component of the angular momentum perpendicular to the plane $L_\perp$ is conserved In this quantity there is a contribution from the magnetic field

$$L_\perp = uv - u\,v + \frac{1}{2}H(u^2+v^2) \tag{2 26}$$

That both quantities are indeed conserved is easily checked using (2 23)

Because the particle has two degrees of freedom, the existence of two integrals of the motion implies that the system is integrable [16] This means that all the solutions of (2 23) are regular In order to solve (2 23) we have to specify the appropriate boundary conditions for the solutions we are looking for These boundary conditions can best be determined by looking at the continuum Hamiltonian for the stationary problem

$$\mathcal{H}_0 = \frac{1}{2}c^2 \int_{-\infty}^{\infty} d\xi \,\{\frac{1}{2}(u'^2+v'^2)+\frac{1}{2}H(uv - u\,v)+\frac{1}{2}r(u^2+v^2) + \frac{1}{4}s(u^2+v^2)^2+\frac{r^2}{4s}\} \tag{2 27}$$

This Hamiltonian is easily derived from (2 9) by transforming the complex field Q in the real fields u and v (see (2 18-19)) and subtracting the (infinite) energy of the ground state The solutions we are looking for must have a localised Hamiltonian (energy) density and a finite energy In view of (2 27) this is accomplished by the following boundary conditions

$$\lim_{\xi\to\pm\infty} \begin{bmatrix} u(\xi) \\ v(\xi) \end{bmatrix} = 0 \quad \text{and} \quad \lim_{\xi\to\pm\infty} \{u^2(\xi)+v^2(\xi)\} = -\frac{r}{s} \tag{2 28}$$

$\sqrt{\frac{-r}{s}}$ is the radius where the Mexican hat has its minimum If we combine (2 28) with (2 25) and (2 26) we see that the solutions we are looking for are characterised by

$$\varepsilon = 0 \quad \text{and} \quad L_\perp = -\frac{rH}{2s} \tag{2 29}$$

The boundary conditions (2 28) correspond in the mechanical model to very special initial conditions The particle has to start in the infinite past on the brim of the inverted Mexican hat with an infinitesimal velocity directed inwards in order to end in the infinite future on the brim with a zero velocity It is clear that this is a very unstable solution of the mechanical problem When H is zero the angular momentum is zero, which means that the particle will move through the origin in the u-v plane This is prohibited when H is non-zero, because then the particle experiences an effective centrifugal repulsion at the origin So there are two qualitatively different solutions of (2 23), depending whether H is zero or non-zero In the next two sections we will analyse these two cases

We end this section with the following observation In the discrete model (2 1) a commensurate ground state has by definition a finite degeneracy (cf (2 5)) This is no longer true in the present continuum model, as is clear from the Mexican hat However, in going further away from the transition point (i e effectively lowering the temperature), the ground state configuration no longer can be described as a condensation of the fundamental mode alone (2 3) Also the higher harmonics will be present in the ground state configuration due to the non-linear coupling So when the fundamental mode is excited, also the higher harmonics will be excited This will break the infinite degeneracy of the Mexican hat and lead to phase pinning within the continuum model This will be the subject of section 4 5

4.3 Solitary wave excitations for H = 0

In this section we will analyse the stationary problem (2 23) when H = 0, i e

$$\begin{aligned} u'' &= ru + su(u^2+v^2) \\ v'' &= rv + sv(u^2+v^2) \end{aligned} \tag{3 1}$$

This is the case that the Lifshitz invariant b vanishes, i e at the minimum of the dispersion curve in the P-phase The solutions of this problem with the boundary conditions (2 28) are determined by (cf (2 29))

$$\varepsilon = \frac{1}{2}(u'^2+v'^2) - \frac{1}{2}r(u^2+v^2) - \frac{1}{4}s(u^2+v^2)^2 - \frac{r^2}{4s} = 0 \tag{3 2}$$

$$I_\perp = uv' - u'v = 0 \tag{3 3}$$

From (3 3) it follows that v is proportional to u, say

$$v = \lambda u \tag{3 4}$$

If we substitute (3 4) into (3 1) we get one equation, namely

$$u'' = ru + su^3(1+\lambda^2) \tag{3 5}$$

Thus $w \equiv u\sqrt{1+\lambda^2}$ satisfies

$$w'' = rw + sw^3 \tag{3 6}$$

The boundary conditions (2 28) imply that

$$\lim_{\xi\to\pm\infty} w'(\xi) = 0 \quad \text{and} \quad \lim_{\xi\to\pm\infty} w^2(\xi)(= u^2(\xi)+v^2(\xi)) = -\frac{r}{s}, \tag{3 7}$$

which leads to the unique solution

$$w(\xi) = \sqrt{\frac{-r}{s}}\tanh\left(\sqrt{\frac{-r}{2}}\xi\right) \tag{3 8}$$

Thus the solution of (3 1) satisfying (3 2) and (3 3) is

$$u(\xi) = \sqrt{\frac{-r}{s}}\tanh\left(\sqrt{\frac{-r}{2}}\xi\right)\sin\phi_o$$

$$\phi_o \in [0,2\pi) \tag{3 9}$$

$$v(\xi) = \sqrt{\frac{-r}{s}}\tanh\left(\sqrt{\frac{-r}{2}}\xi\right)\cos\phi_o$$

in which ϕ_o is related to λ through $\sin\phi_o = \dfrac{1}{\sqrt{1+\lambda^2}}$ This constant phase ϕ_o is a free parameter and reflects the infinite degeneracy of the ground state at this stage of the continuum model Fig 2 shows the trajectory of this $H = 0$ kink in the u-v plane It is clear from Fig 2 that the winding number η of the $H = 0$ kink is $\frac{1}{2}$ This is the winding number of an elementary excitation (excitation with the lowest energy) only for the case $N = 2$ For any other N this $H = 0$ kink will be a composite excitation

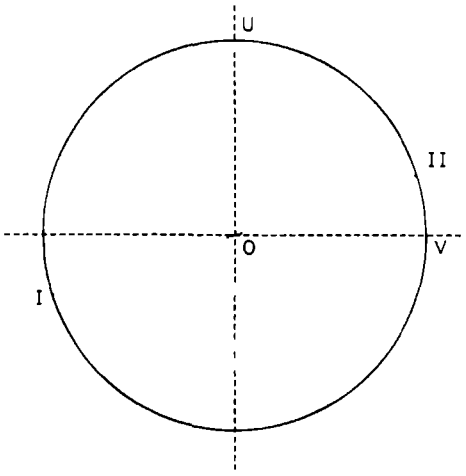

Figure 2. Top view of the trajectory of the H = 0 kink (3 9) starting at $\xi = -\infty$ in I and ending at $\xi = +\infty$ in II

A moving H = 0 kink is obtained from (3 9) by applying (2 22)

$$u(\xi-vt) = \sqrt{\frac{-r}{s}}\tanh(\gamma\sqrt{\frac{-r}{2}}(\xi-vt))\sin\phi_o$$
$$v(\xi-vt) = \sqrt{\frac{-r}{s}}\tanh(\gamma\sqrt{\frac{-r}{2}}(\xi-vt))\cos\phi_o \qquad (3\ 10)$$

The creation energy of the static H = 0 kink E_o follows directly from (2 27)

$$E_o(H=0) = \frac{1}{2}c^2\int_{-\infty}^{\infty} d\xi\{\frac{1}{2}(u'^2+v'^2)+\frac{1}{2}r(u^2+v^2)+\frac{1}{4}s(u^2+v^2)^2+\frac{r^2}{4s}\} \qquad (3\ 11)$$

so by using (3 2) one obtains

$$E_o(0) = c^2\int_{-\infty}^{\infty} d\xi\{\frac{1}{2}r(u^2+v^2)+\frac{1}{4}s(u^2+v^2)^2+\frac{r^2}{4s}\}$$

$$= \frac{1}{4}sc^2\int_{-\infty}^{\infty} d\xi\{u^2+v^2+\frac{r}{s}\}^2 = \frac{r^2c^2}{4s}\int_{-\infty}^{\infty} d\xi\ \frac{1}{\cosh^4(\sqrt{\frac{-r}{2}}\xi)}$$

$$= \frac{\sqrt{-2r^3}c^2}{3s} \tag{3 12}$$

The creation energy of a moving H = 0 kink $E_v(0)$ is given by

$$E_v(0) = \gamma E_o(0) = \gamma \frac{\sqrt{-2r^3}c^2}{3s} \tag{3 13}$$

with $\gamma \equiv \frac{1}{\sqrt{1-v^2/c^2}}$, a result which follows from eq (2 22)

The stability of the H = 0 kink may be investigated by looking at a solution of the form

$$\begin{aligned} u(\xi,t) &= u_o(\xi) + \delta u(\xi,t) \\ v(\xi,t) &= v_o(\xi) + \delta v(\xi,t) \end{aligned} \tag{3 14}$$

with $\{u_o,v_o\}$ the H = 0 kink in the rest frame (3 9) and $\{\delta u,\delta v\}$ sufficiently small We only have to study the stability problem for the kink in the rest frame because the equations of motion are Lorentz-invariant Therefore (in)stability in the rest frame implies (in)stability in any other frame connected to the rest frame by a Lorentz transformation Inserting (3 14) in (2 20) and using the fact that $\{u_o,v_o\}$ is a solution of (3 1) leads to the following set of equations linear in $\{\delta u,\delta v\}$

$$[\frac{\partial^2}{\partial\xi^2} - \frac{1}{c^2}\frac{\partial^2}{\partial t^2} - r - s(3u_o^2+v_o^2)]\delta u - 2su_ov_o\delta v = 0 \tag{3 15}$$

$$-2su_ov_o\delta u + [\frac{\partial^2}{\partial\xi^2} - \frac{1}{c^2}\frac{\partial^2}{\partial t^2} - r - s(u_o^2+3v_o^2)]\delta v = 0$$

Because (3 15) is a linear problem it is sufficient to consider

$$\begin{aligned} \delta u(\xi,t) &= u_1(\xi)e^{i\omega t} \\ \delta v(\xi,t) &= v_1(\xi)e^{i\omega t} \end{aligned} \tag{3 16}$$

If we substitute this ansatz in (3 15) we get the eigenvalue problem

$$\begin{bmatrix} -\frac{d^2}{d\xi^2} + r + s(3u_o^2+v_o^2) & 2su_ov_o \\ 2su_ov_o & -\frac{d^2}{d\xi^2} + r + s(u_o^2+3v_o^2) \end{bmatrix} \begin{bmatrix} u_1 \\ v_1 \end{bmatrix} = \frac{\omega^2}{c^2} \begin{bmatrix} u_1 \\ v_1 \end{bmatrix} \tag{3 17}$$

So the criterion for the linear stability of $\{u_o\ v_o\}$ is that the eigenvalues of the operator above are non negative, or in other words that ω must be real Using (3 9) this operator **L** becomes

$$\mathbf{L} = \begin{bmatrix} -\frac{d^2}{d\xi^2} + r[1 - 2w + w\cos 2\phi_o] & -rw\sin 2\phi_o \\ -rw\sin 2\phi_o & -\frac{d^2}{d\xi^2} + r[1 - 2w - w\cos 2\phi_o] \end{bmatrix} \tag{3 18}$$

with $w(\xi) \equiv \tanh^2(\sqrt{\frac{-r}{2}}\xi)$ **L** can be diagonalised by the orthogonal transformation

$$\mathbf{S} = \begin{bmatrix} \cos\phi_o & \sin\phi_o \\ -\sin\phi_o & \cos\phi_o \end{bmatrix} \tag{3 19}$$

leading to

$$\mathbf{L}' \equiv \mathbf{S}^T \mathbf{L}\mathbf{S} = \begin{bmatrix} -\frac{d^2}{d\xi^2} + r[1 \quad w(\xi)] & 0 \\ 0 & -\frac{d^2}{d\xi^2} + r[1 - 3w(\xi)] \end{bmatrix} \tag{3 20}$$

Thus the spectrum of **L** consists of the union of the spectra of the operators

$$L'_{11} = -\frac{d^2}{d\xi^2} + r\,\mathrm{sech}^2(\sqrt{\frac{-r}{2}}\xi) \tag{3 21}$$

and

$$L'_{22} = -\frac{d^2}{d\xi^2} + r[3\,\mathrm{sech}^2(\sqrt{-\frac{r}{2}}\xi) - 2] \tag{3 22}$$

The eigenvalues and the corresponding eigenvectors of these hermitian operators are completely known L'_{22} is the same operator as the one which appears in the linear stability problem of the kink in the ordinary ϕ^4 model [17] Its lowest eigenvalue is a discrete one and equal to zero Thus L'_{22} has a non-negative spectrum The lowest eigenvalue of L'_{11}, however, is discrete but negative, namely $\frac{1}{2}r$ The function $r\,\mathrm{sech}^2(\sqrt{\frac{-r}{2}}\xi)$ is the simplest reflectionless potential [18], well-known from the inverse scattering transform in the theory of solitons This implies that the lowest eigenvalue of **L** is negative and therefore that the $H = 0$ kink is linearly unstable The origin of this instability is physically

clear S (3 19) is the transformation to a very natural frame a frame with one axis parallel to the trajectory in the u-v plane (see Fig 2) and the other one perpendicular to it It is clear that the spectrum of L'_{22} determines the longitudinal stability and the spectrum of L'_{11} the transversal stability Longitudinal and transversal perturbations are of course independent, this is why L' (3 20) is diagonal The fact that the H = 0 kink is unstable with respect to transversal perturbations is just a reflection of the rotational invariance of the Mexican hat

4.4 Solitary wave excitations for H ≠ 0.

When H is non-zero the angular momentum $L_\perp$ (2 29) of the analogous mechanical particle is non-zero This means that the particle experiences an effective centrifugal repulsion near the origin, therefore its trajectory will avoid the origin Thus the solution of the stationary problem (2 23) when H ≠ 0 is qualitatively different from the one when H = 0 Because the problem depends continuously on H there is also a unique solution of the stationary equations when H ≠ 0 This solution approaches in a continuous manner the solution of the previous section as H goes to zero Using the stationary equations (2 23) and the expressions for the angular momentum ((2 26) and (2 29)) we easily arrive at

$$u''u + v''v = [r-\frac{1}{2}H^2](u^2+v^2)+s(u^2+v^2)^2-\frac{rH^2}{2s} \qquad (4\ 1)$$

If we now combine this with (2 25), (2 29) and the relation

$$(u^2+v^2) = 2(uu''+vv'')+2(u'^2+v'^2) \qquad (4\ 2)$$

we finally obtain the following equation for u^2+v^2, which we will denote by Ω from now on

$$\Omega'' = \frac{r^2-rH^2}{s} + (4r-H^2)\Omega + 3s\Omega^2 \qquad (4\ 3)$$

The constant function $\Omega = -\frac{r}{s}$ is a solution of this equation, therefore

$$\underline{\Omega} \equiv \Omega+\frac{r}{s} \qquad (4\ 4)$$

satisfies

$$\underline{\Omega}'' = -(H^2+2r)\underline{\Omega} + 3s\underline{\Omega}^2 \tag{4 5}$$

The boundary conditions for $\underline{\Omega}$ follow from (2 28) They are

$$\lim_{\xi\to\pm\infty} \underline{\Omega}(\xi) = \lim_{\xi\to\pm\infty} \underline{\Omega}'(\xi) = 0 \tag{4 6}$$

As is shown in appendix B (4 5) and (4 6) only have a non-trivial solution when

$$v^2 \equiv -(H^2+2r) > 0 \tag{4 7}$$

This unique solution is

$$\underline{\Omega}(\xi) = -\frac{v^2}{2s}\,\mathrm{sech}^2(\tfrac{1}{2}v\xi) \tag{4 8}$$

Actually (4 5) is *related* to the Korteweg-de Vries equation [18] Thus

$$\begin{aligned}\Omega(\xi) &= -\frac{r}{s} - \frac{v^2}{2s}\mathrm{sech}^2(\tfrac{1}{2}v\xi) \\ &= -\frac{r}{s}\tanh^2(\tfrac{1}{2}v\xi) + \frac{H^2}{2s}\mathrm{sech}^2(\tfrac{1}{2}v\xi) > 0\end{aligned} \tag{4 9}$$

From this we see that Ω approaches u^2+v^2 for the $H = 0$ kink (3 9) when H goes to zero

In order to derive the equation for the phase $\phi(\xi)$ of this solution we substitute

$$\begin{aligned}u(\xi) &= \sqrt{\Omega(\xi)}\,\sin\phi(\xi) \\ v(\xi) &= \sqrt{\Omega(\xi)}\,\cos\phi(\xi)\end{aligned} \tag{4 10}$$

into (2 26) and use (2 29) This leads to

$$\Omega\phi' = \tfrac{1}{2}H\Omega - L_\perp = \tfrac{1}{2}H\Omega + \frac{rH}{2s} \tag{4 11}$$

This equation can easily be integrated after substitution of Ω (4 9) The result is

$$\phi(\xi) = \phi(-\infty) - \mathrm{arctg}(\frac{v}{H}) - \mathrm{arctg}(\frac{v}{H}\tanh(\tfrac{1}{2}v\xi)) \tag{4 12}$$

So the phase difference $\Delta\phi$, defined by

$$\Delta\phi \equiv \phi(+\infty) - \phi(-\infty) \tag{4 13}$$

equals

$$\Delta\phi = -2 \operatorname{arctg}(\frac{v}{H}). \tag{4.14}$$

This means that the winding number η (2.8) of this solution varies continuously with r and H

$$\eta = -\frac{1}{\pi} \operatorname{arctg}(\frac{\sqrt{-(H^2+2r)}}{H}). \tag{4.15}$$

From now on we refer to this solution as the $H \neq 0$ solitary wave. It follows from (2.22) that the phase difference $\Delta\phi$ for a moving $H \neq 0$ solitary wave depends on its velocity v through the Lorentz-factor γ

$$\Delta\phi = -2 \operatorname{arctg}(\frac{\sqrt{-(\gamma^2H^2+2r)}}{\gamma H}). \tag{4.16}$$

It is clear that a moving $H \neq 0$ solitary wave only exists when

$$\gamma^2H^2 < -2r. \tag{4.17}$$

The initial phase $\phi(-\infty) \equiv \phi_0$ is just as in the case of the $H = 0$ kink a free parameter which reflects the infinite degeneracy of the ground state at this stage of the continuum model. Fig. 3 shows the trajectory of the $H \neq 0$ solitary wave in the u-v plane.

The creation energy of a static $H \neq 0$ solitary wave can again be calculated using (2.27). The result is

$$E_0(H) = \frac{c^2}{2s} \sqrt{-(H^2+2r)}(-\frac{2}{3}r+\frac{1}{6}H^2). \tag{4.18}$$

One can easily show that this is always smaller than the creation energy of the static $H = 0$ kink (3.12). For small values of H we have

$$E_0(H) \simeq E_0(0) - \frac{c^2}{16s} \frac{H^4}{\sqrt{-2r}}. \tag{4.19}$$

The creation energy of a moving $H \neq 0$ solitary wave is not simply related to the creation energy of a static one, like in the case of the $H = 0$ kink (cf. (3.12) and (3.13)). It is given by

$$E_v(H) = \gamma \frac{c^2}{2s} \sqrt{-(\gamma^2H^2+2r)}(-\frac{2}{3}r+[\frac{1}{2}-\frac{1}{3}\gamma^2]H^2). \tag{4.20}$$

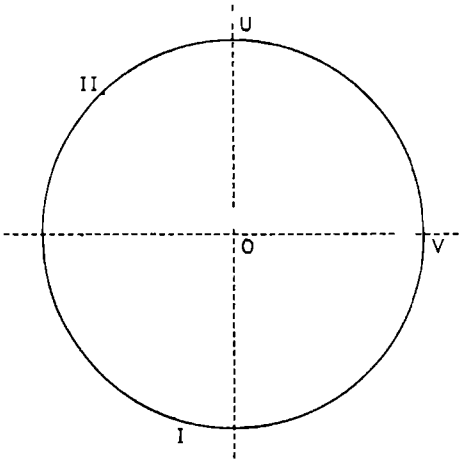

Figure 3. Top view of the trajectory of the $H \neq 0$ solitary wave starting at $\xi = -\infty$ in I and ending at $\xi = +\infty$ in II

Although we may expect that the $H \neq 0$ solitary wave is unstable, because its initial phase ϕ_0 is a free parameter and because the $H = 0$ kink is unstable which is a limiting case, the proof of this is not trivial and can only partly be given The stability here is determined by the sign of the lowest eigenvalue of the following hermitian operator

$$\mathbf{L} = \begin{bmatrix} -\frac{d^2}{d\xi^2}+r+s(3u_o^2+v_o^2) & H\frac{d}{d\xi}+2su_ov_o \\ -H\frac{d}{d\xi}+2su_ov_o & -\frac{d^2}{d\xi^2}+r+s(u_o^2+3v_o^2) \end{bmatrix} \tag{4 21}$$

with $\{u_o,v_o\}$ the static $H \neq 0$ solitary wave Thus we will first analyse the stability of the static $H \neq 0$ solitary wave Later on we will come back to the moving case Because $\mathbf{L}$ is a 2×2 hermitian operator there is a 2×2 unitary operator $\mathbf{U}$ which will diagonalize $\mathbf{L}$ But this is only a formal statement because finding $\mathbf{U}$ is a very complicated problem as is clear from the fact that the matrix elements of $\mathbf{L}$ consist of differential operators Therefore we will proceed along a somewhat different line First we will move the single derivative from the off-diagonal elements of $\mathbf{L}$ to the diagonal ones This is accomplished by the following unitary transformation

$$\mathbf{S} = \frac{1}{\sqrt{2}} \begin{bmatrix} 1 & \imath \\ \imath & 1 \end{bmatrix} \tag{4 22}$$

The result is

$$\mathbf{L}' \equiv \mathbf{S}^{+}\mathbf{L}\mathbf{S} = \begin{bmatrix} -\frac{d^2}{d\xi^2} + \imath H \frac{d}{d\xi} + r + 2s(u_o^2 + v_o^2) & s[2u_o v_o + \imath(u_o^2 - v_o^2)] \\ s[2u_o v_o - \imath(u_o^2 - v_o^2)] & -\frac{d^2}{d\xi^2} - \imath H \frac{d}{d\xi} + r + 2s(u_o^2 + v_o^2) \end{bmatrix} \tag{4 23}$$

After insertion of (4 10) this becomes

$$\mathbf{L}' = \begin{bmatrix} -\frac{d^2}{d\xi^2} + \imath H \frac{d}{d\xi} + r + 2s\Omega(\xi) & -\imath s e^{2\imath\phi(\xi)}\Omega(\xi) \\ \imath s e^{-2\imath\phi(\xi)}\Omega(\xi) & -\frac{d^2}{d\xi^2} - \imath H \frac{d}{d\xi} + r + 2s\Omega(\xi) \end{bmatrix}. \tag{4 24}$$

The single derivative in the diagonal elements of $\mathbf{L}'$ can then be removed by the following gauge transformation

$$\mathbf{G} = \begin{bmatrix} e^{\frac{1}{2}\imath H\xi} & 0 \\ 0 & e^{-\frac{1}{2}\imath H\xi} \end{bmatrix} \tag{4 25}$$

This last unitary transformation leads to

$$\mathbf{L} = \mathbf{G}^{+}\mathbf{L}\mathbf{G} = \begin{bmatrix} \mathbf{M} & \mathbf{V}^* \\ \mathbf{V} & \mathbf{M} \end{bmatrix} \tag{4 26}$$

where

$$\begin{aligned} \mathbf{M} &\equiv -\frac{d^2}{d\xi^2} + r - \frac{1}{4}H^2 + 2s\Omega(\xi) \\ &= -\frac{d^2}{d\xi^2} - v^2 \operatorname{sech}^2\left(\frac{1}{2}v\xi\right) - \left(r + \frac{1}{4}H^2\right) \end{aligned} \tag{4 27}$$

and

$$V \equiv is\, e^{-i(2\phi(\xi)-H\xi)}\Omega(\xi)$$

$$= e^{-i(2\phi(\xi)-H\xi+\frac{\tau}{2})}[r + \frac{1}{2}v^2\mathrm{sech}^2(\frac{1}{2}v\xi)] \tag{4 28}$$

The spectrum and the eigenstates of M are exactly known (see for instance [19]) This spectrum consists of one isolated eigenvalue

$$\varepsilon_b^{(0)} = -\frac{1}{16}(-3+\sqrt{17})^2v^2 - (r+\frac{1}{4}H^2) \equiv -\lambda v^2 - (r+\frac{1}{4}H^2) \tag{4 29}$$

with corresponding eigenstate $|b>$ and a continuum starting at $-(r+\frac{1}{4}H^2)$ with energies and states denoted by

$$\{\varepsilon_k^{(0)}, |k> \quad , \quad -\infty < k < \infty\} \tag{4 30}$$

These eigenstates form a complete orthonormal set, i e

$$<b|b> = 1, \quad <k|k'> = \delta(k-k'), \quad <b|k> = 0 \quad (\forall\, k)$$

$$\text{and} \quad |b><b| + \int_{-\infty}^{\infty} dk\, |k><k| = \mathbf{1} \tag{4 31}$$

These facts we will use in the subsequent analysis of $\mathbf{L}$ (4 26) Suppose now that the ground state of $\mathbf{L}$ is given by the normalised spinor

$$\Psi = \begin{bmatrix} |\psi> \\ |\phi> \end{bmatrix} \quad , \quad <\psi|\psi> + <\phi|\phi> = 1 \tag{4 32}$$

and the ground state energy by ε So we have

$$\begin{aligned} M|\psi> + V^*|\phi> &= \varepsilon|\psi> \\ V|\psi> + M|\phi> &= \varepsilon|\phi> \end{aligned} \tag{4 33}$$

For the moment we will assume that ε does not belong to the spectrum of M In that case we can formally invert the operator $M-\varepsilon\mathbf{1}$, so that we can write the second equation of (4 33) as

$$|\phi> = (\varepsilon\mathbf{1}-M)^{-1}V|\psi> \tag{4 34}$$

If we now substitute this in the first equation of (4 33) we get

$$[M + V^*(\varepsilon 1 - M)^{-1}V]\,|\psi> = \varepsilon\,|\psi>. \tag{4.35}$$

So ε is determined by the following equation

$$\varepsilon = \frac{<\psi|M|\psi>}{<\psi|\psi>} + \frac{<\psi|V^*(\varepsilon 1 - M)^{-1}V|\psi>}{<\psi|\psi>}. \tag{4.36}$$

By using the closure property of the eigenstates of M (cf. (4.31)) this transcendental equation becomes

$$\varepsilon - \frac{<\psi|M|\psi>}{<\psi|\psi>} = \frac{|<b|V|\psi>|^2}{<\psi|\psi>}\,\frac{1}{\varepsilon - \varepsilon_b^{(0)}} + \int_{-\infty}^{\infty} dk\,\frac{|<k|V|\psi>|^2}{<\psi|\psi>}\,\frac{1}{\varepsilon - \varepsilon_k^{(0)}}. \tag{4.37}$$

Because $|\psi>$ is not the ground state of M we have by the variational principle

$$\varepsilon_b^{(0)} < \frac{<\psi|M|\psi>}{<\psi|\psi>} \equiv \mu. \tag{4.38}$$

If we now plot both sides of (4.37) as a function of ε we get schematically Fig. 4.

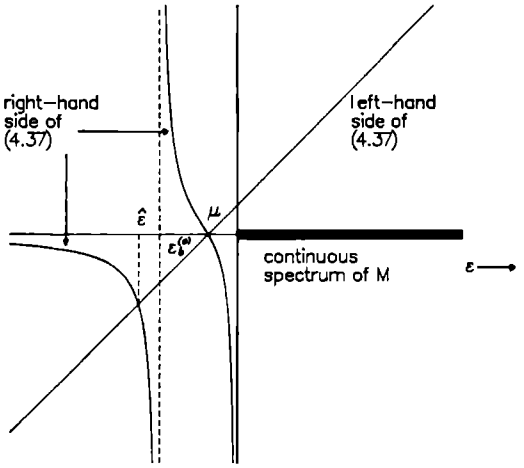

Figure 4. Plot of r h s and l h s of equation (4 37) as a function of ε. The intersection gives the discrete negative eigenvalue of M, which has also a continuous spectrum

Thus from this graphical analysis we may conclude that the ground state energy $\varepsilon(\equiv \hat{\varepsilon})$ is lower than $\varepsilon_b^{(0)}$, which is in agreement with the assumption we made about ε at the beginning. We will now use the variational principle to derive an upper and a lower limit for ε. These limits, although crude, are sufficient for our purpose. The variational principle for the operator $M+V^*(\varepsilon\mathbf{1}-M)^{-1}V$ tells us that

$$\begin{aligned}\varepsilon &< \langle b|M|b\rangle + \langle b|V^*(\varepsilon\mathbf{1}-M)^{-1}V|b\rangle \\ &= \varepsilon_b^{(0)} + \frac{|\langle b|V|b\rangle|^2}{\varepsilon-\varepsilon_b^{(0)}} + \int_{-\infty}^{\infty} dk \frac{|\langle k|V|b\rangle|^2}{\varepsilon-\varepsilon_k^{(0)}} \\ &< \varepsilon_b^{(0)} + \frac{|\langle b|V|b\rangle|^2}{\varepsilon-\varepsilon_b^{(0)}}. \end{aligned} \tag{4.39}$$

The last inequality follows from the fact that the integrand, and thus the integral, is negative for $\varepsilon < \varepsilon_k^{(0)}$ So (4.39) leads to

$$\varepsilon < \varepsilon_b^{(0)} - |\langle b|V|b\rangle| \leq \varepsilon_b^{(0)} - \inf_{-\infty<\xi<\infty} |V(\xi)|. \tag{4.40}$$

On the other hand by using the variational principle for the operators M and $(\varepsilon\mathbf{1}-M)^{-1}$ separately we get

$$\varepsilon = \frac{\langle\psi|M|\psi\rangle}{\langle\psi|\psi\rangle} + \frac{\langle\psi|V^*(\varepsilon\mathbf{1}-M)^{-1}V|\psi\rangle}{\langle\psi|\psi\rangle} > \varepsilon_b^{(0)} + \frac{\langle\psi|V^*V|\psi\rangle}{\langle\psi|\psi\rangle}\frac{1}{\varepsilon-\varepsilon_b^{(0)}} \tag{4.41}$$

and this leads to

$$\varepsilon > \varepsilon_b^{(0)} - \left[\frac{\langle\psi|V^*V|\psi\rangle}{\langle\psi|\psi\rangle}\right]^{1/2} \geq \varepsilon_b^{(0)} - \sup_{-\infty<\xi<\infty} |V(\xi)|. \tag{4.42}$$

So the conclusion is

$$\varepsilon_b^{(0)} - \sup_{-\infty<\xi<\infty} |V(\xi)| < \varepsilon < \varepsilon_b^{(0)} - \inf_{-\infty<\xi<\infty} |V(\xi)|. \tag{4.43}$$

From (4.28) it follows that

$$|V(\xi)| = |r+\frac{1}{2}\nu^2\operatorname{sech}^2(\frac{1}{2}\nu\xi)| \tag{4.44}$$

thus

$$\inf_{-\infty<\xi<\infty} |V(\xi)| = \min_{-\infty<\xi<\infty} |V(\xi)| = |V(0)| = \frac{1}{2}H^2 \qquad (4\ 45)$$

and

$$\sup_{-\infty<\xi<\infty} |V(\xi)| = |V(\xi\to\pm\infty)| = -r \qquad (4\ 46)$$

Therefore the upper limit for ε becomes

$$\varepsilon_b^{(0)} - \inf_{-\infty<\xi<\infty} |V(\xi)| = \lambda(H^2+2r) - (r + \frac{1}{4}H^2) - \frac{1}{2}H^2$$

$$= (\lambda-\frac{3}{4})H^2 + (2\lambda-1)r \qquad (4\ 47)$$

Because $\lambda = \frac{1}{16}(-3+\sqrt{17})^2 \simeq 0\ 079$ this upper limit for ε has no definite sign (the first contribution is negative while the second one is positive because r is negative). Therefore, this somewhat crude analysis only gives a definite answer to the stability question when the magnetic field H exceeds a certain threshold field H_c, which is given by

$$H_c = \sqrt{-r\frac{4-8\lambda}{3-4\lambda}} \simeq 1\ 12\ \sqrt{-r} \qquad (4.48)$$

In this case the $H \neq 0$ solitary wave is linearly unstable For a magnetic field below this threshold this upper limit is non-negative and therefore the question of stability of the $H \neq 0$ solitary wave is left open However as we mentioned before we may also expect that for these values of H this solitary wave will be unstable For a moving $H \neq 0$ solitary wave with velocity v the threshold field is reduced

$$H_c = \frac{1}{\gamma} H_c < H_c \quad , \quad \gamma = \left[1-\frac{v^2}{c^2}\right]^{-1/2} \qquad (4\ 49)$$

It is clear that when this $H \neq 0$ solitary wave is unstable, this unstability will neither be of a pure longitudinal nor of a pure transversal nature, but somewhere in between This is due to the fact that for a $H \neq 0$ solitary wave there is both a variation in the amplitude and in the phase

4.5 Phase pinning through mode-coupling

The continuum model (2 9) has rotational symmetry which implies that the ground state is degenerate in the phase For periodic structures, however, this phase freedom vanishes as a consequence of pinning mechanisms There are two types of such mechanisms When N = 2 or 4, additional terms in the Hamiltonian density appear leading to phase pinning This will be discussed in section 4 6 When N ≠ 1, 2 or 4 pinning may occur nevertheless as a consequence of mode coupling Because of the nonlinearity of the model the ground state will contain not only the basic mode with wave vector q but also higher harmonics The idea then is to devise an effective theory for the fundamental mode alone by eliminating the higher harmonics using their equations of motion This method can be applied in principle to the case of an arbitrary large superstructure, i e an arbitrary large value of N However the amount of algebra increases exceedingly with N Therefore we will show the method for a low value of N From this case it will become clear that when N increases, the magnitudes of the pinning terms decrease This means that this kind of pinning is absent in a truly incommensurate case

Let us start with the derivation of the continuum model which is appropriate for a ground state containing a fundamental mode and several higher harmonics The starting point is again the discrete Hamiltonian (1 1)

$$\mathcal{H} = \sum_n \{\frac{1}{2}x_n^2 + \frac{1}{2}Ax_n^2 + \frac{1}{4}x_n^4 + Bx_nx_{n-1} + Dx_nx_{n-2}\} \tag{5 1}$$

For convenience we assume periodic boundary conditions with a period $\mathcal{N}$, i e

$$x_{n+\mathcal{N}} = x_n \tag{5 2}$$

Let us first transform the Hamiltonian (5 1) to a reciprocal space form, using

$$x_n(t) = \frac{1}{\sqrt{\mathcal{N}}} \sum_k e^{ikn}\tilde{x}_k(t) \tag{5 3}$$

where the sum runs over the discrete k-values consistent with the periodic boundary conditions within the first Brillouin zone $(-\pi,\pi]$ This results in

$$\mathcal{H} = \sum_k \{\frac{1}{2}\tilde{x}_k\tilde{x}_{-k} + \frac{1}{2}\omega^2(k)x_k\tilde{x}_{-k}\}$$

$$+ \frac{1}{4\mathcal{N}} \sum_{k_1 k_2 k_3 k_4} \tilde{x}_{k_1}\tilde{x}_{k_2}\tilde{x}_{k_3}\tilde{x}_{k_4}\,\Delta(k_1+k_2+k_3+k_4) \tag{5 4}$$

$$\omega^2(k) = A+2B\cos(k)+2D\cos(2k) \tag{5 5}$$

and

$$\Delta(k) \equiv \sum_{p\in Z} \delta_{k\, 2\pi p} \tag{5 6}$$

the so-called "lattice Kronecker delta" Notice that $\omega^2(k)$, given by (5 5) is equal to the coefficient a (2 11) in the continuum Hamiltonian (2 9) Now suppose that the parameters A, B and D are such that $\omega^2(k)$ looks like in Fig 5

We take the fundamental wave vector to be

$$q = 2\pi\frac{L}{N} \quad , \quad L < N \quad , \quad L \text{ and } N \text{ relative prime} \tag{5 7}$$

The Fourier spectrum of the ground state configuration contains the following wave vectors

$$\{k = \ell q \,|\, \ell \in I_G\} \qquad \begin{array}{l} \text{with } I_G \equiv \{-\frac{N}{2}+1,-\frac{N}{2}+2, \quad ,\frac{N}{2}\} \text{ when N is even} \\ \text{or } I_G \equiv \{-\frac{N-1}{2},-\frac{N-1}{2}+1, \quad ,\frac{N-1}{2}\} \text{ when N is odd} \end{array} \tag{5 8}$$

We describe non-linear excitations in the system by taking into account a small dispersion around each of the modes which are present in the ground state (5 8), i e by

$$\begin{array}{l} \tilde{x}_k \neq 0 \ , \ k = \ell q+\varkappa \\ \qquad\qquad\qquad\qquad \ell \in I_G, |\varkappa| < k_c \\ \tilde{x}_k = 0 \ , \ k \neq \ell q+\varkappa \end{array} \tag{5 9}$$

This small dispersion is of course just a reflection of the fact that we want to describe low-lying non-linear excitations by slowly varying fields The inverse of the cut-off k_c^{-1} is the smallest scale over which these field vary This cut-off k_c is rather arbitrary, but it at least has to obey

$$k_c \leq \frac{\pi}{N} \tag{5 10}$$

To shorten the notation we write the non-zero Fourier modes $\tilde{x}_{\ell q+\varkappa}$ as

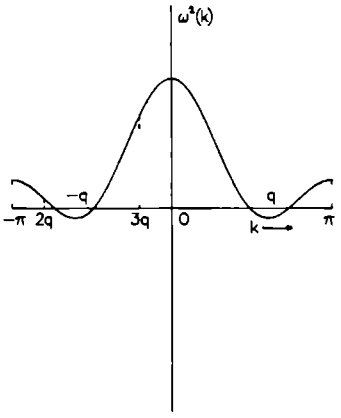

Figure 5 Graph of $\omega^2(k)$ well below the transition from the normal to modulated phase The positions of some higher harmonics of q are shown

$$Q_{\ell\varkappa} \quad , \quad \ell \in I_G \quad , \quad |\varkappa| < k_c \tag{5 11}$$

So our Hamiltonian (5 4) becomes

$$\mathcal{H} = \sum_{\ell \in I_c} \sum_{|\varkappa| < k_c} \{\frac{1}{2} Q_{\ell\varkappa} Q_{-\ell\,-\varkappa} + \frac{1}{2}\omega^2(\ell q+\varkappa) Q_{\ell\varkappa} Q_{-\ell\,-\varkappa}\}$$

$$+ \frac{1}{4N} \sum_{\substack{\ell_1 \ell_2 \ell_3 \ell_4 \\ \in I_c}} \sum_{\substack{\varkappa_1 \varkappa_2 \varkappa_3 \varkappa_4 \\ |\varkappa| < k_c \\ (i=1 \quad 4)}} Q_{\ell_1 \varkappa_1} Q_{\ell_2 \varkappa_2} Q_{\ell_3 \varkappa_3} Q_{\ell_4 \varkappa_4} \Delta([\ell_1+\ell_2+\ell_3+\ell_4]q$$

$$+ \varkappa_1+\varkappa_2+\varkappa_3+\varkappa_4) \tag{5 12}$$

Now in [13] one observed that only the lowest harmonics have a non-negligible amplitude in the ground state Furthermore, the magnitude of $\omega^2(\ell q, \ell \neq \pm 1)$ is large compared to the magnitude of $\omega^2(q)$ (see Fig 5) Therefore, we only consider in the description of the non-linear excitations slow variations of those modes which have a non negligible amplitude in the ground state

$$\begin{aligned} &\omega^2(\ell q+\varkappa) \simeq \omega^2(\ell q) \qquad \text{for } \ell \neq \pm 1 \\ &\omega^2(\pm q \pm \varkappa) \simeq \omega^2(q) - 2b\varkappa + c^2\varkappa^2 \end{aligned} \tag{5 13}$$

with b and c^2 given by (2 12) and (2 13) respectively If the cut-off k_c is small enough then

$$\Delta([\ell_1+\ell_2+\ell_3+\ell_4]q+\varkappa_1+\varkappa_2+\varkappa_3+\varkappa_4) = \Delta([\ell_1+\ell_2+\ell_3+\ell_4]q)\times\delta(\varkappa_1+\varkappa_2+\varkappa_3+\varkappa_4) \tag{5 14}$$

This last relation is actually the core of the continuum limit With these approximations the Hamiltonian becomes

$$\begin{aligned}\mathcal{H} \simeq \sum_{|\varkappa|<k_c}\{\sum_{\ell}(\frac{1}{2}Q_{\ell\varkappa}Q_{-\ell\,-\varkappa} + \frac{1}{2}\omega^2(\ell q)Q_{\ell\varkappa}Q_{-\ell\,-\varkappa}) - 2b\varkappa Q_{1\varkappa}Q_{-1\,-\varkappa} \\ + c^2\varkappa^2 Q_{1\varkappa}Q_{-1\,-\varkappa}\} + \frac{1}{4\mathcal{N}}\sum_{\ell_1\ell_2\ell_3\ell_4}\Delta([\ell_1+\ell_2+\ell_3+\ell_4]q) \\ \times \sum_{|\varkappa_1|<k_c}\sum_{\varkappa_2<k_c}\sum_{\varkappa_3<k_c} Q_{\ell_1\varkappa_1}Q_{\ell_2\varkappa_2}Q_{\ell_3\varkappa_3}Q_{\ell_4\,-(\varkappa_1+\varkappa_2+\varkappa_3)}\end{aligned} \tag{5 15}$$

We now Fourier transform this Hamiltonian This transformation results in

$$\begin{aligned}\mathcal{H} = \int d\xi\{\sum_{\ell}(\frac{1}{2}|Q_\ell|^2+\frac{1}{2}\omega^2(\ell q)|Q_\ell|^2)+ib(Q_1Q_1^*-Q_1Q_1^*) \\ + c^2|Q_1|^2+\frac{1}{4}\sum_{\ell_1\ell_2\ell_3\ell_4}\Delta([\ell_1+\ell_2+\ell_3+\ell_4]q)Q_{\ell_1}Q_{\ell_2}Q_{\ell_3}Q_{\ell_4}\}\end{aligned} \tag{5 16}$$

Notice that when only the fundamental mode is taken into account, i e when in the sums only the terms with $\ell = 1$ and $\ell = -1$ contribute, we end up again with (2 10) We will now restrict ourselves to the stationary version of (5 16), i e

$$\begin{aligned}\mathcal{H}_o = \int d\xi\{\frac{1}{2}\sum_{\ell}\omega^2(\ell q)|Q_\ell|^2+ib(Q_1Q_1^*-Q_1Q_1^*) \\ + c^2|Q_1|^2+\frac{1}{4}\sum_{\ell_1\ell_2\ell_3\ell_4}\Delta([\ell_1+\ell_2+\ell_3+\ell_4]q)Q_{\ell_1}Q_{\ell_2}Q_{\ell_3}Q_{\ell_4}\}\end{aligned} \tag{5 17}$$

The equations of motion associated with this stationary Hamiltonian are

$$\begin{aligned}\frac{\delta\mathcal{H}_o}{\delta Q_\ell^*} &= 0 \qquad , \ \ell \neq \pm 1 \\ (\frac{\delta\mathcal{H}_o}{\delta Q_\ell^*}) - \frac{\delta\mathcal{H}_o}{\delta Q_\ell^*} &= 0 \ , \ \ell = \pm 1\end{aligned} \tag{5 18}$$

or explicitly

$$\omega^2(\ell q)Q_\ell + \sum_{\ell_1 \ell_2 \ell_3} \Delta([\ell_1+\ell_2+\ell_3-\ell]q)Q_{\ell_1} Q_{\ell_2} Q_{\ell_3} = 0 \ , \ \ell \neq -1$$

$$c^2 Q_1 - 2ibQ_1 - \omega^2(q)Q_1$$

$$- \sum_{\ell_1 \ell_2 \ell_3} \Delta([\ell_1+\ell_2+\ell_3-1]q)Q_{\ell_1} Q_{\ell_2} Q_{\ell_3} = 0 \qquad + c.c \tag{5.19}$$

As we mentioned earlier in this section the idea is to use the equations of motion of the higher harmonics to eliminate these modes in $\mathcal{H}_0$, or equivalently in the equation-of-motion of the fundamental mode In this way we end up with an effective theory for the fundamental mode In general this is a difficult procedure, therefore we will show the procedure for a simple case, namely N = 6 In that case the third harmonic $3q = \pi$ cannot be neglected in the ground state After some combinatorics, we end up with the following Hamiltonian

$$\mathcal{H}_0 = \int d\xi \{\omega^2(\frac{\pi}{3})|Q_1|^2 + \frac{3}{2}|Q_1|^4 + ib(Q_1 Q_1^* - Q_1 Q_1^*) + c^2|Q_1|^2$$

$$+ \frac{1}{2}\omega^2(\pi)Q_3^2 + \frac{1}{4}Q_3^4 + Q_3(Q_1^3 + Q_1^{*3}) + 3Q_3^2|Q_1|^2\} \tag{5.20}$$

and with the following equation-of-motion for Q_3

$$\omega^2(\pi)Q_3 + Q_3^3 + 6Q_3|Q_1|^2 + Q_1^3 + Q_1^{*3} = 0 \tag{5.21}$$

Now we make the following plausible assumptions

$$\begin{aligned} |Q_3| &\ll 1 \\ |Q_1|^2 &\ll \omega^2(\pi) \end{aligned} \tag{5.22}$$

With these assumptions, we deduce from (5.21) that approximately

$$Q_3 \simeq -\frac{1}{\omega^2(\pi)}[Q_1^3 + Q_1^{*3}] \tag{5.23}$$

If we now substitute this back in (5.20), we get the following effective Hamiltonian for Q_1

$$\mathcal{H}_0^{\text{eff}} = \int d\xi \{\omega^2(\frac{\pi}{3})|Q_1|^2 + \frac{3}{2}|Q_1|^4 - \frac{1}{2\omega^2(\pi)}(Q_1^3 + Q_1^{*3})^2$$

$$+ ib(Q_1'Q_1^* - Q_1Q_1'^*) + c^2|Q_1|^2\} \tag{5.24}$$

The structure of this effective Hamiltonian becomes clearer by introducing the real fields ϱ and ϕ, defined by

$$Q_1(\xi) = \varrho(\xi)e^{i\phi(\xi)}. \tag{5.25}$$

This leads to

$$\mathcal{H}_o^{eff} = \int d\xi\{c^2(\varrho'^2 + \varrho^2\phi'^2) - 2b\varrho^2\phi' + U(\varrho,\phi)\} \tag{5.26}$$

with

$$U(\varrho,\phi) = \omega^2(\frac{\pi}{3})\varrho^2 + \frac{3}{2}\varrho^4 - \frac{\varrho^6}{\omega^2(\pi)}(1+\cos 6\phi). \tag{5.27}$$

The ground states follow from

$$\frac{\partial U}{\partial \phi} = \frac{\partial U}{\partial \varrho} = 0. \tag{5.28}$$

It is clear that the phase ϕ is pinned because of the $\cos 6\phi$ term. The correction to the "inverted mexican hat" is small, as is clear from the second assumption in (5.22). Therefore the degenerate ground states are approximately located at

$$\varrho \simeq \left[\frac{-\omega^2(\frac{\pi}{3})}{3}\right]^{1/2} \quad ; \quad \phi = \phi_m = \frac{\pi}{3}m \quad (m = 0,\ldots,5) \tag{5.29}$$

notice that $\omega^2(\frac{\pi}{3}) < 0$ because we are below the transition from the P-phase to the N = 6 superstructure phase.

4.6 Continuum model description in the case of N = 4

The case of N = 4 or $q = \frac{\pi}{2}$ is a special one because already in the one-mode approximation a term is present in the continuum Hamiltonian which pins the phase of the fundamental mode. This extra term originates from the fact that we now have

$$e^{4iqn} = 1 \qquad (\forall\, n). \tag{6.1}$$

Therefore the following term appears in the continuum Hamiltonian

$$\frac{1}{4}(Q^4 + Q^{*4}). \tag{6.2}$$

Thus the complete continuum Hamiltonian is given by

$$\mathcal{H} = \int_{-\infty}^{\infty} d\xi\{|P|^2 + (A-2D)|Q|^2 + \frac{3}{2}|Q|^4 + \frac{1}{4}(Q^4+Q^{*4})$$

$$+ iB(Q'Q^*-QQ'^*) + 4D|Q'|^2\} \tag{6.3}$$

with $P \equiv \dot{Q}$. In this expression we have used the specific values of the coefficients a, b and c^2 ((2.11)-(2.13)) for $q = \frac{\pi}{2}$. In terms of the amplitude field ϱ and the phase field ϕ this Hamiltonian becomes

$$\mathcal{H} \simeq \int_{-\infty}^{\infty} d\xi\{\dot{\varrho}^2 + \varrho^2\dot{\phi}^2 + (A-2D)\varrho^2 + \frac{3}{2}\varrho^4 + \frac{1}{2}\varrho^4\cos 4\phi$$

$$- 2B\varrho^2\phi' + 4D(\varrho'^2+\varrho^2\phi'^2)\}. \tag{6.4}$$

From this last expression it is clear that the pinning term is not small compared to the other potential terms.

The equations of motion associated with (6.3) are

$$\begin{aligned} \ddot{Q}-4DQ''+2iBQ' &= -(A-2D)Q-3|Q|^2Q-Q^{*3} \\ \ddot{Q}^*-4DQ^{*''}-2iBQ^{*'} &= -(A-2D)Q^*-3|Q|^2Q^*-Q^3 \end{aligned} \tag{6.5}$$

or in terms of the real fields u and v (see (2.18-19))

$$\begin{aligned} \ddot{u}-4Du''+2Bv' &= -(A-2D)u-u^3 \\ \ddot{v}-4Dv''-2Bu' &= -(A-2D)v-v^3. \end{aligned} \tag{6.6}$$

These equations decouple for B = 0, then both u and v satisfy

$$\ddot{g} - 4Dg'' = (2D-A)g - g^3. \tag{6.7}$$

From the phase diagram (Fig. 1) it can be seen that the transition from the P-phase to the N = 4 superstructure phase takes place at $(\frac{A}{D} = 2)$. Therefore at

all points ($\frac{A}{D} < 2, B = 0$) we have the following kink solution of (6 7)

$$g(\xi - vt) = \sqrt{2D-A}\ \tanh\left(\frac{1}{4D}\sqrt{2D-A}\,\gamma(\xi - vt)\right) \tag{6 8}$$

with $\gamma \equiv \dfrac{1}{\sqrt{1-v^2/4D}}$

We can now construct the following kink solutions of (6 6) for $B = 0$

$$\begin{aligned}
&(i)\quad u = g \\
&\qquad v = \pm\sqrt{2D-A} \\
&(ii)\quad u = \pm\sqrt{2D-A} \\
&\qquad v = g \\
&(iii)\quad u = \pm v = g
\end{aligned} \tag{6 9}$$

These solutions are shown in Fig 6

It is clear from this figure that the winding number η of these kinks is respectively $\frac{1}{4}$ (phase shift $\frac{\pi}{2}$) for the solutions (i) and (ii) and $\frac{1}{2}$ phase shift π) for the solutions (iii) Therefore the solutions (i) and (ii) correspond to elementary excitations while the solutions (iii) correspond to a composite excitations In fact these composite excitations are actually a superposition of elementary excitations ($\eta = \frac{1}{4}$) of the odd (v)- and even (u) sites It is not hard to show that all these solutions are linearly stable The analysis is the same as for the case of the longitudinal stability of the $H = 0$ kink

For the case $B \neq 0$ we make the additional assumption that only the phase of Q varies, which is known as the Constant Amplitude Approximation (CAA) [20] Thus the Ansatz for solving (6 5) is

$$Q(\xi,t) = \varrho e^{i\phi(\xi\, t)} \quad , \quad \varrho \text{ constant} \tag{6 10}$$

Here ϱ is real and equal to the magnitude of Q in the ground state We substitute this in the Hamiltonian (6 4) we get

$$\mathcal{H} = \int_{-\infty}^{\infty} d\xi\{\varrho^2\phi^2 + (A-2D)\varrho^2 + \frac{3}{2}\varrho^4 + \frac{1}{2}\varrho^4\cos 4\phi + 4D\varrho^2\phi^2\}$$

$$- 2B\varrho^2[\phi(+\infty) - \phi(-\infty)] \tag{6 11}$$

Thus the equation of motion for the phase ϕ, i e

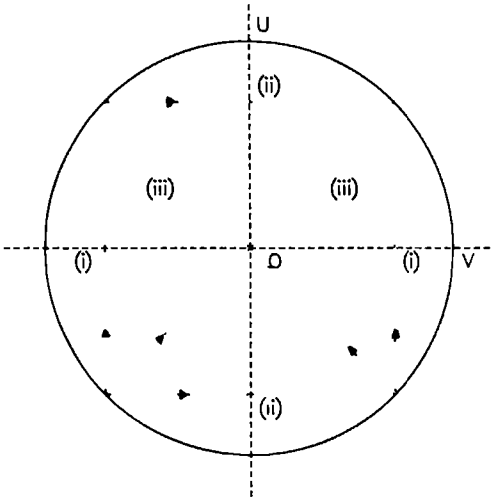

Figure 6. Possible kink solutions of (6 6) when B = 0

$$\frac{\partial}{\partial t}\left(\frac{\delta \mathcal{H}}{\delta \phi}\right) - \frac{\partial}{\partial \xi}\left(\frac{\delta \mathcal{H}}{\delta \phi}\right) = - \frac{\delta \mathcal{H}}{\delta \phi} \tag{6 12}$$

is equal to

$$\phi - 4D\phi = 2\varrho^2 \sin 4\phi \tag{6 13}$$

Therefore $\tilde{\phi}$ defined by

$$\phi(\xi,t) = (2\ell+1)\frac{\pi}{4} + \frac{1}{4}\tilde{\phi}(\sigma,\tau) \quad , \quad \sigma \equiv \frac{2\sqrt{2}}{c}\varrho\xi \, , \, \tau \equiv \frac{2\sqrt{2}}{c}\varrho t$$

$$(\ell = 0, \quad ,3) \tag{6 14}$$

with $c \equiv 2\sqrt{D}$ satisfies

$$\tilde{\phi}'' - \frac{1}{c^2}\ddot{\tilde{\phi}} = \sin\tilde{\phi} \quad , \quad ' \equiv \frac{\partial}{\partial \sigma} \, , \quad \cdot \equiv \frac{\partial}{\partial \tau} \tag{6 15}$$

which is the well-known completely integrable sine-Gordon equation [18] This equation has the following one-soliton solutions

$$\tilde{\phi}(\sigma-v\tau) = 4.\text{arctg}(\exp[\pm\gamma(\sigma-v\tau)]) \tag{6.16}$$

with $\gamma \equiv \dfrac{1}{\sqrt{1-v^2/c^2}}$. These solutions are in the original variables given by

$$\phi(\xi-vt) = (2\ell+1)\frac{\pi}{4} + \text{arctg}(\exp[\pm\frac{2\sqrt{2}}{c}\varrho\gamma(\xi-vt)]). \tag{6.17}$$

It is easy to see that the actual value of ϱ is given by

$$\varrho = \sqrt{\frac{1}{2}(2D-A)} \tag{6.18}$$

and that the energy of these one-soliton solutions is

$$E_{\pm} = (4\gamma^2-1)\sqrt{2D}(\sqrt{\frac{1}{2}(2D-A)})^3$$

$$\pm\frac{\pi}{2}B(2D-A) \tag{6.19}$$

relative to the (infinite) energy of the ground state. The CAA is not restricted to this case only. Also for other values of N one can use this approximation. But it is only a useful approximation if phase pinning terms are taken into account, as in the previous section. In the next section we will see that although the amplitude always varies, the CAA is not a bad approximation.

A somewhat more refined continuum model can be obtained by introducing the following slowly varying fields u and v

$$\begin{aligned} x_{4n}(t) &\equiv u(2n,t) & x_{4n+2}(t) &\equiv -u(2n+1,t) \\ & \text{and} & & \\ x_{4n+1}(t) &\equiv v(2n,t) & x_{4n+3}(t) &\equiv -v(2n+1,t). \end{aligned} \tag{6.20}$$

This leads, after some algebra, to the following continuum Hamiltonian

$$\mathcal{H} = \int_{-\infty}^{\infty} \{\frac{1}{2}(\dot{u}^2+\dot{v}^2) + \frac{1}{2}(A-2D)(u^2+v^2) + \frac{1}{4}(u^4+v^4)$$

$$+ B(uv'-u'v) + 2D(u'^2+v'^2) + 2Bu'v'\}. \tag{6.21}$$

If we write (6.3) in terms of the fields u and v defined by

$$Q = \frac{1}{2}(u - iv) \tag{6 22}$$

we obtain

$$\mathcal{H} \simeq \frac{1}{2}\int_{-\infty}^{\infty} d\xi\{\frac{1}{2}(u^2+v^2) + \frac{1}{2}(A-2D)(u^2+v^2) + \frac{1}{4}(u^4+v^4)$$

$$+ B(uv - u\,v) + 2D(u'^2+v'^2)\} \tag{6 23}$$

If we compare this Hamiltonian to the new one (6 21) we notice a distinct difference, apart from the irrelevant factor $\frac{1}{2}$ in front of (6 23) This difference is the appearance of non-diagonal elements of the so-called "mass tensor" in (6 21) This "mass tensor" M_{ij} is of course defined by the following contribution to the Hamiltonian

$$\frac{1}{2}M_{11}u'^2 + \frac{1}{2}M_{22}v'^2 + \frac{1}{2}(M_{12}+M_{21})u\,v \quad , \quad M_{12} = M_{21} \tag{6 24}$$

The corresponding equations of motion of (6 21) are given by

$$\begin{aligned} \ddot{u} - 4Du - 2Bv + 2B\dot{v} &= -(A-2D)u - u^3 \\ \ddot{v} - 2B\dot{u} - 4Dv - 2B\dot{u} &= -(A-2D)v - v^3 \end{aligned} \tag{6 25}$$

These equations of motion are more complicated than the ones corresponding to (6 23), that is to say (6 6) Once again they decouple for B = 0 leading to

$$\begin{aligned} \ddot{u} - 4Du &= (2D-A)u - u^3 \\ \ddot{v} - 4Dv &= (2D-A)v - v^3 \end{aligned} \tag{6 26}$$

Therefore the same kink solutions (6 9) can be found as for the other model The CAA however does not lead to a manageable problem in this case

4.7 Discrete systems

If the domain walls have a width of several times (≥ 3) the length of a unit-cell, then a continuum approximation is an appropriate way for describing the system However, when the typical width is smaller, effects of the discreteness of the underlying lattice will show up To study the discrete dynamics corresponding to (1 1) we integrate the equations of motion (2 2) numerically using the analytical solutions of the continuum approximation as initial configurations This strategy has been extensively used by many people [1 3,5,8,9 11]

in analogous studies We supplement these equations of motion

$$\ddot{x}_n = -Ax_n - x_n^3 - B(x_{n-1}+x_{n+1}) - D(x_{n-2}+x_{n+2}) \qquad (7\ 1)$$

for a finite system of say $\mathcal{N} = pN$ (p integer) sites with the following boundary conditions

$$x_1 = x_2 = x_{\mathcal{N}-1} = x_{\mathcal{N}} = 0 \qquad (7\ 2)$$

We use these boundary conditions because we will only study the dynamics of single domain walls, for which for instance periodic boundary conditions cannot be used

To integrate (7 1) we first transform this second order system to a first order system in the usual way, thereby doubling the number of equations This first order system is then integrated using a so-called Merson form of the Runge-Kutta method (see for instance [21]) The initial configuration is given by

$$\begin{aligned} x_n(0) &= e^{iqn}Q(n) + e^{-iqn}Q^*(n) \qquad (n=1, \ \mathcal{N}) \\ \dot{x}_n(0) &= -\nu\varkappa[e^{iqn}Q(n) + e^{-iqn}Q^*(n)] \quad (n=3, \ \mathcal{N}-2) \end{aligned} \qquad (7\ 3)$$

in the "sinusoidal" case and by a straightforward generalisation in the "non-sinusoidal" case As we mentioned before Q is an analytical solitary wave solution of the appropriate continuum model The parameter $\varkappa$ determines the "velocity" of the initial configuration The value of this parameter corresponding to the continuum solution is one However other choices of $\varkappa$ offer a possibility for decoupling the width and the velocity of Q in the initial configuration The fact that the width of Q depends on its velocity is due to the Lorentz-like invariance (cf (2 22)) of the equations of motion in the continuum approximation

At times $t > 0$ we can locate the domain wall which is present in the configuration by looking at the displacement of the same particle (any of the N) in each unit-cell of the system It is clear that by this procedure we eliminate the fast-varying n dependence (e^{iqn}) of the displacement-field x_n This procedure does not tell us anything about the structure of the domain wall on scales smaller than the length of a unit-cell, i e N This is however sufficient for most of our purposes Later on in this section we will describe another procedure which interpolates the structure of a domain wall down to the scale of a lattice-constant, i e 1

We will now discuss some of the results which we obtained for two representative cases These representative cases are a chain of 400 particles for which the parameters A, B and C are chosen such that the ground state is a period 4 (N = 4) superstructure and a chain of 360 particles with a period 6

(N = 6) ground state configuration The latter case is of interest because a truly incommensurate ground state with a modulation wave vector q near $\pi/3$ (N = 6) can be described as an N = 6 superstructure with defects, such a defect being a domain wall within this commensurate ground state A single domain wall then corresponds to the limiting situation just before the incommensurate ground state becomes commensurate, the so-called lock-in transition

Fig 7a shows the displacements of every third particle in each of the sixty unit-cells at intervals of ten time-steps The parameters A, B and D are in this case 0 733, −0 480 and 0 26 which implies A/D = 2 822 and B/D = −1 846 respectively In the phase-diagram (Fig 1) this corresponds to a point in the "sinusoidal" region of the N = 6 superstructure phase For reasons of clarity we have connected the displacements of successive points by straight line segments Here Q in the initial configuration is a H ≠ 0 solitary wave with a phase difference $\Delta\phi$ (4 16) of $-\pi/3$ This phase difference is obtained by taking the velocity v equal to 0 5

This figure clearly demonstrates the existence of a propagating domain wall in the discrete system This domain wall connects two neighbouring ground state phases ($\Delta\phi = -\pi/3$) of the system The fact that the wall is very smooth or putting it differently that no noise can be seen on this scale indicates that the domain wall is to a good degree an independent mode of the system which is fairly well described by the continuum model of section 4 2 Although there is no noise visible in this figure, it is surely present albeit with a very small intensity

In section 4 4 we showed that the H ≠ 0 solitary wave is a linearly unstable solution of the equations of motion in the continuum limit at least if the magnetic field H is large enough, that is to say when

$$H > H_c \equiv \frac{1}{\gamma}\sqrt{-r\frac{4-8\lambda}{3-4\lambda}} \sim 1\ 12\ \frac{1}{\gamma}\sqrt{-r} \qquad (7\ 4)$$

with $\lambda \equiv \frac{1}{16}(-3+\sqrt{17})^2 \simeq 0\ 079$ and $\gamma = \frac{1}{\sqrt{1-v^2/c^2}}$ For smaller values of H our crude stability analysis was not conclusive It is easy to verify that for the present choice of the parameters A B, D and v condition (7 4) is satisfied ($H = 0\ 092 > 0\ 088 = H_c$), therefore the H ≠ 0 solitary wave in the initial configuration is linearly unstable It is clear from Fig 7 that at least on the displayed time-scale, i e about 100 time steps, no manifestation of this instability of the initial configuration is noticeable The discrete kink nicely propagates through the system without changing its shape

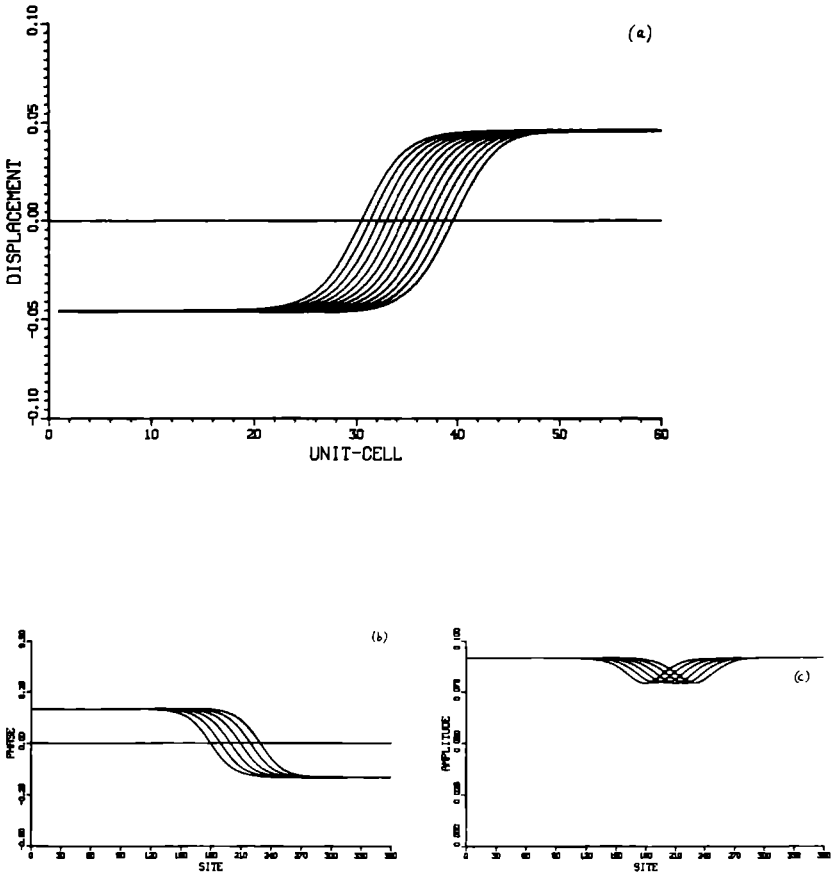

Figure 7. (a) Propagating kink with a width of about 10 unit-cells within an N = 6 superstructure with a sinusoidal modulation (b) Evolution of its phase (c) Evolution of its amplitude

One can also monitor the evolution of the amplitude and the phase of the domain wall at each site This amplitude Δ_n and phase ϕ_n are defined by

$$x_n(t) = \Delta_n(t)\sin(qn+\phi_n(t)) \qquad (n = 1, \ldots \mathcal{N}) \tag{7 5}$$

in the "sinusoidal" case In order to calculate these Δ's and ϕ's for a given set of the x's, we approximate $x_{n+1}(t)$ by

$$x_{n+1}(t) \simeq \Delta_n(t)\sin(qn+q+\phi_n(t)) \qquad (n = 1, \ldots \mathcal{N}-1) \tag{7 6}$$

In this way we obtain at each of the intermediate sites $n = 1, \ldots \mathcal{N}-1$ two equations (7 5-7 6) for two unknowns Δ_n and ϕ_n The solution being

$$\Delta_n(t) = \frac{1}{|\sin q|}\sqrt{x_n^2+x_{n+1}^2-2x_nx_{n+1}\cos(q)}$$

$$\phi_n(t) = \operatorname{arctg}\left[\frac{x_n\sin(qn+q)-x_{n+1}\sin(qn)}{x_{n+1}\cos(qn)-x_n\cos(qn+q)}\right] \qquad (n = 1, \ldots \mathcal{N}-1) \tag{7 7}$$

In practice the approximation (7 6) introduces some numerical noise into Δ_n and ϕ_n, therefore in addition we apply a cubic spline smoothing to these functions

In Fig 7b,c we show this phase (b) and amplitude (c) at successive instants of time ($\Delta t = 20$) Such a phase will always be measured in units of π, so it is clear from Fig 7b that the phase difference is indeed $-\pi/3$ Furthermore one observes no change in shape in either the amplitude or the phase of the discrete wall This is in full agreement with the observation in Fig 7a

In section 4 5 we saw that when the ground state configuration contains higher harmonics this will lead to a pinning of the phase of the fundamental mode Therefore we may expect that this effect will stabilise the domain wall in the discrete system That this is indeed the case is shown in Fig 8a The parameters A, B and D in this case are respectively 0 514, -0 440 and 0 28 Thus A/D = 1 837 and B/D = $-$ 1 571, which in the phase-diagram (Fig 1) is a point well below the transition-point from the P-phase to the region where the N = 6 superstructure is the ground state At this point also the third harmonic $3q \equiv \pi$ is dominantly present in the ground state configuration The rest of the harmonics can still be neglected Therefore the initial configuration for the integration is given by

$$\begin{aligned} x_n(0) &= e^{i\frac{\tau}{3}n}Q_1(n) + e^{-i\frac{\tau}{3}n}Q_1^*(n) + (-1)^nQ_3(n) \\ x_n(0) &= -\nu\dot{x}[e^{i\frac{\tau}{3}n}Q_1(n) + e^{-i\frac{\tau}{3}n}Q_1^*(n) + (-1)^nQ_3(n)] \end{aligned} \tag{7 8}$$

For Q_1 we take the $H \neq 0$ solitary wave For $Q_3(n)$ we take approximately

$$Q_3(n) \simeq \frac{-1}{A-2B+2D} [Q_1^3(n) + Q_1^{*3}(n)]$$

A result which we derived in section 4 5 The phase difference $\Delta\phi$ for this case is again $-\frac{\pi}{3}$ by taking the velocity v equal to 0 8 Just as in the first case we monitor the third particle in each of the 60 unit-cells The time-interval between successive curves is again 10 time steps

It is clear from Fig 8a that this domain wall is less smooth than the one of Fig 7a This is due to the fact that we are actually in a region in the phase diagram where the continuum approximation is no longer a good approximation Therefore the domain wall which is present in the initial configuration will deviate more from the true domain wall in the discrete system Furthermore we approximate Q_1 in (7 8), which is a solution of the equations of motion corresponding to (5 24), by the $H \neq 0$ solitary wave which is only a correct solution in the absence of phase pinning This all will lead to generation of phonons in the system and thus to the appearance of noisy domain walls The apparent change in shape in the wake of the propagating domain wall can be identified with a large emission of phonons into the system from the propagating domain wall In Fig 8b,c we show the phase and the amplitude of the domain wall From these two figures it is clear that this domain wall is practically of the pure phase-type That is to say it involves mainly a variation of the phase with a large but nearly constant amplitude

In their study of the dynamics of kinks in a highly discrete sine-Gordon system, Peyrard and Kruskal [9] discovered that kinks (domain walls) in such a system prefer to propagate at some well-defined velocities and that such a velocity corresponds to, what they call, a quasi-steady state or quasi-steady mode of the system Furthermore if a kink starts with a velocity which is different from one of the preferred velocities, it will relax very fast to the nearest quasi-steady state, thereby radiating phonons at a high rate into the system After staying in this quasi-steady state for quite some time (with a very slow decrease in its velocity) this kink will relax to the next quasi-steady state This again happens in a very short time and is again accompanied by a high rate emission of phonons This process continues until the kink is completely pinned in the system Therefore one can speak of a kind of memory loss of their initial velocity being suffered by these kinks

Peyrard and Kruskal also explain this phenomenon using a simplified model that preserves the discrete character of the system and only focuses on the radiation emitted by the kink, as this is the main source of its energy loss

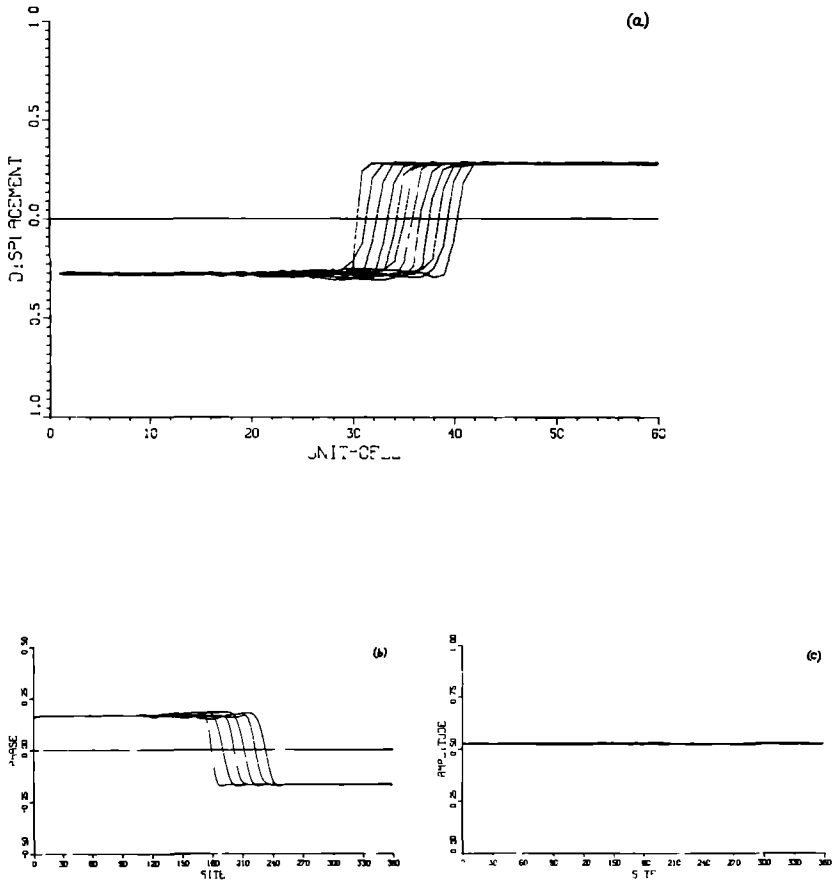

Figure 8. (a) Propagating kink with a width of about 10 unit-cells within an N = 6 superstructure with a non-sinusoidal modulation (b) Evolution of its phase (c) Evolution of its amplitude

This model also predicts the values of the velocities of these quasi-steady states to a very high accuracy Furthermore Peyrard and Kruskal stress the fact that these velocities do not depend on the precise form of the kink but only on the discrete nature of the underlying lattice Therefore they claim that this phenomenon is not only restricted to their discrete sine-Gordon model but will also be present in other one-dimensional lattice models bearing topological kinks Only the time scale of the various phenomena, which depends on the specific form (width) of the kink, will be different for different models In particular they mention that it would be an interesting test to perform a similar study on the discrete ϕ^4 model In a note added in proof they already refer to a paper by Combs and Yip [8] on the discrete ϕ^4 model, which seems to confirm their conjecture To check this conjecture for the frustrated ϕ^4 model, one has to specify the way to determine the kink-velocity

In a continuous system the velocity of a domain wall is defined as the velocity of its "center of gravity", i e the inflection point of the shape function This point is well-defined in a continuous system For a domain wall in a discrete system this center is no longer well-defined, because the wall is not described by a continuous shape function However, a suitable, but nevertheless arbitrary, center can be defined by using some continuous interpolation of the discrete domain wall If we are monitoring the i-th particle in each unit-cell and if for instance $x_{\ell N+i}(t) < 0$ and $x_{(\ell+1)N+i}(t) > 0$ then we take the center to be located at

$$X(t) = \ell N+1 + \frac{x_{(\ell-1)N+i}(t) - N x_{\ell N+i}(t)}{x_{(\ell+1)N+i}(t) - x_{\ell N+i}(t)} \qquad (7\ 9)$$

The velocity X(t) of the domain wall is then obtained from (7 9) simply by

$$X(t) = \frac{X(t+\Delta t) - X(t)}{\Delta t} \qquad (7\ 10)$$

For the steeper kinks this velocity fluctuates strongly when Δt is small This is caused by the noise which is present in the system It even occurs that the amplitude of these fluctuations exceeds the phason velocity, i e the upper limit for the velocity of a propagating kink The phenomenon that Peyrard and Kruskal observe is associated with an average velocity of the domain wall and not with these fluctuations, therefore whenever the fluctuations are large we in addition average X over some suitable time interval T in order to single out the relevant behaviour We checked the conjecture of Peyrard and Kruskal for both systems we mentioned at the beginning of this section, i e the "N = 4" and the "N = 6" system We looked at four different kinks within an N = 6 superstructure, each with a different width and consequently a different initial velocity Each of these

cases correspond to a different point in the N = 6 region of the phase diagram (Fig 1) In the table below the parameters A,B,D, the initial velocity v and v_{phason} in these four cases are given The system-length for each of the cases is 60 unit cells The parameter $\varkappa$ is taken to be 1 in all cases

	A	B	D	v	v_{phason}
I	0 733	-0 480	0 26	0 5	0 872
II	0 514	-0 440	0 28	0 8	0 883
III	0 430	-0 440	0 28	0 825	0 883
IV	0 219	0 440	0 28	0 85	0 883

The first two cases are the ones we discussed earlier in this section Case I corresponds to a very broad domain wall (cf Fig 7a) with a width of approximately 10 unit cells In Fig 9 we plotted the kink-velocity X as a function of time for this case

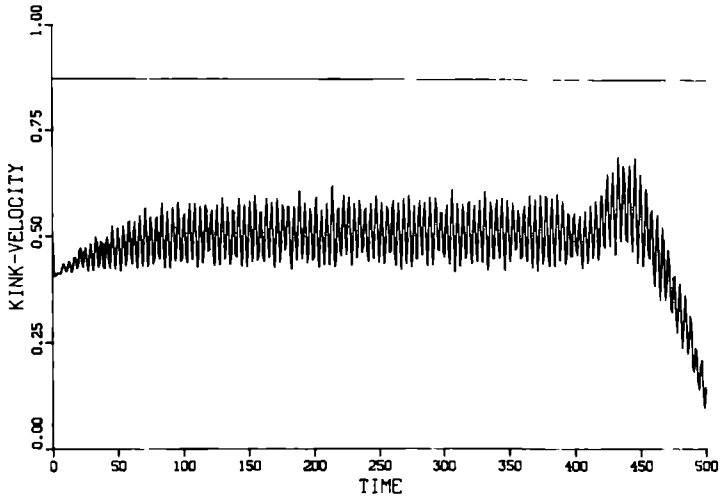

Figure 9 Variation of the kink velocity in the course of time for the kink of Figure 7

In this figure one clearly notices the fluctuations we mentioned earlier but here they are relatively small The origin of the sudden drop in the velocity just after launching the domain wall in the system is not clear to us, but it has definitely nothing to do with the phenomenon of Peyrard and Kruskal We have observed this drop irrespective of the length of the integration step The increase and subsequent decrease in the velocity after about 400 time-steps signals the arrival of the kink at the rigid (cf (7 2)) right end of the system As we mentioned earlier case I is an example of a system with a 'sinusoidal' ground state For all such systems we observed a qualitatively similar behaviour i e that the average velocity of the domain wall is 'equal' to the initial velocity So no memory loss whatsoever in this case The behaviour in case I is an example of what Currie, Trullinger, Bishop and Krumhansl [1] call coherent behaviour The domain wall in case II (cf Fig 8a) has a width of about 3 unit cells In this case discreteness effects are becoming important, because of the "non-sinusoidal" character of the ground state here Fig 10a shows the kink-velocity X as a function of time for this case Here the fluctuations are very much larger The average velocity decreases slowly in time The same behaviour is also observed for different averaging-times T This figure seems to suggest a plateau in the average velocity at about 0 5 This could be such a quasi-steady state of Peyrard and Kruskal It is, however, also possible that we are here observing a behaviour which marks the transition between coherent and incoherent behaviour, as is also observed by Currie, Trullinger, Bishop and Krumhansl [1] The initial drop in velocity seems to be almost instantaneously (cf Fig 10a) like in case I The transition to the first quasi-steady state as observed by Peyrard and Kruskal is also very fast, but it is not an instantaneous transition Therefore, Fig 10b is a bit misleading, because this figure suggests a gradual transition taking place It is just an artefact of the averaging procedure The domain walls in the remaining cases have an even smaller width than the one of case II In the case III this width is about 2 unit cells and in case IV about 1 unit cell Fig 11a shows the evolution of the wall of case III and Fig 12a shows the corresponding evolution in case IV These figures are similar to Fig 8a In case IV we have a complete pinning of the domain wall to the lattice This is what Currie et al [1] call the incoherent regime Although there are fluctuations in the kink-velocity, the average velocity is zero, as is shown in Fig 12b Fig 11b shows the average velocity of the domain wall in case III In this case the decrease in velocity is much faster than the corresponding one in Fig 10b and no plateau is observed From these four cases it is clear that the conjecture of Peyrard and Kruskal is not trivially valid There seems to be some evidence for it, but it is far from conclusive We do observe the complete scenario which was put forward by Currie et al [1] Although we will not go into details here, one can verify very easily that the

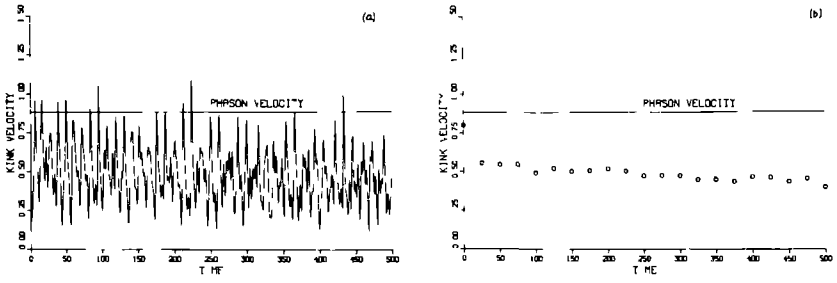

Figure 10. (a) Variation of the kink-velocity in the course of time for the kink of Figure 8 (b) Kink-velocity averaged over intervals of 25 time steps

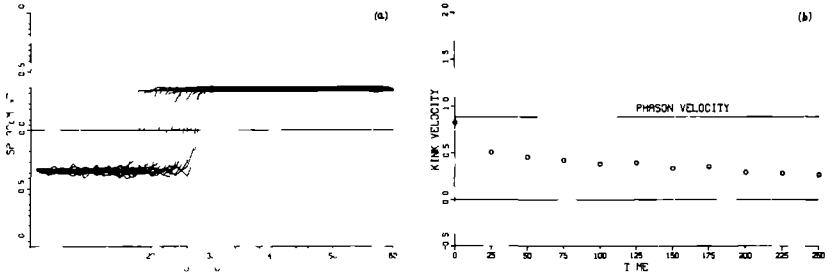

Figure 11. (a) Propagating kink with a width of about 2 unit-cells within an N = 6 superstructure with a non-sinusoidal modulation (b) Its velocity averaged over intervals of 25 time-steps

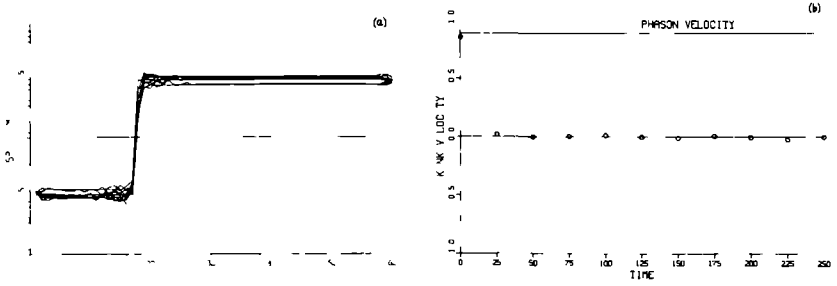

Figure 12. (a) Completely pinned kink with a width of about 1 unit cell within an N = 6 superstructure with a non-sinusoidal modulation (b) Its velocity averaged over intervals of 25 time-steps

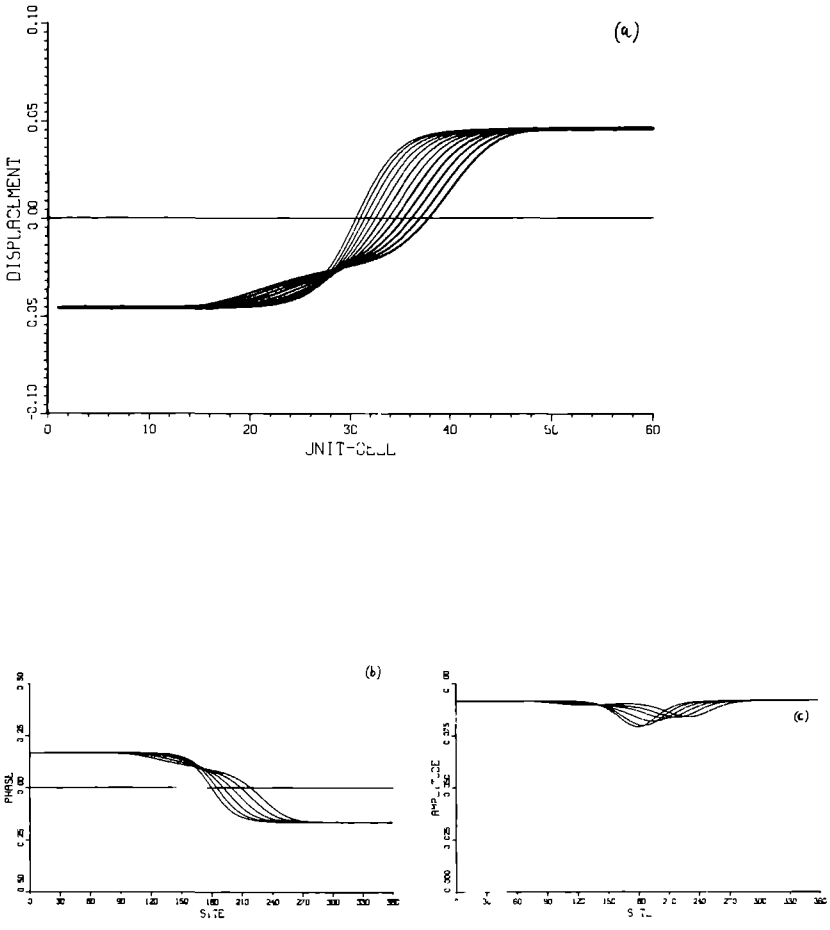

Figure 13. (a) Propagating kink with a width of about 10 unit-cells within an N = 6 superstructure with a sinusoidal modulation The parameter x is here ½ (b) Evolution of its phase (c) Evolution of its amplitude

simple model of Peyrard and Kruskal [9] which seems to explain their observations, is not valid in our case That is to say the corresponding model is much more complicated for a system with frustration and certainly cannot be analysed as easy as the model of Peyrard and Kruskal Therefore, it is not all clear that their conjecture is also valid when frustration is present in the system

The domain wall of Fig 7 becomes unstable when the width and the velocity of the initial $H \neq 0$ solitary wave do not match, that is to say for values of $\varkappa$ differing from one This is shown in Fig 13a,b,c, for $\varkappa = \frac{1}{2}$ All the other parameters are kept fixed In the case of a "smaller" initial velocity $\varkappa = \frac{1}{2}$ we see from Fig 13b that the instability is predominantly present in the phase, while for a "larger" initial velocity also the amplitude of the domain wall is drastically affected

In the previous section we saw that a system for which the ground state is an $N = 4$ superstructure is special, in the sense that in the continuum Hamiltonian in the one-mode approximation there is already a term present which pins the phase of the fundamental mode ($q = \frac{\pi}{2}$) Therefore, a domain wall in that system in the continuum approximation is different from a domain wall in a superstructure with $N \neq 1,2,4$ In that same section we saw that on the line $A/D < 2$, $B = 0$ in the $N = 4$ region in the phase-diagram (Fig 1) one can exactly solve the continuum approximation to the equations of motion, leading to a number of possible kinks (see (6 8)-(6 9) and Fig 6) At all other points in the $N = 4$ region of the phase-diagram one has to resort to the constant amplitude approximation (CAA), which leads to a sine-Gordon kink(s) (cf (6 17)) We now use again these solutions as initial configurations in the integration of the discrete equations of motion (cf (7 1)-(7 3)) Fig 14a shows the displacements of every fourth particle in each of the hundred unit cells of a system with $A = 1\ 75$, $B = 0$ and $D = 1$, at regular intervals of five time-steps The initial velocity is equal to 1 9, while the phason velocity equals 2 (cf (6 8)) in this case The asymptotic phase difference which this wall separates is equal to $\pi/2$ This figure shows a number of things First of all it demonstrates clearly the existence of a domain wall in this discrete system, which propagates at a nearly constant velocity through the system Furthermore, in the wake of this kink one notices a burst of phonons, something which we also saw in several of the "N = 6" cases The shape of this domain wall hardly changes during its propagation in the system Its velocity actually decreases very slowly as can be seen in Fig 14b A similar behaviour is observed for other systems with $A/D < 2$, $B = 0$ and with an initial velocity smaller than the local phason velocity It is clearly not the rapid decay which Peyrard and Kruskal observe Fig 15 shows the same system (same parameters A, B and D) as in Fig 14 but with a velocity

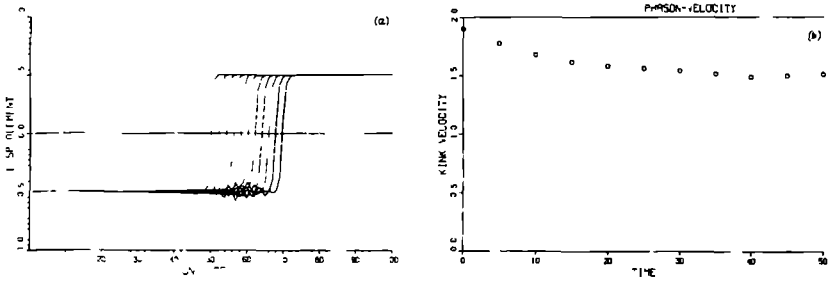

Figure 14. (a) B = 0 propagating kink within an N = 4 superstructure with an initial velocity below the phason velocity (b) Its velocity averaged over intervals of 5 time-steps

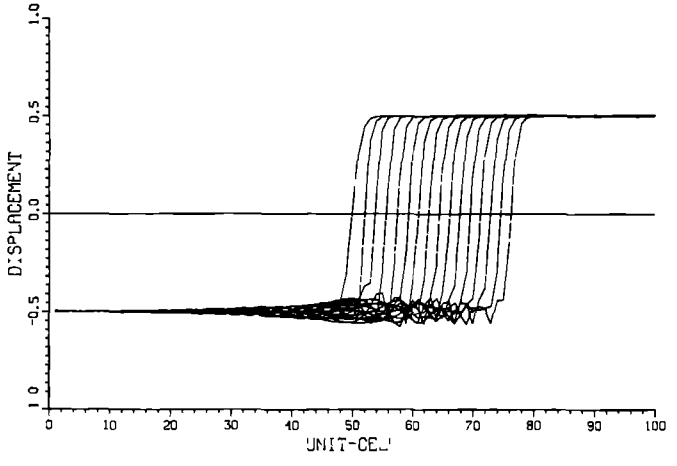

Figure 15. B = 0 propagating kink within an N = 4 superstructure with an initial velocity above the phason velocity

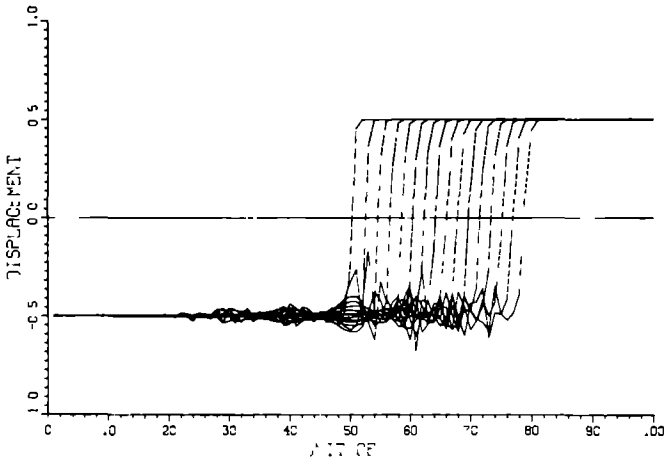

Figure 16. $B \neq 0$ propagating kink within an $N = 4$ superstructure with an initial velocity above the phason velocity

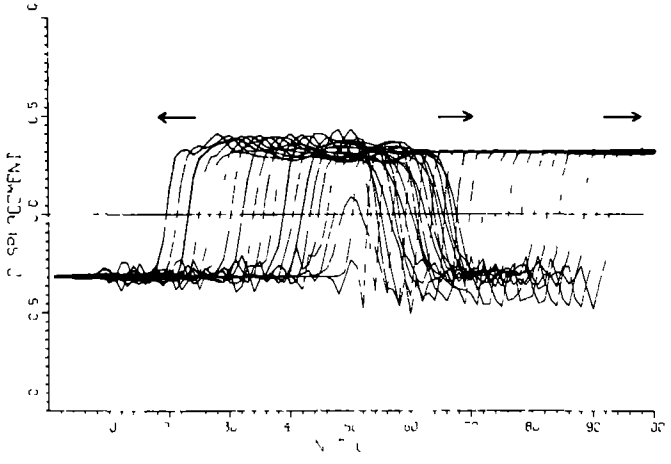

Figure 17. The breaking up of a kink into a kink and a kink - anti kink pair above a critical velocity. The arrows indicate the direction of propagation of each kink

equal to $\sqrt{2}$ and with the parameter $\varkappa$ equal to 2 Therefore this kink is launched into the system with an initial velocity $2\sqrt{2}$, which is larger than the phason velocity In this figure one sees very clearly that the velocity drops fast to an almost constant value This we observe in similar systems as long as the initial velocity exceeds the local phason velocity The phonon creation in this case is the analogue of Cerenkov radiation Furthermore it seems that the duration of this drop is independent of the initial velocity, again as long as the initial velocity is larger than the local phason velocity The same picture holds for systems with $B \neq 0$ An example of such a system is shown in Fig 16 The parameters in this case are $A = 1\ 75$, $B = 0\ 3$ and $D = 1$ The initial velocity is equal to 1 and $\varkappa$ is equal to 3 In this figure the displacements of every third particle are shown The phason velocity is again in this system equal to 2 So also for $B \neq 0$ there exists a propagating domain wall in the discrete system Although the initial configuration for a system with $B \neq 0$ is the same as in the study by Peyrard and Kruskal, the equations of motion are clearly different This is why we probably only find a similar behaviour for initial velocities larger than the local phason velocity

In these "N = 4" systems one can also observe kink - anti-kink production This happens when the initial kinetic energy exceeds a certain threshold value (something like the excitation energy of two widely separated kinks) An example of this phenomenon is shown in Fig 17 The parameters in this case are $A = 1\ 9$, $B = 0\ 3$, $D = 1$, the initial velocity is here equal to 1 and $\varkappa$ is equal to 4 75 The original kink, moving to the right breaks up in a kink moving to the left and a kink - anti-kink pair moving to the right

4.8 Concluding remarks

In linear chain systems with frustration, in which incommensurate modulations occur, the presence and properties of solitary wave excitations have been investigated The procedure was a combination of analytical techniques applied to a continuum approximation of the model and numerical integration of the equations of motion The most important results are the following

- In systems with an incommensurate or long period commensurate small amplitude modulation, kinks are not stable

- In going further away from the phase transition these kinks are stabilised by pinning mechanisms

- There is an analogous pinning mechanism for period four modulations, i e discommensurations near N = 4 may become stable

- Moving kinks keep their form over long distances, but loose energy by emission of phonons

- The velocity of kinks is restricted by the phason velocity

- Kinks with a velocity higher than the phason velocity loose rapidly their energy Above a critical velocity, a kink may break into three or more kinks and anti-kinks

4.9 Appendix A

In this appendix we will give the details of the derivation of the continuum Hamiltonian (2 10) Starting point is the discrete Hamiltonian (2 3)

$$H = \sum_n \{\frac{1}{2}x_n^2 + \frac{1}{2}Ax_n^2 + \frac{1}{4}x_n^4 + Bx_nx_{n-1} + Dx_nx_{n-2}\} \qquad (A\ 1)$$

and the ansatz (2 9)

$$x_n(t) = e^{iqn}Q(n,t) + e^{-iqn}Q^*(n,t) \qquad (A\ 2)$$

where the "order parameter" field $Q(\xi\ t)$ is supposed to be a slowly varying function of ξ i e when

$$Q = O(1) \text{ then } Q = O(\varepsilon) \text{ and } Q, Q^2 = O(\varepsilon^2) \text{ etc}$$

with $\varepsilon \ll 1$

When we substitute (A 2) in (A 1) we get two kinds of terms which we have to sum over n, namely fast - and slowly varying ones Let us illustrate this by looking at the x_n^2 term in (A 1) This term gives

$$x_n^2(t) = e^{2iqn}Q^2(n,t) + e^{-2iqn}Q^{*2}(n,t) + 2|Q(n,t)|^2 \qquad (A\ 3)$$

It is clear that the first two terms are fast varying terms and the third one is slowly varying If we sum a fast varying term over a complete period N (unit cell) all the appearing terms will approximately cancel each other, because a fast varying term is almost periodic It is not hard to see that this correct to $O(\varepsilon^2)$ This means that (A 3) will give

$$\sum_n x_n^2(t) = \sum_n \{2|Q(n,t)|^2\} + O(\varepsilon^2) \qquad \text{(A 4)}$$

Similarly the other on-side terms will give

$$\sum_n x_n^2(t) = \sum_n \{2|Q(n\,t)|^2\} + O(\varepsilon^2) \qquad \text{(A 5)}$$

and

$$\sum_n x_n^4(t) = \sum_n \{6|Q(n,t)|^4\} + O(\varepsilon^2) \qquad \text{(A 6)}$$

Of course this is only true when $N \neq 1,2$ or 4 The derivative terms in (2 10) originate from the remaining terms in (A 1) For instance the $x_n x_{n-1}$ terms gives rise to (we drop both arguments of Q to shorten the notation)

$$x_n x_{n-1} \approx (e^{iqn}Q + e^{-iqn}Q^*)(e^{iq(n-1)}[Q - Q + \frac{1}{2}Q] + e^{-iq(n-1)}[Q^* - Q^{*\prime} + \frac{1}{2}Q^*]$$

$$= e^{-iq}e^{2iqn}[Q^2 - QQ + \frac{1}{2}QQ] + e^{iq}[|Q|^2 - QQ^* + \frac{1}{2}QQ^*]$$

$$+ e^{-iq}[|Q|^2 - Q\,Q^* + \frac{1}{2}Q^*Q] + e^{iq}e^{-2iqn}[Q^{*2} - Q^*Q^* + \frac{1}{2}Q^*Q^*] \qquad \text{(A 7)}$$

so that

$$\sum_n x_n x_{n-1} = \sum_n \{2|Q|^2\cos(q) - e^{iq}QQ^* - e^{-iq}Q\,Q^* + \frac{1}{2}e^{iq}QQ^{**}$$

$$+ \frac{1}{2}e^{-iq}Q^*Q\} + O(\varepsilon^2) \qquad \text{(A 8)}$$

The remaining $x_n x_{n-2}$ term leads to similar expression The derivative terms in (A 8) can be rearranged in the following way

$$e^{iq}QQ^* + e^{-iq}Q\,Q^* = [|Q|^2]\cos(q) - i[Q\,Q^* - QQ^*]\sin(q) \qquad \text{(A 9)}$$

and

$$\frac{1}{2}e^{iq}QQ^* + \frac{1}{2}e^{-iq}Q^*Q = \frac{1}{2}e^{iq}[QQ^*] + \frac{1}{2}e^{-iq}[Q^*Q] - |Q|^2\cos(q) \qquad \text{(A 10)}$$

In the continuum limit the sum over n is replaced by an integral over ξ Therefore all the terms which are a total derivative with respect to ξ can be integrated These "surface" terms are either zero or finite in which case we can get rid of them by redefining the Hamiltonian This will not affect the states nor the

dynamics of the continuum model If we now combine all these results we will end up with (2 10)

4.10 Appendix B

In this appendix we will show why the equation

$$\underset{\sim}{\Omega} = -(H^2+2r)\underset{\sim}{\Omega} + 3s\underset{\sim}{\Omega}^2 \tag{B 1}$$

together with the boundary conditions

$$\lim_{\xi \to \pm\infty} \underset{\sim}{\Omega}(\xi) = \lim_{\xi \to \pm\infty} \underset{\sim}{\Omega}(\xi) = 0 \tag{B 2}$$

only has a non-trivial solution when

$$v^2 = -(H^2+2r) > 0 \tag{B 3}$$

This can be understood by examining the conserved quantities for the case $H \neq 0$, in particular the energy ε of the analogous mechanical particle

$$\varepsilon = \frac{1}{2}(u^2+v^2) - \frac{1}{2}r(u^2+v^2) - \frac{1}{4}s(u^2+v^2)^2 - \frac{r^2}{4s} \tag{B 4}$$

Let us first transform the u-v variables in this expression to polar variables ϱ and ϕ by using

$$\begin{aligned} u(\xi) &= \varrho(\xi)\sin\phi(\xi) \\ v(\xi) &= \varrho(\xi)\cos\phi(\xi) \end{aligned} \tag{B 5}$$

This transformation leads to

$$\varepsilon = \frac{1}{2}(\varrho^2+\varrho^2\phi^2) - \frac{1}{2}r\varrho^2 - \frac{1}{4}s\varrho^4 - \frac{r^2}{4s} \tag{B 6}$$

ϕ can be eliminated by using the conserved quantity $L_\perp$ which in the polar variables is given by

$$L_\perp = -\varrho^2\phi + \frac{1}{2}H\varrho^2 \tag{B 7}$$

The result is

$$\varepsilon = \frac{1}{2}\varrho^2 + U(\varrho) \tag{B 8}$$

with

$$U(\varrho) \equiv -\frac{1}{2}r\varrho^2-\frac{1}{4}s\varrho^4-\frac{r^2}{4s}+\frac{1}{8}H^2\varrho^2+\frac{r^2H^2}{8s^2}\quad\frac{1}{\varrho^2}+\frac{rH^2}{4s} \tag{B 9}$$

In this last expression we used the fact that the $H \neq 0$ solitary wave has an angular momentum $I_{\perp}$ equal to (cf 2 29)

$$L_{\perp} = -\frac{rH}{2s} \tag{B 10}$$

The first three terms in (B 9) constitute the inverted mexican hat, which can be written as

$$U_{IMH}(\varrho) = -\frac{1}{4}s(\varrho^2-\varrho_o^2)^2 \tag{B 11}$$

with $\varrho_o \equiv \sqrt{-\frac{r}{s}}$ the radius of the mexican hat The remaining three terms in (B 9) constitute the effective centrifugal potential This can be written as

$$U_{CF}^{eff}(\varrho) = \frac{1}{8}\,H^2\,\frac{1}{\varrho^2}(\varrho^2-\varrho_o^2)^2 \tag{B 12}$$

So U becomes

$$U(\varrho) = \frac{1}{4}s(\varrho^2-\varrho_o^2)^2(\frac{\varrho_H^2}{\varrho^2}-1) \tag{B 13}$$

where we have introduced $\varrho_H^2 \equiv \frac{H^2}{2s}$ Some plots of U are given in Fig 18 Now ϵ is zero for a $H \neq 0$ solitary wave Thus a solution starting at $\varrho = \varrho_o$ and $\dot{\varrho} = 0$ for $\xi = -\infty$ will stay there in both cases (b) and (c) Only in case (a) there is possibility for a non-trivial motion ($\varrho \neq \varrho_o, \dot{\varrho} \neq 0$) So the desired condition is

$$\varrho_o > \varrho_H \tag{B 14}$$

or in other words

$$H^2 < -2r \tag{B 15}$$

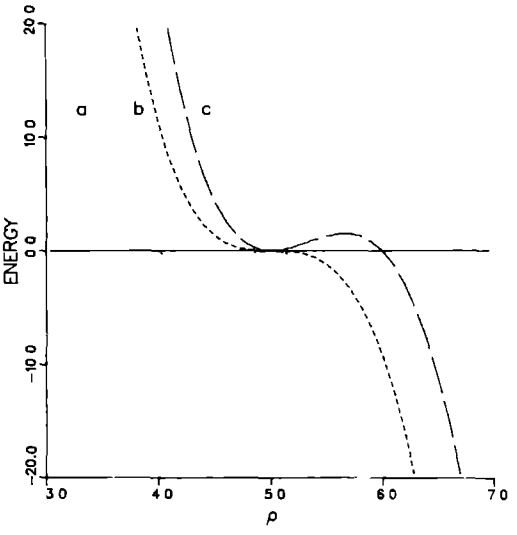

Figure 18. Schematic graph of $U(\varrho)$ for the three possible cases a) $\varrho_0 > \varrho_{11}$ b) $\varrho_0 = \varrho_{11}$ and c) $\varrho_{11} > \varrho_0$ (arbitrary units)

4.11 References

[1] J.F. Currie, S E. Trullinger, A R. Bishop and J A. Krumhansl, Phys. Rev. B **15** (1977) 5567.

[2] T Schneider, in: Solitons, S E. Trullinger, V E Zakharov and V L. Pokrovsky, eds (North-Holland, Amsterdam 1986), 389-343.

[3] W. Hasenfratz and R. Klein, Physica **98A** (1977) 191

[4] S Aubry, in: Solitons and Condensed Matter Physics, A. Bishop and T. Schneider, ed., Solid-State Sciences, vol. 8 (Springer-Verlag, Berlin, 1978), p. 264 and references therein

[5] P Prelovsek and I Sega, J Phys C: Solid State Phys., **14** (1981) 5609.

[6] M. Peyrard and M Remoissenet, Phys Rev. B **26** (1982) 2886.

[7] M Hogh Jensen, Per Bak and A. Popielewicz, J. Phys A Math. Gen . **16** (1983) 4369.

[8] J A Combs and S Yip, Phys Rev B **28** (1983) 6873
[9] M Peyrard and M D Kruskal, Physica **14D** (1984) 88
[10] M Peyrard and H Buttner, J Phys C Solid State Phys , **20** (1987) 1535
[11] N Flytzanis, S Pnevmatikos and M Remoissenet, Physica **26D** (1987) 311
[12] T Janssen, Jap J Appl Phys , **24** (1985) 747
[13] T Janssen and J A Tjon, Phys Rev B **25** (1981) 2245
[14] T Janssen and J A Tjon, J Phys C Solid State Phys , **16** (1983) 4789
[15] E M Lifshitz, Zh Eksp & Teor Fiz , **11** (1941) 253
[16] J Moser, Lectures on Hamiltonian Systems, Memoirs Am Math Soc , **81** (1968) 1
[17] S Aubry, J Chem Phys **64** (1976) 3392
[18] R K Dodd, J C Eilbeck, J D Gibbon and H C Morris, Solitons and Nonlinear Wave Equations (Academic Press, 1982)
[19] L D Landau and E M Lifshitz, Quantum Mechanics (non-relativistic theory), Course of Theoretical Physics, vol 3 (Pergamon Press 1959) p 69
[20] I E Dzyaloshinskii, Sov Phys JETP, **20** (1965) 665
[21] G Hall and J M Watt (eds), Modern Methods for Ordinary Differential Equations (Clarendon Press, 1976) p 59

CHAPTER 5†

MULTI-KINKS IN MODULATED CRYSTALS: THE SOLITON LATTICE OF THE FRUSTRATED ϕ^4 MODEL

J J M Slot and T Janssen

Institute for Theoretical Physics, University of Nijmegen, Toernooiveld, 6525 ED Nijmegen, The Netherlands

Abstract

The dynamics of multi-kinks (soliton lattices) in a linear chain system with frustration, in which incommensurate phases occur, is studied using a combination of analytical and numerical techniques

The multi-kinks are found to have a complex structure when frustration is present in the system, this in contrast to multi-kinks in non-frustrated systems

† Submitted for publication to Journal of Physics A Mathematical and General, IOP Publishing Ltd

5.1 Introduction

In a recent paper [1] we studied the dynamics of single kinks in a model for crystals with a quasiperiodic distortion, the so-called incommensurate displacively modulated crystal structures This model, the DIFFF (Discrete Frustrated ϕ^4) model, consists of a chain of classical particles. Each particle has one degree of freedom denoted by x_n, and is harmonically coupled to its nearest and next-nearest neighbours. In addition each particle moves in an anharmonic (quartic) site potential The Hamiltonian of the system is therefore given by

$$\mathcal{H} = \sum_n \{\frac{1}{2}p_n^2 + \frac{1}{2}Ax_n^2 + \frac{1}{4}x_n^4 + Bx_nx_{n-1} + Dx_nx_{n-2}\}. \qquad (1.1)$$

The ground state of the model was studied in detail as function of the parameters [2]. This ground state depends on the two ratios A/D and B/D Fig 1 shows the various ground state configurations as a function of these ratios.

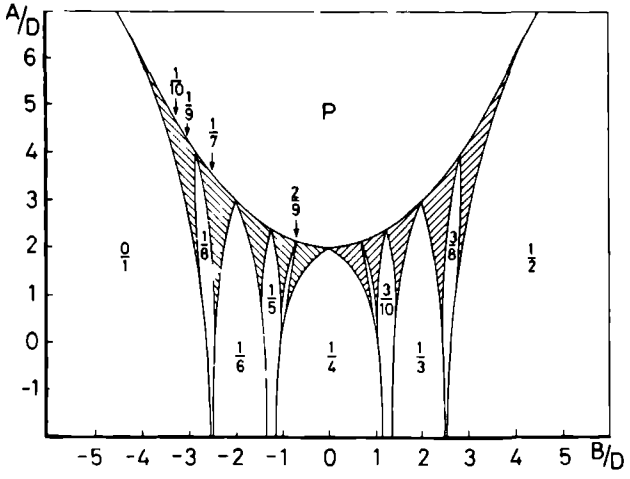

Figure 1. Phase diagram of the discrete frustrated ϕ^4 model Each point in this diagram corresponds to a ground state of the model Indicated are the small period commensurate phases by their wave vector The hatched regions correspond to incommensurate phases and to long-period commensurate phases

When $|B/D| < 4$ an incommensurate ground state is possible (hatched regions) Essential for this is the competition between first and second neighbour interaction, in particular a non-zero value of D

The strategy we followed in [1] to study the dynamics corresponding to the above Hamiltonian was two-fold On the one hand we numerically integrated the corresponding equations of motion for finite chains but in doing so we were guided by the results we obtained from an analysis of a continuum approximation to (1 1) Within this one-mode continuum approximation which is valid for a system with a ground state in one of the so-called "sinusoidal" regions of the phase diagram (Fig 1), we found the explicit form of the single kink This solution of the equations of motion of the continuum model consists of a non-trivial variation of the amplitude and the phase of the ground state configuration This kink is different from the well-known kink of the ordinary (non-frustrated) ϕ^4 model For instance its so-called topological charge i e the asymptotic phase difference in units of 2π which the kink spans, is not fixed to $\frac{1}{2}$ as for the ordinary ϕ^4 kink, but can have any value between 0 and 1 depending on the parameters of the model (A, B and D), the wave vector of the ground state configuration and the velocity of propagation The reason for this difference can be found in the appearance, in general, of the so-called Lifshitz term in the Landau-Ginzburg like continuum Hamiltonian which can be derived starting from (1 1) The equations of motion of the continuum approximation are formally identical to those for a particle with two degrees of freedom in a potential The coefficient of this Lifshitz term can be interpreted as a magnetic field strength, as was shown in [1] Now when this strength goes to zero the "frustrated" kink reduces to the "non-frustrated" continuum kink We also showed in [1] that when we use this "frustrated" continuum kink as initial configuration in the integration of the discrete equations of motion for a finite system, it very rapidly relaxes to a "frustrated" discrete kink

For the ordinary ϕ^4 model, but also for other models like the sine-Gordon model and the Takayama-Lin-Liu-Maki (TLM) model for trans-polyacetylene, one can also find, besides the single kink solution, the so-called soliton lattice solution or multi-kink solution This was for instance done by Horovitz [3] in the case of the TLM model The soliton lattice in these models consists of regularly spaced alternating kinks and anti-kinks Such a solution can also be found in the one-mode continuum limit of the DIFFT model, although as we will see this will not be a periodic solution in general This solution and some of its properties will be the main subject of the present paper Furthermore, we will give some numerical evidence of the existence of a corresponding solution in the discrete system

In the next section we will briefly discuss the continuum model in the one-mode approximation starting from Hamiltonian (1 1) More details of this derivation can be found in [1] Furthermore in this section we will give the single kink solution of the corresponding equations of motion The third section is devoted to the actual soliton lattice solution in both the continuum and discrete model The soliton lattice solution in the continuum model is a more general solution of the corresponding equations of motion than the single kink solution Therefore, this single kink solution can be recovered from the soliton lattice solution by taking an appropriate limit This limit will be discussed in section 4 Finally some conclusions will be given in section 5

5.2 Continuum model

In this section we will briefly discuss the continuum limit of the discrete Hamiltonian (1 1) in the so-called one-mode approximation This procedure was treated at length in [1], therefore we will present here only the result and the main line of reasoning The idea of the one-mode approximation stems from the observation that when the model parameters A, B and D are chosen such that we are in a region of the phase diagram (Fig 1) just below the transition line from the P (para)-phase to one of the modulated phases, the ground state configuration is approximately described by

$$x_n^{(0)} = \Delta \sin(qn + \phi) \tag{2 1}$$

This ground state configuration can be periodic (a superstructure) or incommensurate The latter we also approximate by a superstructure, therefore we can write

$$q = 2\pi \frac{L}{N} \tag{2 2}$$

with L and N relative prime and possibly very large Various values of $\frac{L}{N}$ are shown in Fig 1 In the remainder of this paper we will restrict ourselves to the case $N \neq 1,2$ or 4 The reason is that both cases $N = 1$ and $N = 2$ lead to the ordinary ϕ^4 model and thus to the ordinary ϕ^4 soliton lattice solution The case $N = 4$ is more complicated as we showed in [1] In the so-called constant amplitude approximation (CAA) [4], however, the continuum model reduces to the well-known sine-Gordon model [1], and leads therefore to the soliton lattice solution corresponding to this model [5] The ground state configuration (2 1) with fundamental "wave vector" q (2 2) is an N-fold superstructure This

superstructure will be M-fold degenerate, where M = N if N is even and M = 2N if N is odd These M degenerate phases all have the same amplitude Δ, but a different phase-angle ϕ, i e

$$\phi = \phi^{(j)} \equiv 2\pi \frac{j}{M} + \text{constant} \qquad (j=0, \ldots, M-1) \tag{2 3}$$

It is clear that due to this degeneracy of the ground state, kinks or domain walls naturally appear as low-lying static excitations of the system, because they locally connect different degenerate ground state phases

To derive the appropriate continuum Hamiltonian in this "sinusoidal" region of the phase diagram, we make the following ansatz

$$x_n(t) = e^{iqn}Q(n,t) + e^{-iqn}Q^*(n,t) \tag{2 4}$$

where the complex "order-parameter" field $Q(\xi,t)$ is a slowly varying function of ξ By slowly varying we mean here that if

$$Q = O(1) \text{ then } Q \equiv \frac{\partial Q}{\partial \xi} = O(\varepsilon) \text{ and } Q\,,Q^2 = O(\varepsilon^2) \text{ etc} \tag{2 5}$$

where $\varepsilon \ll 1$ This assumption is justified when the typical width of a kink in the system is large enough ($\geq$ 3 unit-cells) The procedure to follow consists of substituting (2 4) in the Hamiltonian (1 1), sum out all the fast varying terms (i e those terms which have as a factor some power of exp(iqn), replace the sum over n by an integral over ξ and eliminate all appearing "surface" terms This then will lead to the following continuum Hamiltonian, correct to $O(\varepsilon^2)$

$$\mathcal{H} = \frac{c^2}{2} \int_{-\infty}^{\infty} d\xi \{ \frac{1}{2}(u^2+v^2) + \frac{1}{2c^2}(u^2+v^2) + \frac{1}{2}H(uv - u\,v)$$

$$+ \frac{1}{2}r(u^2+v^2) + \frac{1}{4}s(u^2+v^2)^2 + \frac{r^2}{4s}\} \tag{2 6}$$

In this Hamiltonian we have replaced the complex field Q by the pair of real fields u and v, which are defined by

$$u \equiv Q + Q^* \tag{2 7}$$

$$v \equiv i(Q - Q^*) \tag{2 8}$$

Furthermore we have shifted the Hamiltonian density by a constant, such that the ground state of this continuum model has a zero energy This of course does not affect the dynamics of the model The parameters r, s and H in (2 6)

are given by

$$r \equiv \frac{a}{c^2} < 0, \quad s \equiv \frac{3}{4c^2} \quad \text{and} \quad H \equiv \frac{2b}{c^2} \tag{2 9}$$

with

$$a \equiv A + 2B\cos(q) + 2D\cos(2q) \tag{2 10}$$
$$b \equiv B\sin(q) + 2D\sin(2q) \tag{2 11}$$
$$c^2 \equiv -[B\cos(q) + 4D\cos(2q)] \tag{2 12}$$

Because we are below the transition-point from the P-phase to the modulated phase described by q (2 2), r is negative and s is positive Therefore the rotationally invariant (in the u-v space) potential in (2 6) is known as the 'mexican hat" potential Its brim is located at

$$u^2 + v^2 = -\frac{r}{s} = \varrho_o^2 \tag{2 13}$$

The term with coefficient H is the Lifshitz-term, which we mentioned in the introduction The static configuration which minimizes (2 6) is $\varrho^2 = -r/s+H^2/4s$, $\phi = -H\xi/2$ The true ground state, which appears in Fig 1, is generally different because of other terms which are neglected in the one-mode continuum approximation We shall consider kinks with respect to the latter

The equations of motion for the fields u and v follow from (2 6) by using Hamilton's principle of the least action These equations of motion are

$$\begin{aligned} u - \frac{1}{c^2}u - Hv &= ru + su(u^2+v^2) \\ v - \frac{1}{c^2}v + Hu &= rv + sv(u^2+v^2) \end{aligned} \tag{2 14}$$

We shall consider in the following, special solutions of these equations of motion, those which depend on ξ and t in the combination $\xi - vt$ In other words these solutions travel through the system at a constant speed without changing their shape Therefore it is easy to see that it is sufficient to study (2 14) in the rest frame ($v = 0$) Each solution $\{u_o, v_o\}$ of this stationary problem leads to a whole family traveling solutions of the full problem (2 14), via the correspondence

$$\begin{bmatrix} u_o(\xi,H) \\ v_o(\xi,H) \end{bmatrix} \rightarrow \begin{bmatrix} u(\xi,t,H) = u_o(\gamma(\xi-vt),\gamma H) \\ v(\xi,t,H) = v_o(\gamma(\xi-vt),\gamma H) \end{bmatrix} \tag{2 15}$$

with $\gamma \equiv \left[1-v^2/c^2\right]^{-1/2}$, where c is actually the phason-velocity [1] By viewing ξ as a "time" variable, the stationary problem

$$\begin{aligned} u &= ru + Hv + su(u^2+v^2) \\ v &= rv - Hu + sv(u^2+v^2) \end{aligned} \tag{2 16}$$

can be interpreted as the equations of motion of an integrable classical system with two degrees of freedom, i e a particle moving in a plane perpendicular to a homogeneous magnetic field with strength H, in a non-linear central potential (inverted "mexican hat")

$$U(\varrho) = -\frac{1}{2}r\varrho^2 - \frac{1}{4}s\varrho^4 - \frac{r^2}{4s} = -\frac{1}{4}s(\varrho^2-\varrho_0^2)^2\,, \quad \varrho^2 = u^2+v^2 \tag{2 17}$$

It is integrable because there are two integrals of the motion, namely the "energy" ε and the "angular momentum" $L_\perp$

$$\varepsilon = \frac{1}{2}(u^2+v^2) + U(\varrho) \tag{2 18}$$

$$L_\perp = uv - uv + \frac{1}{2}H(u^2+v^2) \tag{2 19}$$

The solution of the stationary problem is completely determined once these two integrals are specified For instance in [1] we showed that the single kink solution, which we referred to as the $H \neq 0$ solitary wave, corresponds to

$$\varepsilon = 0 \quad \text{and} \quad L_\perp = -\frac{rH}{2s} = \frac{1}{2}H\varrho_0^2 \tag{2 20}$$

This solution, which only exists for $H^2 < -2r$, is given by

$$\begin{aligned} u(\xi) &= \sqrt{\Omega(\xi)}\,\sin\phi(\xi) \\ v(\xi) &= \sqrt{\Omega(\xi)}\,\cos\phi(\xi) \end{aligned} \tag{2 21}$$

with

$$\Omega(\xi) = -\frac{r}{s} - \frac{\nu^2}{2s}\,\mathrm{sech}^2(\frac{1}{2}\nu\xi), \quad \nu^2 \equiv -(H^2+2r) > 0 \tag{2 22}$$

and

$$\phi(\xi) = \phi(-\infty) - \mathrm{arctg}(\frac{\nu}{H}) - \mathrm{arctg}(\frac{\nu}{H}\tanh(\frac{1}{2}\nu\xi)) \tag{2 23}$$

So the topological charge or winding number η of this solution is equal

$$\eta \equiv \frac{\phi(+\infty)-\phi(-\infty)}{2\pi} = -\frac{1}{\pi}\,\mathrm{arctg}\left(\frac{v}{H}\right) \tag{2 24}$$

In the next section we will construct the soliton lattice solution of (2 16)

5.3 Soliton lattice solution

The origin of the specific values (2 20) for the two integrals of the motion in the case of the single kink is to be found in the boundary conditions for the single kink, namely

$$\lim_{\xi\to\pm\infty}\begin{bmatrix} u(\xi) \\ v(\xi) \end{bmatrix} = 0 \quad \text{and} \quad \lim_{\xi\to\pm\infty} \varrho^2(\xi) = \varrho_o^2 \tag{3 1}$$

because by definition a single kink connects in an asymptotic sense two degenerate ground state phases $\{\varrho = \varrho_o, \varphi \in [0,2\pi)\}$ and has a finite creation energy with respect to the ground state energy The interpretation of these boundary conditions is clear within the mechanical model The mechanical particle has to start in the infinite part on the brim of the inverted mexican hat with an infinitesimal velocity directed inwards, in order to end in the infinite future on that same brim with a zero velocity When its angular momentum $L_\perp$ is non-zero it will experience a centrifugal repulsion near the origin and will therefore avoid the origin during its course through the inside of the inverted mexican hat The condition for the existence of the single kink which we mentioned in the previous section, i e $H^2 < -2r$, is in fact a condition for the existence of a local minimum between 0 and ϱ_o of the effective radial potential, as was shown in appendix B of [1] It is easy to verify that the effective radial potential (see the appendix) maximally has one local minimum in combination with one local maximum, the condition for this being in general

$$0 \leq L_\perp^2 < \frac{4}{27}\, s\left(\varrho_o^2 + \frac{H^2}{4s}\right)^3 \tag{3 2}$$

It is clear because of the unboundedness of the inverted mexican hat, and therefore of the effective radial potential, that one needs such a local minimum in order to have a bounded motion of the mechanical particle For an angular momentum $L_\perp$ which satisfies (3 2) these local extrema are located at

$$\varrho_{min} \equiv \{\frac{1}{3}(\varrho_o^2+\frac{H^2}{4s})[1-2\cos(\frac{\pi}{3}+\frac{\alpha}{3})]\}^{1/2}$$
$$\varrho_{max} \equiv \{\frac{1}{3}(\varrho_o^2+\frac{H^2}{4s})[1+2\cos\frac{\alpha}{3}]\}^{1/2} \qquad (3.3)$$

where α is defined through

$$\cos\alpha = 1 - \frac{L_\perp^2}{2s[\frac{1}{3}(\varrho_o^2+\frac{H^2}{4s})]^2} \qquad (3.4)$$

For instance in the case of the single kink one has $\varrho_{max} = \varrho_o$ In general, however, ϱ_{max} can be everywhere with respect to ϱ_o The same is true for ϱ_{min}, although one always has $\varrho_{min} < \varrho_{max}$

It is clear that the motion of the mechanical particle is completely determined once we specify its initial position and its initial velocity (four initial conditions) Alternatively we can also specify $L_\perp$, $\varrho_1 \equiv \varrho(0)$ and $\varrho_1 \equiv \varrho(0)$ Of course in this case the motion is not completely determined, because the initial phase $\phi_1 \equiv \phi(0)$ is still free Without loosing generality one can always assume that the initial point is a so-called turning point of the motion, i e $\varrho_1 = 0$ The initial angular velocity $\phi_1 \equiv \phi(0)$ and the energy ε now follow from

$$\phi_1 = \frac{1}{2}H - \frac{L_\perp}{\varrho_1^2} \qquad (3.5)$$

$$\varepsilon = \frac{1}{2}\varrho_1^2\phi_1^2 - \frac{1}{4}s(\varrho_1^2-\varrho_o^2)^2 \qquad (3.6)$$

Furthermore, one can always assume that $\varrho_{min} \leq \varrho_1 \leq \varrho_{max}$ It is now easy to see that when $\phi_1 = 0$ one can only have $\varrho_1 \leq \varrho_o \leq \varrho_{max}$ For a non-zero ϕ_1 one can also have $\varrho_o \leq \varrho_1$

Generally speaking a soliton lattice is a configuration which consists of a regular array of degenerate (near-)ground state phases separated by domain walls This is why one also uses the name multi-kink or kink lattice for such a configuration Furthermore one assumes that the typical width of the kinks is small compared to their mutual distance, so large portions of ground state phase separated by narrow walls This means that the order-parameter field Q will show a slow variation between two kinks, and a relative fast variation when passing through a kink Now let us translate all of this in terms of our mechanical model First of all we have to bear in mind that every orbit of the mechanical particle corresponds to an order-parameter varying in the system, i e an order-parameter field $Q(\xi)$, and that the velocity-field of the particle therefore

corresponds to Q (Ξ) We know that near a classical turning point (here we have actually a turning circle) the particle will have a small radial velocity which eventually becomes zero at the turning point The angular velocity, however, does not have to be small near or at a turning point The motion near one of the the turning circles has to correspond to a (near-)ground state phase Thus one of the turning circles $\varrho = \varrho_1$ or the other one, has to be close to $\varrho = \varrho_0$ Now when the angular velocity is non zero at the turning circle closest to the ground state $\varrho = \varrho_0$, one will have no single (near-)ground state phase between two kinks, but one will pass gradually through a whole bunch of (near-)ground state phases in going from one kink to the next one So we have to conclude that our soliton lattice solution has to correspond to a motion for which ϕ_1 is small We take here the extreme case $\phi_1 = 0$ and thus $\varrho_1 \leq \varrho_0$ We can therefore write

$$\varrho_1^2 = \varrho_0^2 - \Delta \quad \text{with } \Delta \geq 0 \text{ and small} \tag{3 7}$$

Furthermore from (3 5-3 6) it follows that for a soliton lattice solution we have

$$L_\perp = \frac{1}{2}H\varrho_1^2 = \frac{1}{2}H\varrho_0^2 - \frac{1}{2}H\Delta \tag{3 8}$$

and

$$\varepsilon = U(\varrho_1) = -\frac{1}{4}s(\varrho_1^2 - \varrho_0^2)^2 = -\frac{1}{4}s\Delta^2 < 0 \tag{3 9}$$

By using the equations of motion for u and v (2 16) and the two integrals ε and $L_\perp$ (2 18-2 19) and doing a little algebra, it is not hard to derive the following equation for u^2+v^2, which we will denote by Ω from now on

$$\Omega = 4\varepsilon + 2HL_\perp + \frac{r^2}{s} + (4r - H^2)\Omega + 3s\Omega^2 \tag{3 10}$$

The constant term in this equation is positive This can be deduced using (3 8-3 9)

$$4\varepsilon + 2HL_\perp + \frac{r^2}{s} = (H^2 + 2s\Delta)\Omega_1 + s\Omega_1^2 > 0 \tag{3 11}$$

with $\Omega_1 \equiv \varrho_1^2$ By integrating (3 10) once we get

$$\frac{1}{2}\Omega^2 - [(H^2+2s\Delta)\Omega_1 + s\Omega_1^2]\Omega + \frac{1}{2}(H^2-4r)\Omega^2 - s\Omega^3 = \text{constant} \tag{3 12}$$

The value of this constant follows from the boundary condition

$$\Omega = 0 \quad \text{when} \quad \Omega = \Omega_1 \tag{3 13}$$

Therefore it is easy to see that this constant is equal to $-\frac{1}{2}H^2\Omega_1^2$ Thus (3 12) can be written as

$$\Omega'^2 = 2s\{\Omega^2 - (2\Omega_o + \frac{H^2}{2s})\Omega^2 + [\Omega_1^2 + 2(\Delta + \frac{H^2}{2s})\Omega_1]\Omega - \frac{H^2}{2s}\Omega_1^2\} \tag{3 14}$$

The solution of this last equation is implicitly given by the quadrature

$$\xi = \xi_- + \frac{1}{\sqrt{2s}} \int_{\Omega}^{\Omega} dt \, \frac{1}{\sqrt{R(t)}} \tag{3 15}$$

with R(t) the following third-order polynomial in t

$$R(t) = t^3 - (2\Omega_o + \frac{H^2}{2s})t + [\Omega_1^2 + 2(\Delta + \frac{H^2}{2s})\Omega_1]t - \frac{H^2}{2s}\Omega_1^2 \tag{3 16}$$

The zeros of this polynomial can easily be found and are given by

$$\Omega_1 = \Omega_o - \Delta \tag{3 17}$$

$$\Omega_\pm = \frac{1}{2}[\Omega_o + \Delta + \frac{H^2}{2s}] \pm \frac{1}{2}([\Omega_o + \Delta - \frac{H^2}{2s}]^2 + \frac{4H^2}{s}\Delta)^{1/2} \tag{3 18}$$

These zeros are arranged in a definite order

$$0 < \Omega_- < \Omega_1 < \Omega_o + \Delta < \Omega_+ \tag{3 19}$$

The proof of this ordering is given in the appendix In this same appendix we show by an analysis of the effective radial potential, that the condition for the existence of a non-trivial motion is given by (equivalent to (3 2))

$$0 < \Omega_- < \Omega_1 \tag{3 20}$$

For a non-zero value of Δ this is always true, irrespective of the value of the magnetic field H This is in contrast to the case of the single kink ($\Delta = 0$), because there a similar condition as (3 2) is only fulfilled when

$$H^2 < -2r \tag{3 21}$$

as was shown in [1] Now the radial motion of the mechanical particle takes place between the following bounds

$$\Omega_- \leq \Omega \leq \Omega_1 \tag{3 22}$$

As initial position we take for reasons of convenience $\Omega(0) = \Omega_-$ instead of $\Omega(0) = \Omega_1$ Thus (3 15) becomes

$$\xi = \frac{1}{\sqrt{2}s} \int_{\Omega}^{\Omega} dt \, \frac{1}{\sqrt{(t-\Omega_-)(\Omega_1-t)(\Omega_+-t)}} \tag{3 23}$$

This last integral can be expressed as an incomplete elliptic integral of the first kind $F(\phi,k)$ (see for instance [6]), namely

$$\xi = \frac{1}{\lambda} F(\arcsin(\left[\frac{\Omega-\Omega_-}{\Omega_1-\Omega_-} \right]^{1/2}),k) \tag{3 24}$$

with $\lambda = \left[\frac{s(\Omega_+-\Omega_-)}{2} \right]^{1/2}$ and elliptic modulus $k = \left[\frac{\Omega_1-\Omega_-}{\Omega_+-\Omega_-} \right]^{1/2}$ where $0 < k < 1$ on account of (3 19) Therefore $\Omega(\xi)$ can be expressed in terms of the Jacobi elliptic function $sn(u,k)$, the so-called sine-amplitude, by inverting (3 24)

$$\Omega(\xi) = \Omega_- + [\Omega_1-\Omega_-]sn^2(\lambda\xi,k) \tag{3 25}$$

This sine-amplitude $sn(u,k)$ is a periodic function of u with period

$$4K(k) \equiv 4F(\frac{\pi}{2},k) = 4 \int_0^{\pi/2} \frac{d\theta}{\sqrt{1-k^2\sin^2\theta}} \tag{3 26}$$

$K(k)$ is known as the complete elliptic integral of the first kind Because $sn(-u,k) = -sn(u,k)$, we have that Ω is periodic with period

$$T \equiv \frac{2K(k)}{\lambda} \tag{3 27}$$

This period lies somewhere between $\frac{\pi}{\lambda}(= \frac{2K(0)}{L})$ and $\infty(= \frac{2K(1)}{\lambda})$

The equation for the phase $\phi(\xi)$ is easily obtained by transforming $L_\perp$ (2 19) using (2 21)

$$L_\perp = \frac{1}{2}H\Omega_1 = -\Omega\phi + \frac{1}{2}H\Omega \tag{3 28}$$

or

$$\phi = \frac{1}{2}H(1 - \frac{\Omega_1}{\Omega}) \tag{3 29}$$

If we now substitute (3 25) in this expression, we end up after some algebra with

$$\phi(\xi) = \frac{1}{2}H\beta^2 \frac{1-sn^2(\lambda\xi,k)}{1-\beta^2 sn^2(\lambda\xi,k)} \quad , \quad \beta^2 \equiv 1 - \frac{\Omega_1}{\Omega_-} \tag{3 30}$$

or

$$\phi(\xi) = \phi(0) + \frac{H}{2\lambda}\beta^2 \int_0^{\lambda\xi} du \frac{1-sn^2(u,k)}{1-\beta^2 sn^2(u,k)} \tag{3 31}$$

where on account of (3 19) we have $0 < -\beta^2 < \infty$ Again we can express this last integral in terms of an incomplete elliptic integral, but now one of the third kind $\Pi(\phi,\beta^2,k)$ [6], namely

$$\phi(\xi) = \phi(0) + \frac{H}{2\lambda} \{\lambda\xi + (\beta^2-1)\Pi(am(\lambda\xi,k),\beta^2,k)\} \tag{3 32}$$

where the amplitude am(u,k) is defined by

$$sin(am(u,k)) \equiv sn(u,k) \tag{3 33}$$

and $\Pi(\phi,\beta^2,k)$ by

$$\Pi(\phi,\beta^2,k) = \int_0^{\phi} \frac{d\theta}{(1-\beta^2 sin^2\theta)\sqrt{1-k^2 sin^2\theta}} \tag{3 34}$$

The phase $\phi(\xi)$ (3 32) has the following property If we write ξ as

$$\xi = nT + \hat{\xi} \qquad \text{for some } n \in Z \tag{3 35}$$

with T given by (3 27) and $-\frac{1}{2}T < \hat{\Gamma} \leq \frac{1}{2}T$ (this is unique), then

$$\phi(\xi) = \phi(\hat{\xi}) + n\Delta\phi \tag{3 36}$$

where

$$\Delta\phi \equiv \frac{H}{\lambda}\{K(k) + (\beta^2-1)\Pi(\frac{\pi}{2},\beta^2,k)\} \tag{3 37}$$

which we define as the phase difference of the soliton lattice It now follows that when this phase difference is some rational multiple of 2π, we have a periodic soliton lattice, i e when

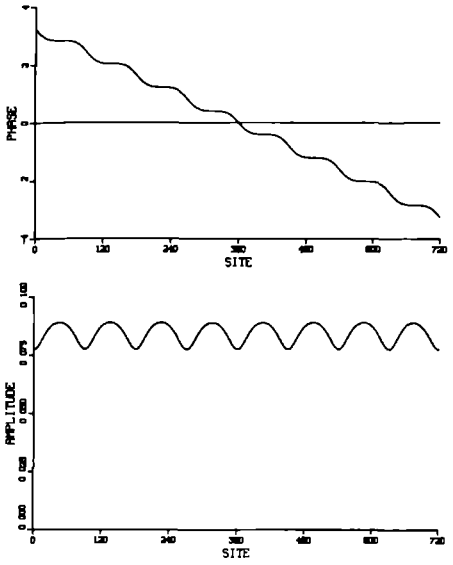

Figure 2 Sketch of the phase ϕ and the amplitude $\varrho = \sqrt{\Omega}$ as a function of ξ

$$\Delta\phi = 2\pi\frac{n}{m} \qquad \text{for some } n,m \in Z \tag{3 38}$$

When this is not the case we have an incommensurate soliton lattice Fig 2 shows an example of the phase and amplitude of an incommensurate soliton lattice Needless to say is that a moving soliton lattice can be obtained by the prescription (2 15) This will again imply, just as in the case of the single kink, that the phase difference will depend on the velocity of propagation v The total energy of a static soliton lattice configuration is of course infinite However because the energy density (Hamiltonian density) can be expressed entirely in terms of $\Omega(\xi)$, we can calculate the energy per period T (3 27), i e

$$\delta_0 = \frac{1}{2}c^2 \int_{-\frac{1}{2}T}^{\frac{1}{2}T} d\xi\{\frac{1}{2}(u^2+v^2) + \frac{1}{2}H(uv - u\,v) + \frac{1}{2}r(u^2+v^2)$$

$$+ \frac{1}{4}s(u^2+v^2)^2 + \frac{r^2}{4s}\} \tag{3 39}$$

This can be written, using the integrals of the motion, as

$$\delta_o = \frac{sc^2}{2\lambda} \int_{-K(k)}^{K(k)} dw\{\frac{1}{4}\Delta^2 + (\Delta+\frac{H^2}{4s})(\Omega_1-\Omega_-)cn^2(w,k)$$

$$+ \frac{1}{2}(\Omega_1-\Omega_-)^2cn^4(w,k)\} \tag{3 40}$$

with cn(w,k) the so-called cosine amplitude, which is related to the sine amplitude via $cn^2(w,k) = 1-sn^2(w,k)$ All the integrals in (3 40) can be done, leading to

$$\delta_o = \frac{sc^2}{2\lambda} \{K(k)\Delta^2 + 2(\Delta+\frac{H^2}{4}s)(\Omega_+-\Omega_-)[E(k)-(1-k^2)K(k)]$$

$$+ \frac{2}{3}(\Omega_+-\Omega_-)^2[(2k^2-1)E(k) + \frac{1}{2}(1-k^2)(2-3k^2)K(k)]\} \tag{3 41}$$

In this last expression E(k) is the so-called complete elliptic integral of the second kink, which is defined by

$$E(k) = E(\frac{\pi}{2},k) = \int_0^{\pi/2} \sqrt{1-k^2\sin^2\theta}d\theta \tag{3 42}$$

In the case of the single kink we argued in [1], that it is linearly unstable The main reason for this instability is the fact that the initial phase is a free parameter combined with the fact that the potential in the one-mode continuum limit is rotationally invariant in the u-v plane The same is true for the soliton lattice solution, therefore we may expect that this solution is also linearly unstable in this continuum limit The proof of this conjecture is, however, far more difficult than in the case of the single kink and is at the present time not known to us

Mechanisms, like we discussed in [1], which pin the phase of the single kink are of course also valid for the soliton lattice solution, i e phase pinning via coupling to higher harmonics of the fundamental mode

We will end this section with a short discussion concerning the existence of the soliton lattice configuration in the discrete system One way to reveal such a solution in a discrete system is to integrate the discrete equations of motion,

thereby using the continuum solution as initial condition. The hope is then that this continuum solution is near the discrete one, so that it quickly relaxes to this discrete solution. The details of the method we use for integrating the discrete equations of motion can be found in [1]. The result of one such calculation is shown in Fig. 3. In this picture we have plotted the displacement of every third site in each of the 240 unit-cells, containing six particles each, of this finite system, at successive intervals of 20 time steps The parameters A, B and D are in this case 0.734, −0.480 and 0.260, which implies that A/D = 2.833 and B/D = −1.846. In the phase diagram (Fig. 1) this corresponds to a point in the "sinusoidal" region of the N = 6 superstructure phase. The reason for looking at each third site is of course to eliminate the fast-varying n dependence ($e^{i(qn)}$ in x_n (cf (2.4). The value of Δ we took was 10^{-4}, which is small with respect to the current value or Ω_0, namely 8.10^{-3} The initial velocity we took was v = 0.525. With these values of the parameters the period T of Ω in the initial configuration is about 90 lattice constants and the phase difference $\Delta\phi$ is near $\pi/4$, actually $\Delta\phi = -0.2578\pi$ (which makes it a so-called incommensurate soliton lattice) It is therefore clear that the whole system (16×90=1440 sites) makes up nearly two whole periods of the soliton lattice.

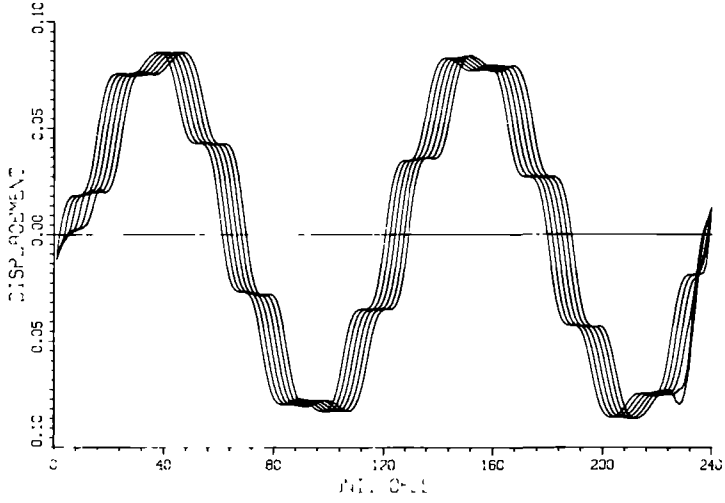

Figure 3. Propagating soliton lattice within an N = 6 superstructure The displacement of the third particle in each unit cell is given for 6 successive times separated by 20 time steps

Concluding we can say that this figure clearly demonstrates the existence of a propagating soliton lattice in the discrete system with no shape change during its propagation through the system At both ends one notices some disturbance This is entirely due to the fixed b c we use in the calculation Notice that such a kink lattice with $\Delta\phi \approx \frac{\pi}{4}$ does not connect degenerate ground states ($\Delta\phi = \pi/3$) and can, therefore, only occur in this sinusoidal region Actually it is surprising that it is so stable in the numerical example

5.4 Single kink limit

In this section we will discuss the single kink limit of the soliton lattice solution This amounts to letting Δ go to zero ($\Omega_1 \to \Omega_0$)

First we will show that when $\Delta \to 0$ (3 28), i e

$$\Omega(\xi) = \Omega_- + (\Omega_1 - \Omega_-)\mathrm{sn}^2(\lambda\xi, k) \tag{4 1}$$

reduces to (2 22), i e

$$\Omega(\xi) = -\frac{r}{s} - \frac{v^2}{2s}\,\mathrm{sech}^2(\frac{1}{2}v\xi) \tag{4 2}$$

Because the single kink only exists for $v^2 \equiv -(H^2+2r) > 0$, we will impose this as an extra condition, while taking the limit $\Delta \to 0$ This condition can also be written as

$$\frac{H^2}{2s} < \Omega_0 \equiv -\frac{r}{s} \tag{4 3}$$

In this limit Ω_1 (3 17) and $\Omega_\pm$ (3 18) go to

$$\Omega_1 \to \Omega_0$$

and

$$\Omega \to \frac{H^2}{2s} \quad , \quad \Omega_+ \to \Omega_0 \tag{4 4}$$

Therefore λ (3 26) and k (3 27) go to

$$\lambda \to \frac{1}{2}v \quad \text{and} \quad k = \left[\frac{\Omega_1 - \Omega}{\Omega_+ - \Omega}\right]^{\frac{1}{2}} \to 1 \tag{4 5}$$

In this last limit, when the elliptic modulus k goes to 1, the sine-amplitude will go to the hyperbolic tangent, i e

$$sn(\lambda\xi,k) \rightarrow \tanh(\frac{1}{2}\nu\xi) \tag{4 6}$$

Thus if we combine all these results, we see that Ω (4 1) goes to

$$\Omega(\xi) \rightarrow \frac{H^2}{2s} - (\frac{r}{s}+\frac{H^2}{2s})\tanh^2(\frac{1}{2}\nu\xi)$$

which is equal to (4 2) Now let us look at the phase ϕ (3 33), i e

$$\phi(\xi) = \phi(0) + \frac{H}{2\lambda}\{\lambda\xi + (\beta^2-1)\Pi(am(\lambda\xi,k),\beta^2,k)\} \tag{4 7}$$

with $\beta^2 = 1 - \frac{\Omega_1}{\Omega_-}$ First of all when $k \rightarrow 1$, the incomplete elliptic integral of the third kind $\Pi(\phi,\beta^2,k)$ goes to (see for instance [6])

$$\Pi(\phi,\beta^2,k) \rightarrow \frac{-1}{\beta^2-1}\{\ell n(tg\phi+sec\phi)-\frac{1}{2}\beta\ell n\left[\frac{1+\beta sin\phi}{1-\beta sin\phi}\right]\} \tag{4 8}$$

Because $\phi = am(\lambda\xi,k)$ we have that $sin\phi = sn(\lambda\xi,k) \rightarrow \tanh(\frac{1}{2}\nu\xi)$ The coefficient β which is imaginary (cf (3 19)) goes to

$$\beta = i\left[\frac{\Omega_1-\Omega_-}{\Omega_-}\right]^{1/2} \rightarrow i\frac{\nu}{H} \tag{4 9}$$

Therefore ϕ (4 7) becomes in this limit

$$\phi(\xi) \rightarrow \phi(0) + \frac{1}{2}H\{\xi-\xi+\frac{1}{H}\ell n\left[\frac{1+\frac{i\nu}{H}\tanh(\frac{1}{2}\nu\xi)}{1-\frac{i\nu}{H}\tanh(\frac{1}{2}\nu\xi)}\right]\} \tag{4 10}$$

$$= \phi(0) - \frac{1}{2i}\ell n\left[\frac{1+\frac{i\nu}{H}\tanh(\frac{1}{2}\nu\xi)}{1-\frac{i\nu}{H}\tanh(\frac{1}{2}\nu\xi)}\right]\} \tag{4 11}$$

It is now not hard to see that this last expression is equal to

$$\phi(0) - \text{arctg}(\frac{\nu}{H} \tanh(\frac{1}{2}\nu\xi)) \qquad (4\ 12)$$

which is (2 23) apart from a constant So both the phase and the amplitude of the single kink can be recovered from the corresponding quantities of the soliton lattice when $\Delta \to 0$ Finally by using the following results

$$K(k) \to \ell n \frac{4}{\sqrt{1-k^2}} \quad , \quad E(k) \to 1 \qquad (4\ 13)$$

and

$$\Delta \sim 1-k^2 + O((1-k^2)^2) \quad \text{when } k \to 1 \qquad (4\ 14)$$

one can easily recover from (3 41), the energy of a static single kink which we calculated in I, namely

$$\mathcal{E}_o \text{ (single kink)} = \frac{\nu c^2}{2s}(-\frac{2}{3}r + \frac{1}{6}H^2) \qquad (4\ 15)$$

5.5 Concluding remarks

We have investigated the presence and some of the properties of a multi-kink or soliton lattice in a linear chain system with frustration in which incommensurate modulations occur The procedure was, as in the case of the single kinks [1] a combination of analytical techniques applied to a continuum approximation of the model and numerical integration of the equations of motion The main results are the following

- In contrast to soliton lattices in systems without frustration, the soliton lattices in a system with frustration has a rather complex structure

- A soliton lattice in a frustrated system does not have to be periodic at the level of the continuum approximation This is due to the fact that the amplitude of the soliton lattices, which is a periodic function, and the increase in the phase in such a period, are in general incommensurate with respect to one another

- Even if the soliton lattice is commensurate in the above sense, it will in general be incommensurate with respect to the underlying discrete lattice

- Just as in the case of the single kinks we have again that the phason-velocity is the upper-limit for the velocity of propagating soliton lattices

- Moving soliton lattices keep their form over long distances, which establishes the presence of well-defined soliton lattices in a discrete system

5.6 Appendix

In this appendix we will analyse the effective radial potential which the mechanical particle feels in the case of the soliton lattices solution In particular we will give a proof of the definite ordering (3 19), i e

$$O < \Omega_- < \Omega_1 < \Omega_o + \Delta < \Omega_+ \tag{1}$$

This effective radial potential can be derived by first transforming the energy ε of the particle ((2 18)+(3 9))

$$\varepsilon = -\frac{1}{4}s\Delta^2 = \frac{1}{2}(u^2+v^2) - \frac{1}{2}r(u^2+v^2) - \frac{1}{4}s(u^2+v^2)^2 - \frac{r^2}{4s} \tag{2}$$

to polar variables ϱ and ϕ by using

$$\begin{aligned} u(\xi) &= \varrho(\xi)\sin\phi(\xi) \\ v(\xi) &= \varrho(\xi)\cos\phi(\xi) \end{aligned} \tag{3}$$

This leads to

$$\varepsilon = \frac{1}{2}(\varrho^2+\varrho^2\phi^2) - \frac{1}{2}r\varrho^2 - \frac{1}{4}s\varrho^4 - \frac{r^2}{4s} \tag{4}$$

ϕ can be eliminated from this last expression by using the angular momentum $L_\perp$ in polar variables

$$L_\perp = \frac{1}{2}H\varrho_1^2 = -\varrho^2\phi + \frac{1}{2}H\varrho^2 \tag{5}$$

Thus

$$\varepsilon = \frac{1}{2}\varrho^2 + U_{eff}(\varrho) \tag{6}$$

with

$$U_{eff}(\varrho) = -\frac{r^2}{4s} - \frac{1}{2}r\varrho^2 - \frac{1}{4}s\varrho^4 + \frac{1}{8}H^2\frac{1}{\varrho^2}(\varrho^2 - \varrho_1^2)^2 \tag{7}$$

This potential only depends on ϱ through $\Omega \equiv \varrho^2$, therefore it is more convenient to analyse $\bar{U}_{eff}(\Omega) \equiv U_{eff}(\sqrt{\Omega})$, which can be written as

$$\bar{U}_{eff}(\Omega) = -\frac{1}{4}s(\Omega-\Omega_0)^2 + \frac{1}{8}H^2\frac{1}{\Omega}(\Omega-\Omega_1)^2 \tag{8}$$

The first term constitutes the inverted mexican hat $\bar{U}_{IMH}(\Omega)$ and the second term the effective centrifugal potential $\bar{U}_{CF}^{eff}(\Omega)$ A sketch of both these potentials and their sum is shown in Fig 4

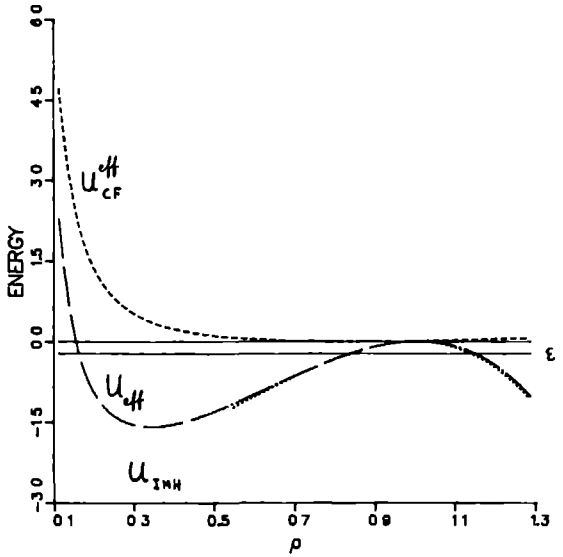

Figure 4. Sketch of $U_{IMH}(\varrho)$ $U_{CF}^{eff}(\varrho)$ and $U_{eff}(\varrho) = U_{eff}(\varrho) = U_{IMH}(\varrho) + U_{CF}^{eff}(\varrho)$ as functions of ϱ (arbitrary units)

It is not hard to see that the solutions of the equation

$$\bar{U}_{\text{eff}}(\Omega) = \varepsilon = -\frac{1}{4}s\Delta^2 \tag{9}$$

are given by (3 17) and (3 18), i e

$$\begin{aligned} \Omega_1 &= \Omega_o - \Delta \\ \Omega_\pm &= \frac{1}{2}[\Omega_o+\Delta+\frac{H^2}{2s}] \pm \frac{1}{2}([\Omega_o+\Delta-\frac{H^2}{2s}]^2+\frac{4H^2}{s}\Delta)^{1/2} \end{aligned} \tag{10}$$

For the expression for Ω_+ it is immediately clear that

$$\Omega_+ > \Omega_o + \Delta \tag{11}$$

and because Δ is positive, we also have

$$\Omega_1 = \Omega_o - \Delta < \Omega_o + \Delta \tag{12}$$

When $\Omega \to 0$ we have that $\bar{U}_{CF}^{\text{eff}}(\Omega) \to +\infty$, while $\bar{U}_{IMF}(\Omega)$ remains finite and negative Therefore we have that for sufficiently small values of Ω

$$\bar{U}_{\text{eff}}(\Omega) > \varepsilon \tag{13}$$

The same is true for $\Omega_1 < \Omega < \Omega_o+\Delta$, as can be seen in Fig 4 So in order to have a non-trivial motion ($\varrho \neq \varrho_1$, $\dot{\varrho} = 0$), we need that

$$0 < \Omega_- < \Omega_1 \tag{14}$$

or in other words

$$\bar{U}_{\text{eff}}(\Omega) \leqslant \varepsilon \quad \text{for } \Omega_- \leqslant \Omega \leqslant \Omega_1 \tag{15}$$

By using (10) we see that (14) boils down to

$$-\Omega_o + 3\Delta + \frac{H^2}{2s} < ([\Omega_o+\Delta-\frac{H^2}{2s}]^2 + \frac{4H^2}{s}\Delta)^{1/2} \tag{16}$$

For $\Delta = 0$ this inequality is satisfied when

$$\frac{H^2}{2s} < \Omega_o \quad \text{or} \quad H^2 < -2r \tag{17}$$

which is the condition for the existence of the single kink solution Now suppose that

$$\frac{1}{3}\Omega_o \leqslant \Delta < \Omega_o \tag{18}$$

then we have $-\Omega_o+3\Delta \geqslant 0$ and thus $-\Omega_o+3\Delta+\frac{H^2}{2s} > 0$ In this case (16) is equivalent to

$$[-\Omega_o+3\Delta+\frac{H^2}{2s}]^2 < [\Omega_o+\Delta-\frac{H^2}{2s}] + \frac{4H^2}{s}\Delta \tag{19}$$

If we work this out we find $8\Delta^2 < 8\Omega_o\Delta$ or $\Delta < \Omega_o$, which is true by supposition Thus (14) is true independently of the magnetic field strength H when Δ obeys (18) Now suppose that

$$0 < \Delta < \frac{1}{3}\Omega_o \tag{20}$$

Then for $\frac{H^2}{2s} < \Omega_o-3\Delta$ we have that

$$-\Omega_o + 3\Delta + \frac{H^2}{2s} < 0 \tag{21}$$

and thus we must conclude that (16) is trivially satisfied On the other hand when

$$\frac{H^2}{2s} \geqslant \Omega_o - 3\Delta \tag{22}$$

we have again $-\Omega_o+3\Delta+\frac{H^2}{2s} \geqslant 0$ and so we can repeat the reasoning which we just gave in the complimentary case (18)

Therefore we can conclude that (14) is always true as long as $\Delta \neq 0$ This completes the proof of the definite ordering (1)

5.7 References

[1] J J M Slot and T Janssen, submitted for publication to Physica D (1987)

[2] T Janssen and J A Tjon, Phys Rev **B25** (1981) 2245

[3] B Horovitz, Phys Rev Lett **46** (1981) 742

[4] I E Dzyaloshinskii, Sov Phys JETP, **20** (1965) 665
[5] See for instance R K Dodd, J C Eilbeck, J D Gibbon and H C Morris, Solitons and Nonlinear Wave Equations (Academic Press, 1982), Chapter 7, p 389
[6] P F Byrd and M D Friedman, Handbook of Elliptic Integrals for Engineers and Physicists (Springer Verlag, 1953)

Summary

The occurrence of commensurately and incommensurately modulated phases in many crystals is to a large extent due to non-linear interactions The resulting ground state is almost always degenerate. The energetically low-lying static excitations consist in that case of domain walls (or discommensurations) between domains corresponding to the various degenerate ground state phases. These non-linear excitations play an important role in the low-temperature behaviour of modulated crystals

In this thesis statics and dynamics of domain walls are studied in two model systems with a linear-chain structure These systems are, consequently, quasi-one-dimensional

The first model is a generalization of the Su-Schrieffer-Heeger (SSH) model which was originally proposed to explain the interesting optical, electrical and magnetic phenomena at low temperature of the quasi-one-dimensional organic conductor trans-polyacetylene $(CH)_x$ However, the model is representative for a whole class of quasi-one-dimensional systems of the charge transfer type In these systems there is an indirect non-linear interaction between the lattice degrees of freedom mediated by the electrons The generalization studied here consists of a strong coupling between the chains, which is fully absent in the original model As a consequence there results a completely different modulated ground state for a half-filled band. Non-linear excitations can no longer be attributed to individual chains and , therefore, have a collective character. Furthermore, the spin-charge relations for the domain walls in this model are very different from those in the original model

The existence of the quasi-one-dimensional conductor $Hg_{3-\delta}AsF_6$ shows the possibility of a strong coupling between chains For this material one has performed calculations to get an insight in the strength and anisotropy of the electron-phonon interaction From these calculations it is seen that the intra-chain coupling is very weak, whereas the inter-chain coupling is indeed very strong With these results a number of experimental findings may be explained, partly qualitatively and partly quantitatively In particular, one understands why there is no Peierls instability

The second model is the so called **D**iscrete **F**rustrated φ^4 (DIFFF) or Janssen-Ijon model In this model one considers a one-dimensional chain of classical particles (atoms) each moving in an anharmonic (quartic) local potential and harmonically coupled to the first and second neighbours It is the simplest model that in principle shows most of the characteristics of modulated crystals. As in the generalized SSH model, the domain walls occurring in such systems have been studied, both in a continuum approximation and by numerical

integration In contrast to the case of the generalized SSH model, attention was also paid to the dynamics of domain walls In the continuum approximation used here, moving domain walls may be obtained from static ones by a Lorentz-like transformation, in which the role of the speed of light is taken over by the phason velocity It turns out that these domain walls cannot be described purely in terms of the phase of the modulation function, but that also the amplitude comes in Individual domain walls as well as lattice systems of domain walls (soliton lattices) have been studied in this model For both types one can find an exact expression for their form if one considers a continuum approximation in which only one mode is taken into account In that case the equations of motion are equivalent with those of a particle with two degrees of freedom in a rotationally invariant potential and in a perpendicular external magnetic field This is an integrable dynamical system It is no longer so when one takes into account more modes The additional terms appearing in this case give, within an effective theory for the fundamental mode, rise to pinning of the modulation phase The exact solutions turn out to correspond to unstable crystal configurations However, when these exact solutions of the continuum approximation are used as starting configuration for the numerical integration of the equations of motion for the discrete system, these excitations are found to have a very long lifetime and to propagate over hundreds of unit-cells In the numerical integration individual domain walls turn out to behave as particles that, depending on their velocity, move almost uniformly, or loose rapidly their energy by the emission of phonon radiation of the Cerenkov type, or disintegrate

De oorsprong van het optreden van commensurabel en incommensurabel gemoduleerde fasen in vele kristallen is voor een groot deel gelegen in de aanwezigheid van niet-lineaire interacties die vrijwel altijd tot een ontaarde grondtoestand leiden De energetisch laagliggende statische excitaties zullen bestaan uit domeinwanden (of discommensuraties) tussen gebieden corresponderende met verschillende ontaarde grondtoestandsfasen Deze niet-lineaire excitaties spelen een belangrijke rol in het lage-temperatuur-gedrag van gemoduleerde kristallen

In dit proefschrift is gekeken naar de statica en de dynamica van domeinwanden in een tweetal modellen voor gemoduleerde systemen met de structuur van een lineaire keten Deze systemen zijn dus quasi-een-dimensionaal

Het eerste model is een uitbreiding van het Su-Schrieffer-Heeger (SSH) model dat oorspronkelijk was opgesteld om allerlei interessante optische, electrische en magnetische verschijnselen bij lage temperaturen te verklaren van de quasi-een-dimensionale organische geleider trans-polyacetyleen $(CH)_x$ Het model is echter generiek voor vele quasi-een dimensionale systemen van het charge transfer type In deze systemen is er een indirecte niet lineaire interactie tussen de rooster-vrijheidsgraden die gemedieerd wordt door de elektronen De uitbreiding hier bestaat uit de invoering van een sterke koppeling tussen de ketens die in het oorspronkelijke model geheel ontbreekt Als gevolg hiervan ontstaat een geheel andere gemoduleerde grondtoestand voor een half-gevulde band Ook de niet lineaire excitaties kunnen niet meer toegeschreven worden aan een individuele keten en hebben dus een collectief karakter Verder zijn de spin-lading relaties voor deze domeinwanden geheel anders dan in het oorspronkelijke model

Dat er een sterke koppeling aanwezig kan zijn tussen ketens blijkt uit het bestaan van de quasi-een-dimensionale incommensurabele geleider $Hg_{3-\delta}AsF_6$ Aan dit materiaal zijn berekeningen gedaan teneinde een inzicht te krijgen in de sterkte en de anisotropie van de elektron-fonon interactie Uit deze berekeningen bleek dat de intra-keten koppelingsconstante zeer klein is, terwijl de inter-keten koppelingsconstante inderdaad zeer groot is Hiermee kunnen een aantal experimentele bevindingen deels kwalitatief deels kwantitatief verklaard worden, in het bijzonder waarom er geen Peierls-instabiliteit waargenomen wordt

Het tweede model is het zogenaamde Discrete geFrustreerde ϕ^4 (DIFFF) model, ook wel Janssen Tjon model genoemd Beschouwd wordt een een-dimensionale keten van klassieke deeltjes (atomen) die ieder in een

anharmonische (4e orde) locale potentiaal bewegen en die met elkaar harmonisch gekoppeld zijn tot en met de tweede buren Het is het eenvoudigst denkbare model dat vrijwel het gehele scala van verschijnselen vertoont die worden waargenomen in gemoduleerde kristallen De domeinwanden die in zo'n systeem optreden zijn bestudeerd, evenals die in het uitgebreide SSH model, in een continuumbenadering èn door middel van numerieke simulatie van het discrete systeem In tegenstelling tot het voorgaande (SSH) is hier ook aandacht geschonken aan de dynamica van domeinwanden In de hier gebruikte continuumbenadering zijn de bewegende domeinwanden uit de statische te verkrijgen door een Lorentz-achtige transformatie, waarbij de rol van de lichtsnelheid gespeeld wordt door de fason-snelheid Het blijkt dat deze domeinwanden niet puur beschreven kunnen worden in termen van de fase van de modulatie-golf, maar dat ook de amplitude een rol speelt. Zowel individuele domeinwanden als een roostersysteem van domeinwanden (soliton rooster) zijn bestudeerd in dit model Van beide kan de exacte gedaante gevonden worden in de continuumbenadering waarbij slechts één mode in beschouwing wordt genomen In dit geval zijn de bewegingsvergelijkingen equivalent met die van een deeltje met twee vrijheidsgraden in een rotatie-symmetrische potentiaal en een loodrecht uitwendig magneetveld. Dit is een integreerbaar dynamisch systeem. Dat is niet meer zo indien men meer modes in beschouwing neemt De extra termen die men in dit geval krijgt in het kader van een effectieve theorie voor de fundamentele mode geven aanleiding tot pinning van de fase van de modulatie-golf De exacte oplossingen blijken te corresponderen met instabiele kristal-configuraties. Echter, indien deze exacte oplossingen gebruikt worden als start-configuratie bij het numeriek integreren van de bewegingsvergelijkingen van het directe systeem, blijken deze excitaties toch een zeer lange levensduur te hebben en zich over honderden eenheids-cellen voort te bewegen Individuele domeinwanden blijken zich bij deze numerieke integratie te gedragen als deeltjes die, afhankelijk van hun snelheid, eenparig bewegen, of hun energie verliezen door fononstraling van het Cerenkov type, of desintegreren.

Curriculum vitae

J J M Slot

geboren 3 maart 1959 te Terneuzen

1965-1971	lagere school, Terneuzen
1971-1977	ongedeeld VWO Zeldenrust College Terneuzen
1977-1982	studie Wis- en Natuurkunde Rijksuniversiteit Utrecht
10 maart 1980	kandidaatsexamen letter N0 cum laude
20 sept 1982	doctoraalexamen theoretische natuurkunde met groot bijvak wiskunde cum laude
1 okt 1982 - 31 sept 1987	wetenschappelijk medewerker afdeling Theoretische Natuurkunde III (Theoretische vaste-stof-fysica) Faculteit der Wiskunde en Natuurwetenschappen Katholieke Universiteit Nijmegen

De promovendus heeft naast het promotie-onderzoek waarvan de resultaten in dit proefschrift verwerkt zijn gedurende deze periode werkcolleges verzorgd in quantummechanica statistische mechanica, vaste-stof-fysica en groepentheorie

STELLINGEN

1) Het model van een twee-dimensionaal gemoduleerd kristal dat door Parlinski met behulp van moleculaire dynamica technieken geanalyseerd wordt, is rekening houdend met het beoogde doel nodeloos gecompliceerd

K Parlinski, Phys Rev B35, 8680 (1987)

2) Voor een grote klasse van maatbehoudende transformaties van het vlak op zichzelf, is integreerbaarheid te formuleren in termen van convergentie van de Campbell-Baker-Hausdorff formule in een geschikt gekozen oneindig-dimensionale Lie-algebra

A J Dragt en J M Finn, J Math Phys 17, 2215 (1976)
J J M Slot, doctoraal scriptie, R U Utrecht (1982)

3) Het zou zeer waardevol zijn om in een georganiseerd verband bestaande programmatuur voor electronische structuur berekeningen van materialen (bandenstructuurberekeningen etc) onderling te vergelijken door middel van zogenaamde "benchmark tests", zoals dat reeds jaren gebruikelijk is voor eindige elementen programmatuur

zie "Benchmark" een maandelijks tijdschrift uitgegeven door de National Agency for Finite Element Methods & Standards (NAFEMS)

4) Gelet op de toenemende behoefte in de industrie en het bedrijfsleven aan deugdelijke simulatie in de meest brede betekenis van het woord, is het jammer om te moeten constateren dat de rol die de theoretisch fysicus hierin zou kunnen vervullen, gezien zijn achtergrond en mentale gesteldheid, nog maar zo weinig doorgedrongen is

5) Bij de toepassing van beeldvormende techniek door middel van nucleaire magnetische resonantie (NMR) in de geneeskunde, maakt men dankbaar gebruik van het feit dat een mens grotendeels uit water bestaat

"Medical applications of MR" in Principles of MR imaging, syllabus Philips Medical Systems 1986

6) De voorspelling van Minnhagen voor het optreden van niet-universele sprongen in de helicïteitsmodulus bij de Kosterlitz-Thouless overgang kan niet geverifieerd worden bij gefrustreerde XY-modellen

P Minnhagen, Phys Rev ***B32****, 7548 (1985)*
J M Thijssen en H J F Knops, preprint, Nijmegen (1987)

7) Iemand aan de tand voelen en iets aan de kaak stellen dient als uitgangspunt voor orthognatisch mond- en kaakchirurgisch ingrijpen

8) De accountantsverklaring dient niet vanuit de koppeling met een bepaald controle-object te worden bezien, doch vanuit de aard van de functievervulling zoals die wordt bepaald door de eisen en verwachtingen van het maatschappelijk verkeer

Prof Drs K P G Wilschut RA "De verwachtingskloof aangaande de dienstverlening door het accountantsberoep", De Accountant, april 1987

9) Het verdient aanbeveling moleculair biologisch onderzoek te verrichten naar mogelijke therapeutische toepassingen van anti-sense fosfaat-gemethyleerde DNA fragmenten